

MANA Progress **R**eport

Research Digest 2011



World Premier International (WPI) Research Center
International Center for
Materials Nanoarchitectonics (MANA)



National Institute for Materials Science (NIMS)

Preface

Masakazu Aono
MANA Director-General
NIMS



MANA was shaken considerably by the Great Tohoku-Kanto earthquake that hit Japan on March 11th, 2011, and by its associated disasters, but fortunately none of us was hurt. Various research facilities at MANA were damaged to some extent, but the damage is repairable. After this disaster happened, lots of friends of MANA, from various countries, kindly sent us messages of sympathy. We appreciate those warm messages very much.

More than four years have passed since MANA was established in October 2007 as one of the five research centers in the WPI Program. In 2011, these five WPI research centers underwent an interim evaluation of their first five years in operation. We are proud that MANA got a high score “A”, which means that MANA can continue its brisk activities for another 5 years at least. Next to the existing MANA Building at NIMS, the construction work of the new MANA and Environmental Research Building is steadily nearing completion. This can be seen as a symbol of the continued success of the MANA project.

This booklet, which is the part “Research Digest 2011” of the MANA Progress Report, summarizes the research activities of *MANA Principal Investigators*, *Group Leaders*, *MANA Independent Scientists* and *ICYS-MANA Researchers* in the calendar year 2011. *MANA Principal Investigators* are world-top class scientists, who take the main role to achieve the MANA research targets and serve as mentors for younger scientists. *Group Leaders* perform MANA research together with a MANA Principal Investigator by heading an own group. *MANA Independent Scientists* are younger researchers at NIMS, who work full-time for MANA and can perform their own research independently. *ICYS-MANA Researcher* is a position for postdoctoral fellows selected from all over the world by open recruitment. *ICYS-MANA Researchers* perform their own research independently by receiving advice from MANA Principal Investigators and other mentors. Other information on MANA research achievements (e.g., the lists of publications and patents) is given in the part “Facts and Achievements 2011” of the MANA Progress Report.

Lastly, on behalf of MANA, I would like to ask you for your continued understanding and support to MANA.

MANA Research Digest 2011

MANA Principal Investigators (24)

Nano-Materials Field

Takayoshi SASAKI (Field Coordinator)	7
Inorganic Nanosheets	
Katsuhiko ARIGA	8
Supramolecular Materials	
Yoshio BANDO (MANA Chief Operating Officer)	9
Inorganic Nanostructured Materials	
Toyohiro CHIKYOW	10
Nano Electrics and Related Materials	
Dmitri GOLBERG	11
Nanotubes' and Graphenes' Properties	
Kazuo KADOWAKI (Satellite)	12
Superconducting Quantum Nanoarchitectonics	
Zhong Lin WANG (Satellite)	13
Self-Powered Nanosensors for Environment Monitoring	

Nano-System Field

Masakazu AONO (MANA Director-General, Field Coordinator)	14
Nano-System Architectonics	
James K. GIMZEWSKI (Satellite)	15
MANA Brain: Neuromorphic Atomic Switch Networks	
Tsuyoshi HASEGAWA	16
Atomic Electronics for Future Computing	
Xiao HU	17
Manipulating Quantum Entanglement of Electron System	
Christan JOACHIM (Satellite)	18
Surface Atomic Scale Logic Gate	
Tomonobu NAKAYAMA	19
Integration of Nano Functionality for Novel Nanosystems	
Hideaki TAKAYANAGI (Satellite)	20
Mesoscopic Superconductivity and Quantum Information Physics	
Kazuhito TSUKAGOSHI	21
Gate-Induced In-Plane p-i-n Tunnel Junction in Bilayer Graphene	
Mark WELLAND (Satellite)	22
Bio-Inspired Materials for Sustainable Energy	

Nano-Green Field

Kohei UOSAKI (Field Coordinator)23
 Construction of Interphases with Atomic/Molecular Order for
 Efficient Conversion of Energy/Materials

Kazunori TAKADA24
 Solid State Batteries

Omar YAGHI25
 Reticular Materials

Jinhua YE26
 Nanoarchitectonics of Hybrid Artificial Photosynthetic System

Nano-Bio Field

Takao AOYAGI (Field Coordinator)27
 Smart Nano-Biomaterials

Guoping CHEN28
 Nano- and Micro-Structured Porous Scaffolds for Tissue Engineering

Yukio NAGASAKI (Satellite)29
 Nanotherapy Based on Novel Materials Nanoarchitectonics

Françoise M. WINNIK (Satellite)30
 Nanoarchitectonics-Inspired Nanoparticles and Interfaces for
 Therapeutic Applications

Group Leaders (11)

Naoki FUKATA (Nano-Materials Field)	31
Next-Generation Semiconductor Nanodevices	
Nobutaka HANAGATA (Nano-Bio Field)	32
Development of Nano Biomedicines	
Masanori KIKUCHI (Nano-Bio Field)	33
Bioactive Ceramics Materials	
Hisatoshi KOBAYASHI (Nano-Bio Field)	34
Materials for Functional Nanomedicine	
Takao MORI (Nano-Materials Field)	35
Functionalization of Atomic Network Materials	
Tadaaki NAGAO (Nano-System Field)	36
Controlling the Light in Nanospace	
Takashi SEKIGUCHI (Nano-Materials Field)	37
Characterization of Semiconductor Nanostructures by Using EBIC and CL Techniques	
Akiyoshi TANIGUCHI (Nano-Bio Field)	38
Development of Sensor Cells for Nanomaterials Safety Evaluation	
Yoshitaka TATEYAMA (Nano-System Field)	39
Nano-System Computational Science	
Kazuya TERABE (Nano-System Field)	40
Nano-Ionics Devices Based on Local Ion Transport	
Akiko YAMAMOTO (Nano-Bio Field)	41
Controlling Initial Degradation of Bioabsorbable Mg Alloys to Improve Biocompatibility	

MANA Independent Scientists (9)

Ryuichi ARAFUNE42
 Laser-Based Inelastic Photoemission Spectroscopy

Alexei A. BELIK43
 Search for New Ferroelectric, Magnetic and Multiferroic Materials
 Using High-Pressure Technique

Satoshi MORIYAMA44
 Graphene-Based Quantum-Dot Devices

Jun NAKANISHI45
 Development of Photoresponsive Biointerfaces

Naoto SHIRAHATA46
 Green Nanochemistry: Bandgap Engineering for Group IV Nanostructures

Lionel VAYSSIERES47
 Metal Oxide Quantum-Confined Structures: Aqueous Design, Electronic
 Structure & Size Dependence on Chemical & Physical Properties

Katsunori WAKABAYASHI48
 Theoretical Research on Electronic Properties of Nano-Carbon Systems

Yusuke YAMAUCHI49
 Synthesis and Application of Mesoporous Pt

Genki YOSHIKAWA50
 Nanomechanical Sensors for Medical, Security and Environmental Applications

ICYS-MANA Researchers (10)

Fatin HAJJAJ51
 Magneto-Responsive Soft Materials: Magnetically Reconfigurable
 in a Nonvolatile Fashion

Ryoma HAYAKAWA52
 Optical Manipulation of Single-Electron Tunneling Through
 Photochromic Molecular Dots

Song-Lin LI53
 Complementary-Like Graphene Logic Gates

Lok Kumar SHRESTHA54
 C₆₀ Microcrystals with Diverse Morphologies

Yoshihiro TSUJIMOTO55
 Low-Temperature Fluorination of Layered Iron Oxide

Ken WATANABE56
 Visualization of the Grain Boundary as the Blocking Layer for
 Oxygen Tracer Diffusion

Xianlong WEI57
 Electron Emission from One-Atom-Thick Solids

Jung-Sub WI58
 Direct Fabrication of Plasmonic Nanoparticles

Tianyou ZHAI59
 High-Performance Solar-Blind Photodetectors

Yuanjian ZHANG60
 Nano-Carbon Materials for Green Energy: Ambipolar Engineering of
 Graphitic Carbon Nitride via Graphene

Inorganic Nanosheets

MANA Principal Investigator

(Field Coordinator)

MANA Scientist
MANA Research Associate

Graduate Student

Takayoshi SASAKI

Minoru Osada, Yasuo Ebina, Renzhi Ma, Tadashi Ozawa
Jianbo Liang, Baowen Li, Shibata Tatsuo,
Xiaohe Liu, Fengxia Geng, Chengxiang Wang
Hikaru Takano, Kazuaki Matsuba, Asuka Fukue



1. Outline of Research

We aim at synthesizing 2D inorganic nanosheets as a unique class of nanoscale materials by delaminating various layered compounds through soft-chemical processes. Particular attention is paid to fine control of their composition and structure via doping and substitution of constituent elements, expecting new or enhanced properties.

We develop a new nanofabrication process for precisely organizing functional nanosheets into multilayer or superlattice assemblies through solution-based processes (Fig. 1). Based on the exotic approach with the nanosheets (soft-chemical materials nanoarchitectonics), we establish the tailoring ability and controllability over nanostructures with a precision down to 1 nm, which is comparable to that in lattice engineering utilizing modern vapor-phase deposition techniques.

In the second stage, we take challenges to develop innovative nanostructured materials and nanodevices through nanoscale assembly of nanosheets and a range of foreign species (organic modules, metal complexes, clusters...). Particularly we attempt to realize new or sophisticated functions by cooperative interaction between nanosheets themselves or between nanosheets and other functional modules.

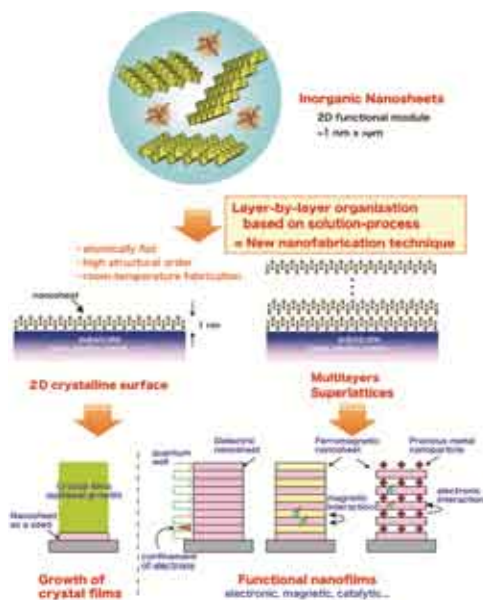


Fig. 1. Conceptual explanation of the research plan.

2. Research Activities

(1) Evolution of Ferroelectricity via Hetero-Assembly of Perovskite Oxide Nanosheet.¹⁾

Two types of perovskite-type nanosheets with different thicknesses, LaNb_2O_7 and $\text{Ca}_2\text{Nb}_3\text{O}_{10}$, were assembled layer-by-layer through Langmuir-Blodgett method. Various

characterizations including UV-visible absorption spectroscopy, XRD and TEM observation (Fig. 2) revealed the formation of a superlattice film where two types of nanosheets are alternately stacked. The hetero-assembled film was found to show ferroelectric property (Fig. 2), despite paraelectric nature for individual nanosheets themselves. This surprising behavior may be ascribed to the formation of soft interface between the two different nanosheets, resulting in loss of centrosymmetry, and may be taken as a new strategy to induce ferroelectric response.

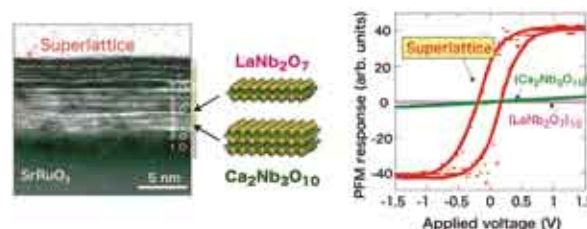


Fig. 2. Cross-sectional TEM images for a superlattice film of LaNb_2O_7 and $\text{Ca}_2\text{Nb}_3\text{O}_{10}$ nanosheets, and its PFM data.

(2) Synthesis of Transition Metal Hydroxide Nanocones.²⁾

We found that microwave-assisted homogeneous precipitation of Co^{2+} salts and surfactant dodecylsulfate (DS) in the presence of alkaline agent (hexamethylenetetramine) produced hydroxide nanocones with a sharp edge angle of $10\text{--}60^\circ$ (Fig.3). This is the first example of such cone-shaped nanomaterials apart from carbon/BN system. Detailed analysis by TEM and XRD demonstrated that the cone is composed of lamellar hydroxide layers accommodating DS ions in the gallery. Interestingly the nanocone can be delaminated into unilamellar nanosheets by dispersing in formamide.

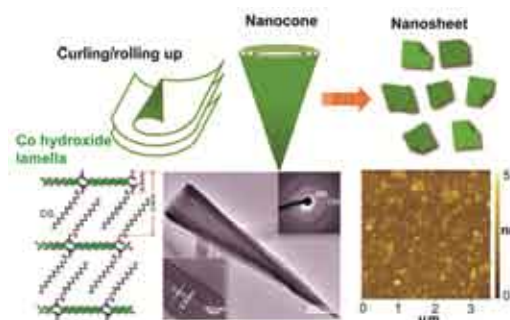


Fig. 3. Formation of nanocone structure in Co hydroxide and their exfoliation into nanosheets.

References

- 1) B. Li, M. Osada, T.C. Ozawa, Y. Ebina, K. Akatsuka, R. Ma, H. Funakubo, T. Sasaki, *ACS Nano* **4**, 6673 (2010); *Jpn. J. Appl. Phys.* **50**, 09NA10 (2011).
- 2) X. Liu, R. Ma, Y. Bando, T. Sasaki, *Angew. Chem. Int. Ed.* **49**, 8253 (2010).

Supramolecular Materials

MANA Principal Investigator

MANA Scientist
MANA Research Associate

Katsuhiko ARIGA

Jonathan P. Hill, Qingmin Ji
Venkata Krishnan, Jan Labuta, Dattatray Sadashiv Dhawale



1. Outline of Research

Functional materials have been wisely constructed via bottom-up approaches as seen in preparation of molecular and nano patterns, complexes, and nanomaterials organized nano- and microstructures, and function materials. In addition, novel concepts to bridge nano (molecular) structures and bulk systems now becomes crucial in order to control real nano and molecular functions from our visible worlds. We have proposed a novel methodology “hand-operating nanotechnology” where molecular orientation, organization and even functions in nanometer-scale can be operated by our bulk (hand) operation. Selected examples of research results on supramolecular materials are shown below.

2. Research Activities

(1) Photo-Driven Molecular Machine.¹⁾

We newly synthesized porphyrin derivatives bearing 2,6-di-*t*-butyl phenol substituents at their 5,15-positions that undergo reversible photoredox switching between porphyrin and porphodimethene states as revealed by UV-vis spectroscopy, fluorescent spectroscopy, and X-ray single crystal analyses. Photoredox interconversion is accompanied by substantial variations in electronic absorption and fluorescence emission spectra, and a change of conformation of the tetrapyrrole macrocycle from planar to roof-shaped (Fig. 1). Our molecular design indicates a simple and versatile method for producing photo-redox macrocyclic compounds, which should lead to a new class of advanced functional materials suitable for molecular devices and machines.

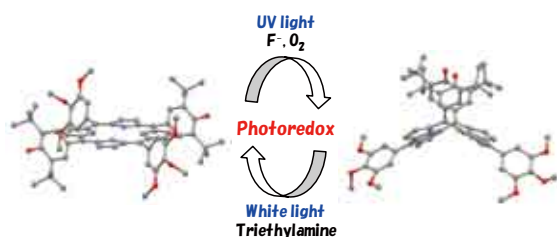


Fig. 1. Photo-driven molecular machine.

(2) Living Molecular Assembly.²⁾

We have observed the self-assembling growth of molecular nanowires of trigeminal porphyrins and investigated their reassembly properties following their obliteration (Fig. 2). Our process is an example of bottom-up self-assembly compounded with top-down nanomanipulation and we are currently assessing the use of this method for controlled growth of surface-anchored nanoscale organic circuit structures, which might be studied as self-assembled molecular electronic devices.

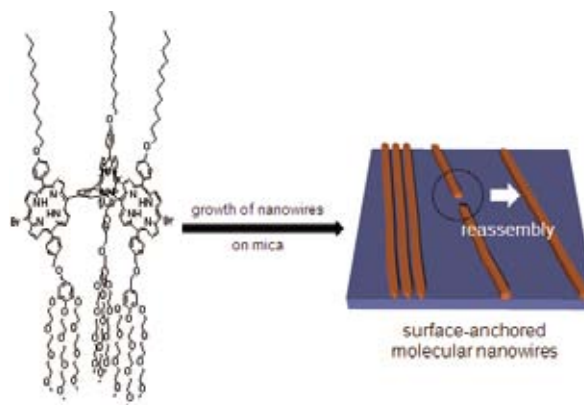


Fig. 2. Living self-assembled nanowire with self-healing capability.

(3) Electro-Chemical Coupling Layer-by-Layer (ECC-LbL) Assembly.³⁾

Electrochemical coupling layer-by-layer (ECC-LbL) assembly is introduced as a novel fabrication methodology for preparing layered thin films (Fig. 3). This method allows us to covalently immobilize functional units, such as porphyrin, fullerene, and fluorene, into thin films of desired thicknesses and designable sequences for both homo- and hetero-assemblies while ensuring efficient layer-to-layer electronic interactions. Films were prepared using a conventional electrochemical set-up by a simple and inexpensive process where various layering sequences can be obtained and photovoltaic functions of a prototype p/n heterojunction device were demonstrated.

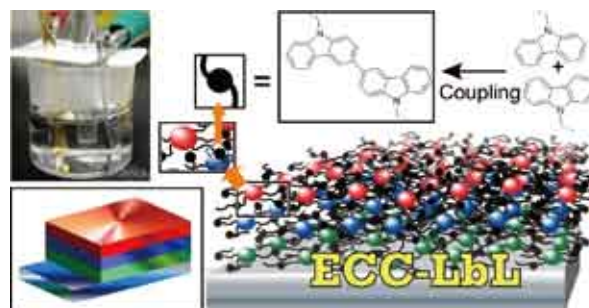


Fig. 3. Electro-Chemical Coupling Layer-by-Layer (ECC-LbL) Assembly.

References

- 1) S. Ishihara, J.P. Hill, A. Shundo, G.J. Richards, J. Labuta, K. Ohkubo, S. Fukuzumi, A. Sato, M.R.J. Elsegood, S.J. Teat, K. Ariga, *J. Am. Chem. Soc.* **133**, 16119 (2011).
- 2) Y. Xie, M. Akada, J.P. Hill, Q. Ji, R. Charvet, K. Ariga, *Chem. Commun.* **47**, 2285 (2011).
- 3) M. Li, S. Ishihara, M. Akada, M. Liao, L. Sang, J.P. Hill, V. Krishnan, Y. Ma, K. Ariga, *J. Am. Chem. Soc.* **133**, 7348 (2011).

Inorganic Nanostructured Materials

Principal Investigator

(MANA Chief Operating Officer)
 MANA Scientist
 MANA Research Associate
 Graduate Student (Waseda Univ.)

Yoshio Bando

Chunyi Zhi, Ryutaro Souda
 Xi Wang, Shimou Chen, Chikkavenkataswamy Nethravathi
 Xuebin Wang, Tian Wei



1. Outline of Research

Our ultimate goal is to explore various applications of one-dimensional nanomaterials, including their optoelectronic applications, composites materials, energy storage etc. At current stage, we are developing controllable methods for synthesis of nanomaterials, investigating their properties, developing novel nanofillers for polymeric composites, and fabricating photodetectors using semiconductor nanowires, nanomaterials for lithium ion battery and supercapacitors etc (Fig. 1).

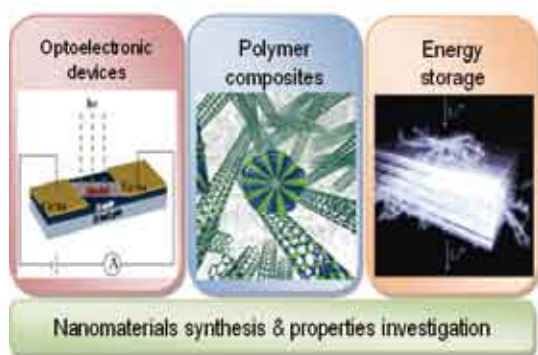


Fig. 1. Three sub-themes and their coordination.

Based on the ultimate goal and our current researches, we set up following three sub-themes.

- (i) Developing highly effective synthesis method for various semiconductor nanomaterials;
- (ii) Systematic property investigation to fabricated nanomaterials;
- (iii) Application studies, including device fabrication, energy storage tests and composite materials studies etc.

2. Research Activity

(1) *Fabrication of Large-Area, Few-Layered BN and C_x-BN Nanosheets by “Chemical Blowing” of Thin-Walled Bubbles.*¹⁾

We have developed a new route of chemical blowing for the production of atomically thin free-standing BN and C_x-BN nanosheets. This technology has two main charac-

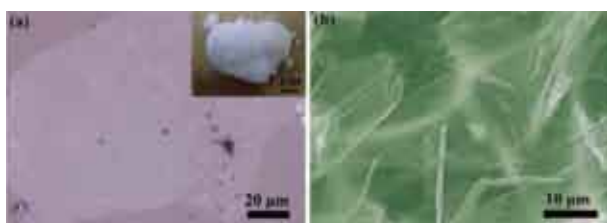


Fig. 2. a) Optical image of a large BN nanosheet transferred on a SiO₂ substrate. b) SEM image of ultrathin BN sheets.

teristic features: high volume yield and laterally large areas. Significant mechanical reinforcement in polycarbonate/BN composites and delicate tuning of nanosheet conductivity are demonstrated in this work (Fig. 2).

(2) *Self-stacked Co₃O₄ Nanosheets for High-performance Lithium Ion Batteries.*²⁾

Self-stacked Co₃O₄ nanosheets were synthesized via a facile method. The obtained Co₃O₄ shows a peculiar multi-lamellar structure which is built up by vertically stacked nanoplates with interspaces preserved by carbon segments between the layers. It is also suggested that further improvements in the electrochemical performance of hierarchical materials can be achieved by optimizing the assembly-mode of the present building nanosheet blocks.

(3) *Highly Thermo-conductive Fluid with Boron Nitride Nanofillers.*³⁾

We demonstrated for the first time how BN nanotubes and nanospheres may effectively be used to achieve remarkable thermal conductivity improvement of a fluid. Benefiting from high thermal conductivity and high aspect ratio of BN nanotubes, at a fraction of 6 vol %, the thermal conductivity of water was remarkably improved, up to 2.6-times. A combination of BN nanotubes and nanospheres was found to increase the fluid's thermal conductivity while keeping its viscosity low (Fig. 3).

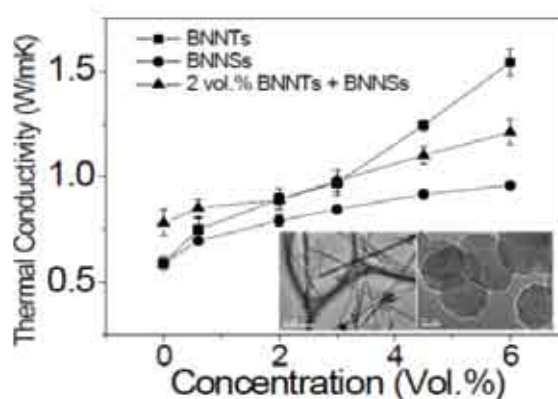


Fig. 3. Thermal conductivity improvement of nanofluids by BN nanofillers. Insets show nanofillers used.

References

- 1) X. Wang, C. Zhi, L. Li, H. Zeng, C. Li, M. Mitome, D. Golberg, Y. Bando, *Adv. Mater.* **23**, 4072 (2011).
- 2) X. Wang, H. Guan, S. Chen, H. Li, T. Zhai, D. Tang, Y. Bando, D. Golberg, *Chem. Commun.* **47**, 12280 (2011).
- 3) C. Zhi, Y. Xu, Y. Bando, D. Golberg, *ACS Nano* **5**, 6571 (2011).

Nano Electrics and Related Materials

MANA Principal Investigator
MANAScientist

Toyohiro CHIKYOW
Masahiro Goto, Yutaka Wakayama



1. Outline of Research

In the future large scale integrated circuit (LSI), due to the scaling of the transistors, new materials exploration and atomically controlled nano interfaces are required.¹⁾ Presently a stack of HfO_2 and SiO_2 are used in a micro processor and this materials will be adopted in memory devices too. However to realize more smaller transistor, another new gate oxide materials, which can contact with Si directly, will become the most serious issue, though a lot of efforts have been made to find new candidates of having higher dielectric property to find the next generation “high-k” materials. For this purpose, La_2O_3 or CeO_2 has been extensively studied.²⁾ To find confirmable metal gate, work function tuning, structure control and thermal stabilities are the key factors in materials screening. To control the work functions, two kinds of metals, which have higher work function and lower work function, are mixed to compose nano-CMOS device. As well recognized, though the work function was successfully tuned, it did not reflect the threshold voltage (V_{th}), due to the Fermi level pinning.³⁾ The other emerging issue is the fluctuation in device performance, such as V_{th} fluctuation in nano CMOS. It is not clearly identified how the V_{th} fluctuates, but some candidates for explanations are pointed out. One of them is edge roughness which comes from polycrystalline structure of the metal gate composed of grains in 20 nm – 200 nm, which are larger than that of gate length. For realizing ideal metal gate, the material must be amorphous with work function tenability and thermal stability with high-k insulator. In this work, we refer to the new materials exploration at first and showed a successful result of new finding in metal gate materials.

2. Research Activities

(1) Combinatorial materials synthesis.

As the new materials exploration tool, the combinatorial synthesis becomes prevalent in the last a decade for the materials research. Recently, we demonstrated the combinatorial ternary alloying as an innovative tool for thin film synthesis⁴⁾ to cover the whole composition. The concept of this combinatorial synthesis is illustrated in Fig. 1a. In this method, the sample rotation and moving mask system was synchronized to form a thin composition spread film. The advantage of this method is the continuous composition spread accompanied by three kinds binary alloying regions as shown in Fig. 1b. This method was already applied for new gate oxide of HfO_2 - Y_2O_3 - Al_2O_3 films.⁵⁾ This method can be applied to the ternary metal alloying to screen the metal gate materials as demonstrated in Fig. 1b.

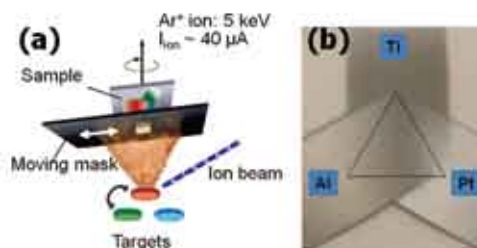


Fig. 1. Concept of ternary combinatorial synthesis (a) and practical combinatorial samples of metal alloys (b).

(2) New amorphous metal gate of Ta-Y-C.⁶⁾

One of the candidate of amorphous structured metal gate is Ta – Y because the Ta and Y has more than 15% atomic size difference and has a great possibility of having amorphous or micro grain structure from the empirical amorphous formation rule. Also C as the impurity will extend the possibility of thermally stable metal alloy on high-k oxide. In addition, Ta has higher work function and Y has lower one and they are suitable coupling for work function tuning. Fig. 2 shows a result of flat band shift of TaC-Y alloy and sample structure for measurement is also shown. It was observed that the flat band shift changed due to the work function and the difference was 0.8 eV, which make CMOS operation possible. Also the structure was found stable and amorphous up to 600 °C in the post annealing in N_2 atmosphere. These results showed that Ta-C-Y alloying had a great possibility as the metal gate materials for the future nano CMOS devices.

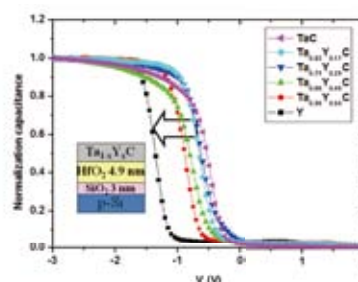


Fig. 2. Flat band shift due to work function tuning by TaC-Y alloying. The shift was 0.8 eV and it was enough for CMOS operation.

References

- 1) For example, *International Technology Road Map in Semiconductors 2011*, (Semiconductor Industry Association, San Jose, CA, 1999), p. 105.
- 2) D. Kukuruzyak et al., *Adv. Mater.* **20**, 3827 (2008).
- 3) Y. Akasaka et al., *Jpn. J. Appl. Phys.* **45**, L1289 (2006).
- 4) T. Nagata et al., *J. Appl. Phys.* **107**, 103714 (2010).
- 5) K. Hasegawa et al., *Appl. Surf. Sci.* **223**, 229 (2004).
- 6) P. Homhuan et al., *Jpn. J. Appl. Phys.* **50**, 10PA03 (2011).

Nanotubes' and Graphenes' Properties

MANA Principal Investigator

MANA Scientist
MANA Research Associate

Dmitri GOLBERG

Masanori Mitome, Naoyuki Kawamoto
Daiming Tang



1. Outline of Research

Nanotubes and graphenes have all the potentials to become the major structural and electronic materials of the 21st century. In order to fully use their rich, but yet entirely understood, unique characteristics, their mechanical and physical properties, in particular, on the individual structural level have to be thoroughly analyzed prior to the materials' smart integration into real technologies. The state-of-the-art microscopy techniques and facilities utilized by the Nanotubes Group, *i.e.* atomic force microscope (AFM) and scanning tunneling microscope (STM) setups merged with a high-resolution transmission electron microscope (HRTEM),¹⁾ allow us to precisely *in situ* measure mechanical, thermal and electrical properties of the most promising nanotube types, namely, C nanotubes (CNTs) and BN nanotubes (BNNTs), and "black" (C) and "white" (BN) graphenes,²⁾ while paying a special attention to the peculiar deformation, electron and heat transport kinetics under various experimental conditions and ultimately high spatial, and temporal resolutions.

2. Research Activities

(1) Temperature profiling inside a CNT interconnect.

CNTs have been assumed for the use as low-resistant interconnects for complex miniaturized electrical circuits. However, understanding resistive (or Joule) heating in such interconnects remains a major challenge, particularly in regards to CNT structural and thermal variations during prolonged periods of electrical stress. We performed real-time imaging of the associated effects of Joule heating in the CNT channels. First, electrical contacts to nanotubes entirely filled with a sublimable material ($Zn_{0.92}Ga_{0.08}S$) were made inside a STM-HRTEM. Upon exposure to a high current density, resistive hot-spots were identified on (or near) the contact points. These migrated and expanded along the CNT, as indicated by the localized sublimation of the encapsulated material. Using the hot-spot edges as markers we calculated the internal longitudinal and transverse temperature profiles inside CNTs, Fig. 1.³⁾

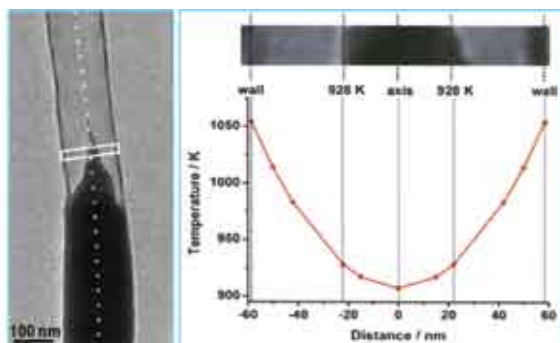


Fig. 1. (left) a CNT with partially sublimated encapsulated nanowire; and (right) the calculated temperature profile across the nanotube.

(2) Tensile properties of bamboo-like BN nanotubes.

BNNTs are structural analogs of CNTs, but they exhibit much higher chemical, thermal and oxidation stabilities that are important for practical applications. The common BNNT morphologies, which may be found on the nanotube market, are those made of bamboo-like joints, but their mechanical properties have never been elucidated. For the first time we performed direct tensile tests on such bamboo-like nanotubes inside AFM-HRTEM (Fig. 2).⁴⁾ The nanotube properties and deformation kinetics were correlated with the joints' interfacial structures under atomic resolution, and a geometry strengthening effect was demonstrated. As a result of such effect, the BNNBs revealed high ultimate tensile strength, of up to ~8 GPa, and the Young's modulus of up to ~220 GPa. The experimental results were verified through comparative molecular dynamics (MD) simulations for the interlocked and loosen interfacial structures between the nano-bamboo joints (Fig. 2).

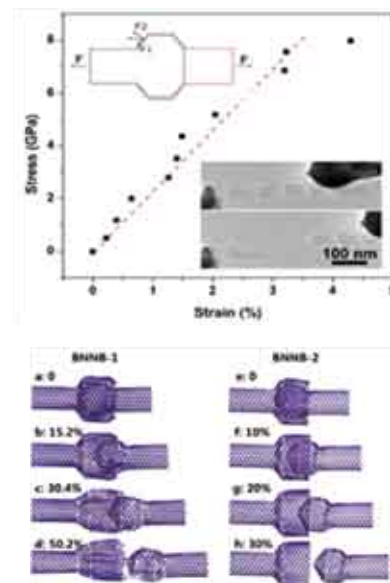


Fig. 2. (top) True stress-strain plot recorded under tensile loading of a bamboo-like BNNT; a force diagram and TEM images of the starting and broken tube stages are shown in the insets; (bottom) The comparative MD simulation results for a tensed interlocked bamboo-joint (BNNB-1, inset in the top diagram) and for that without interlocking (BNNB-2). The tensile strains are marked.

References

- 1) D. Golberg, P.M.F.J. Costa, M.S. Wang, X. Wei, D.M. Tang, Z. Xu, Y. Huang, U.K. Gautam, B. Liu, H. Zeng, N. Kawamoto, C. Zhi, M. Mitome, Y. Bando, *Adv. Mater.* **24**, 177 (2012).
- 2) D. Golberg, *Nature Nanotechn.* **6**, 200 (2011).
- 3) P.M.F.J. Costa, U.K. Gautam, Y. Bando, D. Golberg, *Nature Commun.* **2**, 421 (2011).
- 4) D.M. Tang, C.L. Ren, X.L. Wei, M.S. Wang, C. Liu, Y. Bando, D. Golberg, *ACS Nano* **5**, 7362 (2011).

Superconducting Quantum Nanoarchitectonics

MANA Principal Investigator
(Satellite at Univ. Tsukuba, Japan)
Graduate Student

Kazuo Kadowaki

Shinya Hashimoto, Manabu Tsujimoto, Kaveh Delfanzari,
Yohei Jono, Ryo Nakayama, Takeo Kitamura, Yusuke Suzuki,
Akihiko Nozawa, Masashi Sawamura, Takuya Ishikawa,
Krsto Ivanovic, Pradip Das, Takanari Kashiwagi



1. Outline of Research

Our objective in this research is to develop a new concept of materials science, which is referred to as Nanoarchitectonics, especially in superconductivity using highly developed modern nanotechnology in the ultimate quantum regime of materials. The challenge to accomplish this concept has been set forth on the intrinsic Josephson junctions (IJJ's) with and without magnetic field using high- T_c superconductor (HTSC) $\text{Bi}_2\text{Sr}_2\text{CaCu}_2\text{O}_{8+\delta}$, which can be grown by us in the highest quality of single crystal form available in the world. June in 2007, a remarkable novel phenomenon was discovered in the mesa structure of this material: strong, continuous and coherent electromagnetic waves at THz frequencies were observed. From the sharp spectrum of the radiation it is considered as LASER emission from stacked intrinsic Josephson junctions in the mesa. This achievement has triggered interest because the device may bring us the first full solid state THz sources, which will enable us a variety of important applications in the 21st century.

Concerning new materials, we have started to develop topological insulating materials such as Bi_2Se_3 , Bi_2Te_3 , $\text{TlBi}(\text{S}_{1-x}\text{Se}_x)_2$, etc. this year. Among others, we were successful to grow large single crystals of Bi_2Se_3 doped with Cu and $\text{Bi}_{1.5}\text{Sb}_{0.5}\text{Te}_{1.8}\text{Se}_{1.2}$ compounds and studied not only the basic physical properties but also superconducting behaviors, ARPES, STM, etc.

2. Research Activities

(1) THz radiation from HTSC IJJ's.

The research has been focused on two directions: one is to understand deeply the fundamental aspect of THz radiation and the other is to develop applications.¹⁾ Here, we show an example of applications for the THz imaging as shown in Fig. 1. The radiation is monochromatic so that it is very unique to do imaging, i.e., since the spectrum power density is very high, it is possible to do accurate measure-

ment. On the other hand, it is not possible to take Fourier spectra unless the emission frequency can be varied easily and widely. Using multi branching nature of radiation²⁾ we found that the frequency can be changed between 0.3 and 0.9 THz rather easily. This gives us a great hope that this IJJ THz emitter is promising as a unique variable THz source. Using this radiation we have started an imaging project.¹⁾ The raster image was shown in Fig. 2 as examples, where the clear see-through images of two coins and a razor blade are shown. This can be improved further by exploring faster detector and making more intense sources. We intend to develop this equipment for medical and biological use in near future.

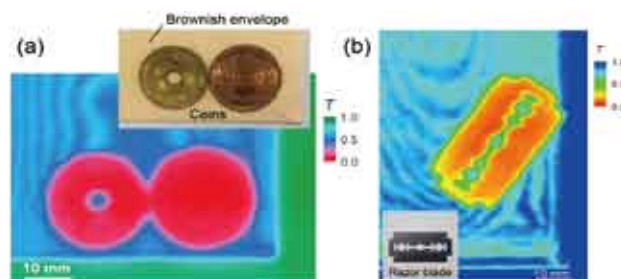


Fig. 2. Two kinds of different see-through images: (a) two Japanese coins, 5 yen with a hole (the diameter is exactly 5 mm) and 10 yen. (b) an image of shaving razor blade inserted in the brown envelope. In both cases fringes are observed due to interference of monochromatic THz the wave from front and back side of the envelope paper.

(2) Single crystal growth of topological insulators.

We have succeeded in growing high quality single crystals of topological insulators $\text{Bi}_2\text{Se}_3\text{:Cu}$ and $\text{Bi}_{1.5}\text{Sb}_{0.5}\text{Te}_{1.8}\text{Se}_{1.2}$ as shown in Fig. 3. We have made fundamental study of these single crystals not only such as electrical resistivity, Hall effect, magnetoresistance, but also STM, ARPES etc. The ARPES data showed a beautiful Dirac cone-like dispersion relation for the surface state and a semiconducting gap behavior for the bulk state.³⁾ The Cu doped Bi_2Se_3 exhibits superconductivity below 3.6 K, where we observed an anomalous magnetization behavior, suggesting a non-trivial exotic superconducting state.⁴⁾



Fig. 3. Large single crystals of $\text{Bi}_{1.5}\text{Sb}_{0.5}\text{Te}_{1.8}\text{Se}_{1.2}$ topological insulator.

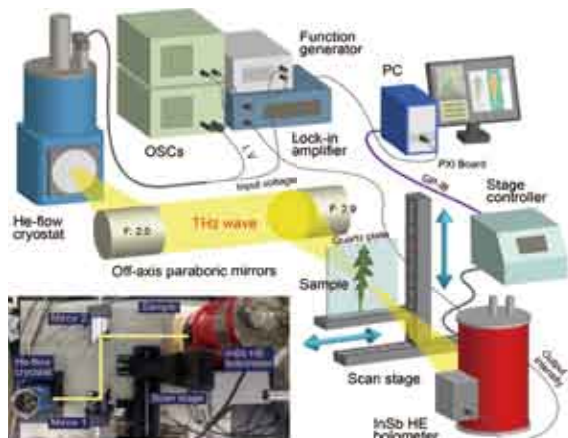


Fig. 1. A stereographic picture of the prototype THz imaging setup developed by us.

References

- 1) M. Tsujimoto et al., submitted.
- 2) M. Tsujimoto et al., *Phys. Rev. Lett.* **105**, 037005 (2010).
- 3) Y. Tanaka et al., submitted.
- 4) P. Das et al., *Phys. Rev. B* **83**, 220513(R) (2011).

Self-Powered Nanosensors for Environment Monitoring

MANA Principal Investigator **Zhong Lin WANG**

(Satellite at Georgia Tech, USA)
Research Scientist
Graduate Student

Youfan Hu
Minbaek Lee, Chen Xu



1. Outline of Research

A nanosystem is an integration of multi-functional nanodevices. The power required to drive such electronics is in the range of microwatt to milliwatt range, which can be harvested from our living environment. Once it reaches an output of milliwatt, it is possible to have self-powered, maintain-free biosensors, environmental sensor, nanorobotics, micro electromechanical system, and even portable/wearable electronics. Taking a nanorobot as an example, it can sense, take action, send signal and receive feed back if it has sufficient power. It is well known that man made electronics are driven by electricity. We must develop innovative technologies for converting other forms of energy into electricity so that it can be used for our purposes.

The working mode of a wireless sensor can have an active mode but most importantly, a standby mode, during which the device is at “sleeping” with minimum energy consumption. The power generated by an energy harvester may not be sufficient to continuously drive the operation of a device, but an accumulation of charges generated over a period of time is sufficient to drive the device for a few seconds. This could be of practical use for devices that have standby and active modes, such as glucose and blood pressure sensors, or even personal electronics such as blue tooth transmitters (driving power ~ 5 mW; data transmission rate ~ 500 kbits/s; power consumption 10 nW/bit), which are only required to be in active mode periodically. The energy generated when the device is in standby mode is likely to be sufficient to drive the device when it is in active mode.

2. Research Activities

We have also fabricated a self-powered environmental sensor (Fig. 1a), which can detect Hg^{2+} ions and indicate their concentration via the emitting intensity of an LED. A single-walled CNT (SWNT) based FET and ZnO NW array served as a Hg^{2+} sensor and an energy harvesting part, respectively. Firstly, drain-source current of a sensor was monitored in various concentrations of Hg^{2+} ions in water droplet to characterize sensing process. Fig. 1b shows measured drain-source current and resistance of a sensor at different concentrations of Hg^{2+} ions in water droplet. Initially, least current ($< 10^{-8}$ A) was only observed as we chose a SWNT FET in *enhancement mode*. When the concentration of solution reached about ~ 10 nM, which is the allowable limit of Hg^{2+} ions in drinking water set by most government environmental protection agencies, a noticeable change of resistance was appeared. To demonstrate an automatic

detection of the local Hg concentration, a light emitting diode was attached on the circuit to serve as an indicator for Hg^{2+} detection. To accomplish self-powered sensing of environmental pollutants with NGs, a circuit was designed with two independent loops. In energy harvesting process, a circuit was connected in the loop ‘A’ (Fig. 1a) with NGs and rectifying diode bridge to store generated charges into the capacitor. After sufficient charging process, connection was changed to the loop ‘B’ in Fig. 1a, thus it was ready to detect Hg^{2+} ions and lit up an LED with a certain intensity depending on the concentration of pollutants in water droplet. Fig. 1c shows photograph images of an LED that was lit up under each concentration of Hg^{2+} ions in water droplet. As shown after the third image of Fig. 1c, noticeable LED light was noticed from the concentration of 10 nM and getting brighter gradually till 1 mM.

The self-powered system demonstrated here can have important applications in environmental monitoring, quarter quality control, oil/gas line inspection. By using the turbulence and pressure change in gas/water/oil pipe, electricity can be generated for driving temperature/flow-meter/velocity/pressure sensors. This can be a good technology for monitoring water quality in the residential area in a city, and even at large scale.

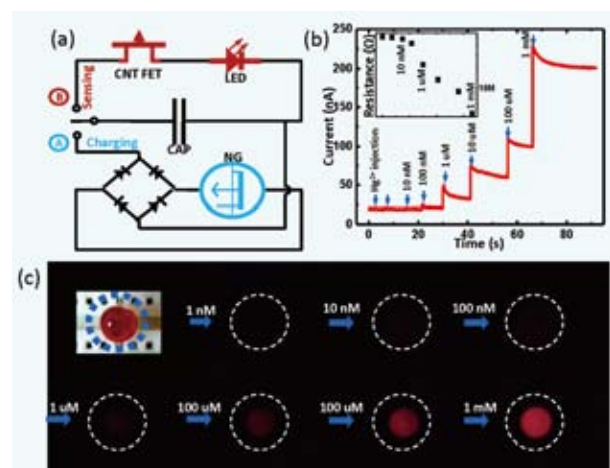


Fig. 1. Characteristics of self-powered Hg^{2+} sensor driven by nanogenerators. (a) Circuit diagram depicting our self-powered sensor composed of nanogenerator, rectifying bridge, capacitor, Hg^{2+} detector and light emitting diode with ‘A’ charging and ‘B’ sensing process selecting switch. (b) Sensing behavior of our fabricated sensor with various concentrations of Hg^{2+} ions in water solution. The inset shows the plot of resistance depending on mercury ion injection. (c) Optic images of a laser emitting diode representing intensity changes owing to resistance changes in the detector depending on the concentration of Hg^{2+} ions in water solution. All measurements were conducted with energy stored by nanogenerators.

Nano-System Architectonics

MANA Principal Investigator Masakazu AONO

(MANA Director-General, Field Coordinator)

MANA Scientist

MANA Research Associate

Yuji Okawa, Makoto Sakurai, Hideo Arakawa

Swapan K. Mandal, Marina Makarova, Kewei Liu, Qi Wang



1. Outline of Research

The goal of our Nano-System Construction Group is to create new nano-systems with novel functionality by the use of various key technologies of “materials nano-architectonics” and put the created nano-systems to practical use to contribute to our society in such forms as next-generation information processing and communication and environmental and energy sustainability. To achieve this interdisciplinary research, we make close collaboration with other research groups in MANA (Fig. 1). We are also making collaboration with MANA’s satellite labs headed by Prof. Jim Gimzewski (UCLA, USA), Prof. Mark Welland (Univ. of Cambridge, UK), and Prof. Christian Joachim (CEMES-CNRS, France).



Fig. 1. Collaboration of the Nano-System Construction Group with other groups in MANA.

2. Research Activities

Our research activities are classified into the following four subjects:

- 1) Novel nanochemistry: Controlled chain polymerization for the formation of electrically conductive polymer chains at designated positions and its application to wire single functional molecules with firm “chemical soldering” aiming at the realization of single-molecule electronics.¹⁻⁵⁾
- 2) Atomic switch: a) Practical application of the atomic switch to programmable ICs;⁶⁻⁸⁾ b) Utilization of the synaptic properties of the atomic switch to develop novel brain-like network circuits.⁹⁻¹¹⁾
- 3) Development and application of novel scanning-probe microscopes (SPMs): a) Novel SPMs for nanoscale magnetic imaging without using a magnetic probe. b) Multiple-probe SPMs for local nanoscale electrical conductivity measurements.¹²⁻¹³⁾
- 4) Development of novel sensors.¹⁴⁾

In what follows, only 1) and 4) will be discussed.

We have developed a method to create a single conductive linear polymer chain at designated positions by initiating chain polymerization of monomers using a scanning tunneling microscope (STM) tip.¹⁻³⁾ By using this method, we made two-terminal wiring for a single phthalocyanine molecule and succeeded in making such nanowiring through “chemical soldering (Fig. 2).^{4,5)}

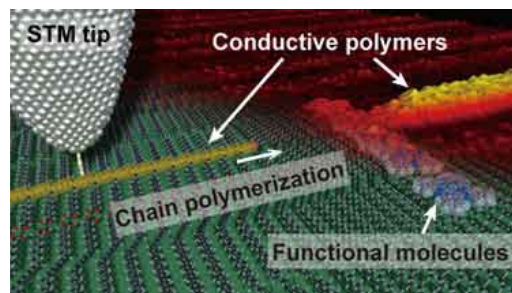


Fig. 2. Nanowiring and nanochemical soldering for a single functional molecule.

We have found novel reversible and nonvolatile metal-insulator transition for SnO₂ (non-piezoelectric). This will pave a way for a novel strain sensor (Fig. 3).¹⁴⁾

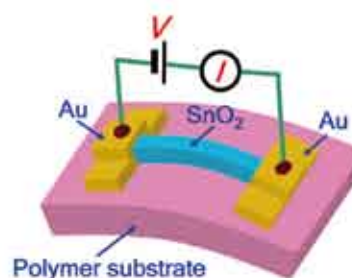


Fig. 3. Novel strain sensor using a SnO₂ rod.

References

- 1) Y. Okawa, M. Aono, *Nature* **409**, 683 (2001).
- 2) Y. Okawa, M. Aono, *J. Chem. Phys.* **115**, 2317 (2001).
- 3) D. Takajo, Y. Okawa, T. Hasegawa, M. Aono, *Langmuir* **23**, 5247 (2007).
- 4) Y. Okawa, S.K. Mandal, C. Hu, Y. Tateyama, S. Goedecker, S. Tsukamoto, T. Hasegawa, J.K. Gimzewski, M. Aono, *J. Am. Chem. Soc.* **133**, 8227 (2011).
- 5) S.K. Mandal, Y. Okawa, T. Hasegawa, M. Aono, *ACS Nano* **5**, 2779 (2011).
- 6) K. Terabe, T. Hasegawa, T. Nakayama, M. Aono, *Nature* **433**, 47 (2005).
- 7) T. Sakamoto, H. Sunamura, H. Kawaura, T. Hasegawa, M. Aono, *Appl. Phys. Lett.* **82**, 3032 (2003).
- 8) T. Tsuruoka, K. Terabe, T. Hasegawa, M. Aono, *Nanotechnol.* **21**, 425205 (2010).
- 9) T. Hasegawa, T. Ohno, K. Terabe, T. Tsuruoka, T. Nakayama, J.K. Gimzewski, M. Aono, *Adv. Mater.* **22**, 1831 (2010).
- 10) T. Ohno, T. Hasegawa, T. Tsuruoka, K. Terabe, J.K. Gimzewski, M. Aono, *Nature Mater.* **10**, 591 (2011).
- 11) T. Hasegawa, Y. Ito, H. Tanaka, T. Hino, T. Tsuruoka, K. Terabe, H. Miyazaki, K. Tsukagoshi, T. Ogawa, S. Yamaguchi, M. Aono, *Appl. Phys. Exp.* **4**, 015204 (2011).
- 12) S. Higuchi, O. Kubo, H. Kuramochi, M. Aono, T. Nakayama, *Nanotechnol.* **22**, 285205 (2011).
- 13) S. Higuchi, H. Kuramochi, O. Laurent, T. Komatsubara, S. Machida, M. Aono, K. Obori, T. Nakayama, *Rev. Sci. Instrum.* **81**, 073706 (2010).
- 14) K. Liu, M. Sakurai, M. Aono, submitted.

MANA Brain: Neuromorphic Atomic Switch Networks

MANA Principal Investigator

(Satellite at UCLA, USA)

MANA Scientific Advisor

Post-doc

Graduate Student

James K. GIMZEWSKI

Adam Z. Stieg

Greg Pawin, Cristina Martin-Olmos

Audrius Avizienis, Henry Sillin



1. Outline of Research

The structure and activity of the brain is intrinsically complex, comprised of billions of neurons interacting recurrently through trillions of synaptic interfaces. Biological neural networks utilize self-configuring, hardware-based architectures capable of dynamic topological alteration and function without the need for pre-programming or an underlying software algorithm. These intrinsically nonlinear, complex systems demonstrate extraordinarily efficient transmission of information and emergent behaviors commonly associated with intelligence such as associative memory, learning, and predictive capacity in non-deterministic environments.

The realization of hardware-based neuromorphic networks requires the ability to fabricate highly interconnected, complex wiring architectures with integrated circuit elements whose nonlinear properties emulate those of biological neurons and synapses. We have set out to develop a neuromorphic device based on a complex, hierarchical network that employs dynamic local rewiring and Hebbian type activity-dependent interfaces fabricated through self-assembly. This multi-scale approach involved the combination of self-assembled nanoscale architectures, solid-state electroelectronics, and electrochemistry.

2. Research Activities

In 2011, we successfully produced functional devices consisting of highly interconnected ($\sim 10^9/\text{cm}^2$) atomic switch synapses embedded in a self-assembled complex network of silver nanowires as seen in Fig. 1.

We have shown this device architecture to self-organize into a persistent critical state clearly characterized by multiple, temporally metastable states requiring no fine-

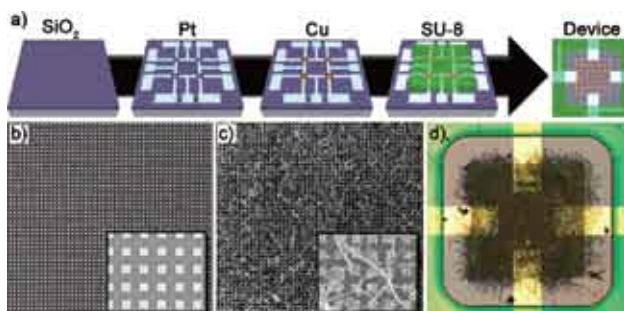


Fig 1. Fabrication scheme for CASA networks. (a) Schematic of substrate/device microfabrication through various lithographic techniques. (b) Cu seed posts ($1 \mu\text{m}^2$, $1 \mu\text{m}$ pitch, 300 nm height) deposited onto the substrate by electron beam lithography react with AgNO_3 within a reaction well formed from SU-8 epoxy photoresist, (c) resulting in electroless deposition of complex Ag nanowire networks. (d) The network extends throughout the device well and is electrically probed via macroscopic Pt electrodes.

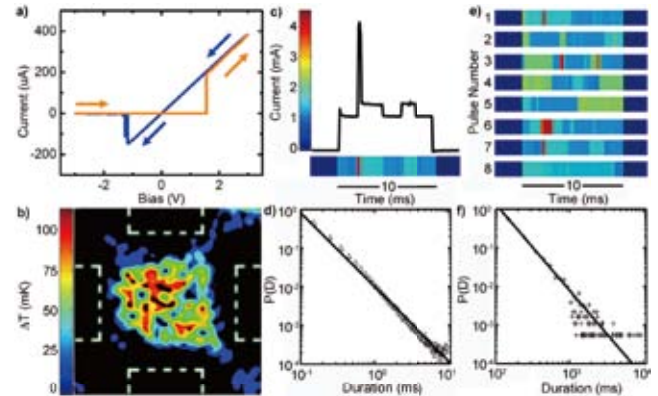


Fig. 2. Electrical characteristics of complex nanoelectronic networks. (a) Experimental I-V curve demonstrating pinched hysteresis; $R_{\text{on}}=8 \text{ K}\Omega$, $R_{\text{off}}>10 \text{ M}\Omega$. (b) Ultrasensitive IR image of a distributed device conductance under external bias at 300K . (c, e) Representative network current response to a 2V pulse showing switching between discrete, metastable conductance states. (d, f) Temporal correlation of metastable states observed during pulsed stimulation demonstrated power law scaling for probability, $P(D)$, of duration. Power law scaling existed for residence time both (d) within a single 10 ms pulse and (f) over 2.5 s during extended periods of pulsed stimulation.

tuning. To our knowledge, this network represents a unique implementation of a purpose-built self-assembled network composed of coupled non-linear elements that clearly demonstrates the essential characteristics of SOC, specifically power-law scaling of: $1/f$ fluctuations, energetic avalanches, as well as temporal metastability shown in Fig. 2.

The emergent complex behaviors observed indicate a capacity for memory and learning via persistent critical states with potential utility for the creation of physically intelligent machines.

Recent Publications with MANA recognition:

- 1) T. Hasegawa, A. Nayak, T. Ohno, K. Terabe, T. Tsuruoka, J.K. Gimzewski, M. Aono, *Appl. Phys. A* **102**, 811 (2011).
- 2) T. Ohno, T. Hasegawa, T. Tsuruoka, K. Terabe, J.K. Gimzewski, M. Aono, *Nature Mater.* **10**, 591 (2011).
- 3) Y. Okawa, S.K. Mandal, C. Hu, Y. Tateyama, S. Goedecker, S. Tsukamoto, T. Hasegawa, J.K. Gimzewski, M. Aono, *J. Am. Chem. Soc.* **133**, 8227 (2011).
- 4) H.I. Rasool, E.B. Song, M.J. Allen, J.K. Wassei, R.B. Kaner, K.L. Wang, B.H. Weiller, J.K. Gimzewski, *Nano Lett.* **11**, 251 (2011).
- 5) H.I. Rasool, E.B. Song, M. Mecklenburg, B.C. Regan, K.L. Wang, B.H. Weiller, J.K. Gimzewski, *J. Am. Chem. Soc.* **133**, 12536 (2011).
- 6) S. Sharma, B.M. Gillespie, V. Palanisamy, J.K. Gimzewski, *Langmuir* **27**, 14394 (2011).
- 7) S. Sharma, E.E. Grintsevich, M.L. Phillips, E. Reisler, J.K. Gimzewski, *Nano Lett.* **11**, 825 (2011).
- 8) A.Z. Stieg, A.V. Avizienis, H.O. Sillin, C. Martin-Olmos, M. Aono, J.K. Gimzewski, *Adv. Mater.* **24**, 286 (2012).
- 9) R. Tanoue, R. Higuchi, N. Enoki, Y. Miyasato, S. Uemura, N. Kimizuka, A.Z. Stieg, J.K. Gimzewski, M. Kunitake, *ACS Nano* **5**, 3923 (2011).

Atomic Electronics for Future Computing

MANA Principal Investigator

MANA Scientist
MANA Research Associate

Tsuyoshi HASEGAWA

Kazuya Terabe, Tohru Tsuruoka
Alpana Nayak, Takami Hino, Soumya R. Mohapatra



1. Outline of Research

We aim to explore new nanosystems showing novel functions based on atomic electronics. The new nanosystems are expected to realize new computing systems such as by achieving fault tolerant logic circuits, nonvolatile logic circuits, optical and chemical sensors, and so on. Since the present-day semiconductor systems based on CMOS devices is approaching to their maximum performance due to the ultimate downsizing, new types of logic systems using beyond-CMOS devices should be developed for further progress in information technology.

In this study, we will use the atomic electronic device, which has been developed by ourselves, for making new nanosystems. The atomic electronic device, such as atomic switch, is operated by controlling movements of cations and/or atoms in a nano-scale using nanoionics phenomena. The atomic electronic device has a possibility for configuring new computing systems, such as beyond von-Neumann computers. For instance, the atomic electronic device is non-volatile, which enables simultaneous logical operation and memorization by a single device. The characteristic could enable for configuring conceptually new logic systems, which changes by itself according to the logical operation. We believe that neural computing systems are ultimate style of the non-volatile logic systems, such as neural computing.

In order to accomplish the purpose, we will conduct 1) basic research on nanoionic phenomena, 2) developing new atomic electronics devices showing the novel functions based on the basic research, 3) developing nanofabrication technique for making the atomic electronics devices, 4) demonstration of novel operation of the atomic electronics devices and basic circuits using them.

2. Research Activities

(1) Synaptic Operations achieved by Atomic Switch.^{1,2)}

Memory is believed to occur in the human brain as a result of two types of synaptic plasticity: short-term plasticity (STP) and long-term potentiation (LTP). STP is achieved through the temporal enhancement of a synaptic connection, which then quickly decays to its initial state. However, repeated stimulation causes a permanent change in the connection to achieve LTP; shorter repetition intervals enable efficient LTP formation from fewer stimuli. Development of artificial (inorganic) synapse that emulates the STP and LTP behaviours is the key-issue in the realization of the Brain-type computer, which we have achieved using Ag_2S -based gap-type atomic switch, as shown in Fig. 1a. Namely, pulse input with a lower repetition rate only caused the temporal increase in conductance (Fig. 1b), corresponding to the STP-mode. Conversely, pulse input with

a higher repetition rate achieved a persistent transition to the higher conductance state (Fig. 1c), corresponding to the LTP mode.

The synaptic behaviours are useful for developing artificial neural networking systems made of all solid-state devices, which do not require any pre-programming.

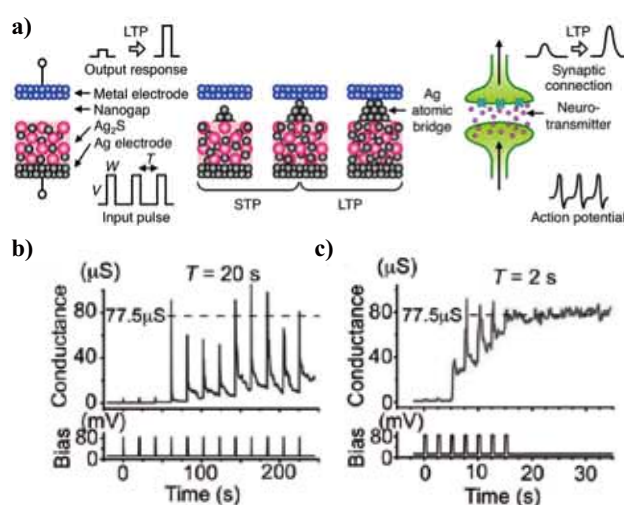


Fig. 1. Schematic of an inorganic synapse made of Ag_2S atomic switch and a biological synapse (a). Changes in the conductance of the Ag_2S gap-type atomic switch corresponding to LTP (b) and STP (c).

(2) Switching mechanism of Gapless Atomic Switch.^{3,4)}

We have revealed the switching mechanism of $\text{Cu}/\text{Ta}_2\text{O}_5/\text{Pt}$ gapless atomic switch by measuring I/V s in a wide ambient temperature range from 88 to 573 K. The SET voltage is primarily determined by supersaturation in the vicinity of the Pt electrode, which is controlled by the application of positive bias. The supersaturation required for spontaneous growth of a Cu nucleus decreases with increasing temperature, resulting in lower SET voltages at higher temperatures. The RESET voltage is determined by the thermal stability of the metal filament formed. We also found that residual water acts an important roll in the switching operation, such as in the oxidation of Cu atoms and their diffusion in the Ta_2O_5 layer. These findings are useful for developing new functions of atomic switches.

References

- 1) T. Ohno, T. Hasegawa, T. Tsuruoka, K. Terabe, J. K. Gimzewski, M. Aono, *Nature Mater.* **10**, 591 (2011).
- 2) T. Ohno, T. Hasegawa, A. Nayak, T. Tsuruoka, J. K. Gimzewski, M. Aono, *Appl. Phys. Lett.* **99**, 203108 (2011).
- 3) T. Tsuruoka, K. Terabe, T. Hasegawa, M. Aono, *Nanotechnol.* **22**, 254013 (2011).
- 4) T. Tsuruoka, K. Terabe, T. Hasegawa, I. Valov, R. Waser, M. Aono, *Adv. Funct. Mater.* **22**, 70 (2012).

Manipulating Quantum Entanglement of Electron System

MANA Principal Investigator

MANA Scientist
MANA Research Associate
Graduate Student

Xiao HU

Masanori Kohno
Zhi Wang, Qi-Feng Liang, Sasmita Mohakud
Yuki Takahashi, Feng Liu, Zhao Huang, Long-Hua Wu



1. Outline of Research

A composite system is in a quantum entangled state when its wave function cannot be given simply by the cross product of those for subsystems. This superposition of wave functions is the essence of quantum systems, without classical counterpart. Entanglement of two polarized laser beams can be kept even they are separated far away. While the laser beams can serve a perfect medium for quantum teleportation, nonlocal entangled electrons are important for many applications, such as quantum recording and quantum computation, where compactness and quick response have high priority. To generate and manipulate nonlocal quantum entanglement of electrons, or quasiparticles in correlated electron systems is therefore one of the frontiers of modern physics.

Spin singlet of two electrons is the most fundamental entanglement state. We focus on the superconductivity since it is nothing but a condensate of quantum entangled electron pairs, namely the Cooper pairs. In order to extract a Cooper pair from the superconductor and move the two electrons separately, we add two leads to the tip of superconductor as shown in the left part of Fig. 1. Since a Cooper pair tends to pass through one of the two paths (co-tunneling), we build a quantum dot on each path, which works as a gate making use of the Coulomb repulsion, and thus a pair of electrons gain certain probability to pass different routes (split tunneling).

If the two electrons lose their spin entanglement when they travel through different paths, a finite resistance occurs when they arrive at the other superconductor electrode. On the other hand, if the spin entanglement is kept all the way and the two electrons recombine at the destination, a current without dissipation, known as Josephson current, is carried by this pair of electrons.

In experiments so far, normal resistances were measured and resistance-resistance correlation between the two branches was detected. While a positive correlation suggests that some Cooper pairs are split into the two branches, it is difficult to make sure whether the electrons keep the quantum entanglement after splitting.

2. Research Activities

(1) Detecting the nonlocal entangled electrons.¹⁾

We propose to measure Josephson current which is purely contributed from entangled electron pairs, either co-tunneling or split-tunneling. In order to figure out how much split Cooper pairs contribute to the total Josephson current, one detects the oscillation of maximal Josephson current with response to the magnetic flux applied through the area enclosed by the two paths. When the contribution from split Cooper pairs equals to that from co-tunneling ones, the oscillation period is $2\Phi_0$, whereas it should be Φ_0

without split tunneling (right of Fig. 1). This measurement gives an unambiguous evidence for the nonlocal quantum entanglement of electrons.

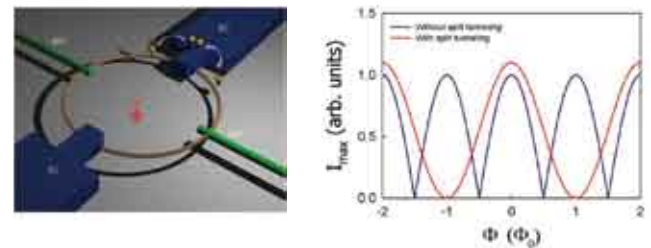


Fig. 1. Left: Schematic setup of the Cooper-pair splitter; Right: Oscillations of the maximal Josephson current in response to the magnetic flux with large (red) and without (blue) contribution from split Cooper pairs.

(2) Nature of high-energy magnetic excitations in quasi-one-dimensional magnets under magnetic field.²⁾

High-energy magnetic excitations are usually caused by magnetic long-range order in a magnet having Ising-like anisotropy or spin-singlet dimer long-range order in a quantum spin system. These high-energy states can be understood as anti-bonding states created from the ordered ground state with multi-site unit cells. However, in quasi-one-dimensional antiferromagnets under magnetic field, high-energy magnetic excitations appear even without magnetic or dimer long-range order. It is found that the high-energy magnetic excitations can be understood in the context of the Mott physics (Fig. 2). Namely, they are attributed to repulsive interactions between down spins. Thus, the Mott physics is relevant not only for strongly correlated electron systems but also for strongly correlated quantum spin systems where excitations are governed by strong quantum fluctuations.

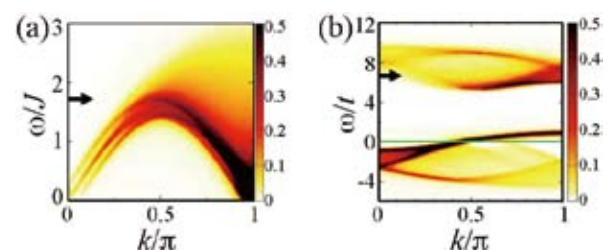


Fig. 2. (a) Dynamical structure factor $S(k, \omega)$ of a spin-1/2 Heisenberg chain in a magnetic field. (b) Single-particle spectral function $A(k, \omega)$ of a Hubbard chain near the Mott transition. Arrows indicate high-energy states which can be understood in the context of the Mott physics.

References

- 1) Z. Wang, X. Hu, *Phys. Rev. Lett.* **106**, 037002 (2011). Cover picture of the issue.
- 2) M. Kohno, *J. Phys: Conf. Ser.* **320**, 012021 (2011).

Surface Atomic Scale Logic Gate

MANA Principal Investigator
(Satellite at CNRS Toulouse, France)

Toulouse Scientist
MANA Research Associate
Graduate Student

Christian JOACHIM

Mohamed Hliwa
Maricarmen Grisolia, Demetra Piachos
Nicolas Renaud, Sabrina Munery



1. Outline of Research

Designing and constructing an atomic scale calculator requires the exploration of:

- The quantum design of a molecule (or atom surface circuit) able to perform alone the logical operations.
- The molecule synthesis (respectively atom by atom UHV-STM construction on a surface) of the molecule logic gate (respectively the atom surface circuit logic gate).
- The development of a surface multi-pad interconnection technology with a picometer precision respecting the atomic order of the surface nano-system assemblage.
- The improvement of specific quantum chemistry software like N-ESQC able to simulate the full logic gate nano-system functionalities with its interconnections and its supportive surface.

The CNRS Toulouse MANA satellite is working on 2 specific areas of this broad academic problem. We expect to understand the physics of surface interconnection of simple single molecule logic gate (or surface atomic circuit logic gate) using atomic wire, to certify logic gate design and pursue the exploration of the molecule logic gate complexity roadmap to embed the maximum possible computing power inside a single molecule or a single surface atomic scale circuit.

2. Research Activities

(1) Surface atomic scale logic gate.

Dangling bond surface atomic wires are constructed using atom by atom vertical manipulation on a semi-conducting surface. Two surfaces are studied by the Toulouse MANA satellite: MoS₂ and Si(100)H. For MoS₂, the STS of a single S extracted atom on the MoS₂ surface have been recorded in NIMS in collaboration with Toulouse in preparation to surface logic gate construction.¹⁾ For Si(100)H, all the 4 symmetric “2-input 1 output” AND, NOR, AND and NAND Boolean logic gates were quantum designed (Fig. 1) but not yet QHC designed.²⁾

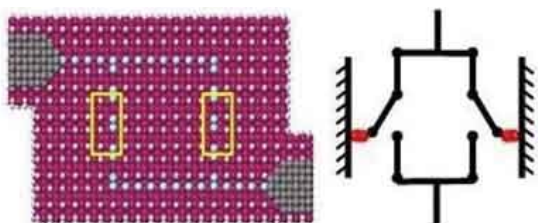


Fig. 1. Design and N-ESQC calculation of a quantum OR dangling bond Boolean logic circuit with its classical equivalent constructed on a Si(100)H 2x1 surface.

(2) Classical molecular devices.

Following the STM surface polymerization of PDA on a MoS₂ surface discovered in NIMS and the interconnection of a Zn Phtahalocyanine molecule to 2 of those PDA wires, we have used the ESQC technique to calculate the non linear I-V characteristics of this molecular junction.

(3) QHC molecule logic gates.

Following the demonstration of a QHC NOR gate with a single starphene molecule,³⁾ a very robust QHC NOR gate is now designed and synthesized with a long version of the previous molecule (Fig. 2). LT-NC-AFM and LT-UHV-STM images have been obtained⁴⁾ and compared to ESQC calculated images (Fig. 2).

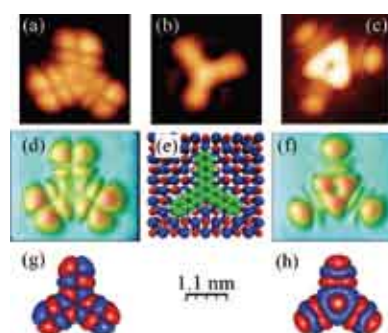


Fig. 2. Constant-current STM images of the NOR molecule adsorbed on NaCl/Cu(111). Imaging conditions: (a) $I_t = 2$ pA, $V_t = -2.7$ V, (b) $I_t = 3$ pA, $V_t = 1.1$ V, (c) $I_t = 3$ pA, $V_t = 1.6$ V. (d) and (e) ESQC images from the model shown in (e). (g) and (h): HOMO and LUMO of the free molecule calculated for an electron density of 10^{-5} \AA^{-3} .

The QHC theory of logic gate design was developed up to the point where our quantum symbolic analysis of a QHC gate design⁵⁾ can be used to pass from a formal valence bond model to a logic gate conjugated molecule.⁶⁾ Using this new symbolic approach, a QHC OR gate (Fig. 3) was designed for single manipulated Au atoms to contact the molecule one at a time performing like a single classical digital input. The classical to quantum conversion of those inputs occurs inside the molecule.

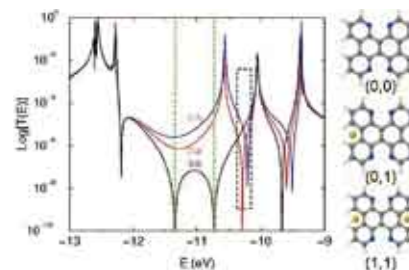


Fig. 3. A QHC OR gate molecule with Au metal atom inputs designed using our new Quantum symbolic analysis. The I(V) characteristics is obtained from this T(E) using the generalized Landauer Formula.

References

- 1) N. Kodoma et al., submitted.
- 2) H. Kawai et al., submitted.
- 3) W.H. Soe et al., *Phys. Rev. B* **83**, 155443 (2011).
- 4) O. Guillermet et al., *Chem. Phys. Lett.* **511**, 482 (2011).
- 5) N. Renaud, C. Joachim, *J. Phys. A* **44**, 155302 (2011).
- 6) N. Renaud et al., *Phys. Chem. Chem. Phys.* **13**, 14404 (2011).

Integration of Nano Functionality for Novel Nanosystems

MANA Principal Investigator

MANA Scientist

MANA Research Associate
Visiting Scientist

Senior Visiting Scientist
Graduate Student (Univ. of Tsukuba)

Tomonobu NAKAYAMA

Takashi Uchihashi, Yoshitaka Shingaya,
Osamu Kubo, Katsumi Nagaoka
Puneet Mishra, Jianxun Xu
Seiji Higuchi, Shinichi Machida, Masato Nakaya,
Shin Yaginuma
Makoto Sawamura, Masami Suganuma
Toshiyuki Kakudate, Amir Pakdel



1. Outline of Research

We develop novel techniques and methodologies toward the realization of novel nanosystems for future information technology. Development and application of multiprobe scanning probe microscopes (MSPM), manipulation of individual atoms and molecules, fabrication of low-dimensional nanostructures and measurements of signal transfer through living cell systems, are explored for a common purpose; creation and characterization of elemental nanostructures and functional nanosystems which transmit and transduce electrical, optical, mechanical, ionic and magnetic signals.

MSPM has simultaneously and independently controlled 2 to 4 scanning probes¹⁻³⁾ which are brought into electrical contact to a single nanostructure and reveal its electrical property.⁴⁾ We have implemented atomic force microscope functions in our MSPM and realized measurements of electrical properties of conductive nanostructures on insulating substrates.^{5,6)}

Fabrication of nanostructures by means of self-organization, atom/molecule manipulation and dynamic shadow mask deposition in addition to the conventional deposition techniques is pursued because such methodologies are keys to realize functional nanosystems.

A nerve cell and a network of the cells are nanosystems of interest because of their sophisticated hierarchical materials systems ultimately devising a human brain. We believe that understanding such “nanosystems in nature” changes the present computing technology. Investigation of signal transmission and transduction through single and conjugated living cells (see Fig. 1) are promoted in collaboration with Nano-Bio Field in MANA.

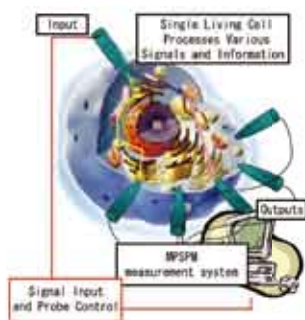


Fig. 1. Schematic illustration of a “cell odyssey” using the MSPM which works in liquid environment.

2. Research Activities

(1) Multiprobe Atomic Force Microscope.⁵⁻⁶⁾

Four metal probes were simultaneously operated in frequency modulation mode using new-type of tuning fork sensors,⁵⁾ which enable us to measure physical properties of conductive nanostructures on insulating substrates. Electrical properties of nanostructured graphenes on SiO₂ substrates were directly measured using our quadruple-probe atomic force microscope (QPAFM),⁶⁾ showing anisotropic

resistivity of the graphene structure grown on a stepped SiC surface (in collaboration with Prof. Tanaka at Kyusyu Univ. and Dr. Tsukagoshi at MANA).

(2) Carbon nanosystems and their functions.⁷⁻¹¹⁾

We have demonstrated that data storage with a bit density of 190 Tbits/in² can be achieved controlling bound and unbound states of fullerene C₆₀ molecules using STM-induced chemical reaction.⁷⁻⁸⁾ Further increase of information density became possible by controlling the degree of polymerization to form dimer, trimer, tetramer and so on, namely by controlling multiple bound states.⁹⁾

Carbon nanohorns (CNHs) aggregates were found to show reversible and irreversible change in conductivity against mechanical deformation, as confirmed by repeatedly pressing and releasing single CNHs aggregates with a conductive AFM probe.¹⁰⁾ Such mechanoelectrical property appears because a CNHs aggregate has multilayered architecture comprising of outer nanohorns part and graphitic inner core part.¹¹⁾

(3) Macroscopic supercurrent flowing through an In-induced surface reconstruction on Si(111).¹²⁾

Superconducting current through an atomically thin superconducting system, that is, a Si(111) $\sqrt{7}\times\sqrt{3}$ -In reconstructed structure, was found to flow over millimeter distance (Fig. 2). Surprisingly, the surface steps involved in a measured area did not disturb transport of Cooper pairs at all. Systematic measurements of critical current and further analysis strongly suggested that the surface atomic step worked as a Josephson junction.¹²⁾

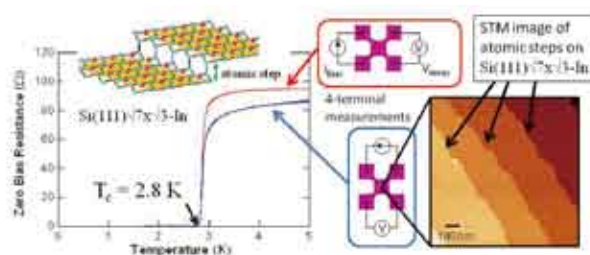


Fig. 2. Macroscopic supercurrent flows through the Si(111) $\sqrt{7}\times\sqrt{3}$ -In reconstructed surface as confirmed by four-terminal electrical measurements in UHV at low temperatures. There are many surface steps involved in the measured area of over millimeter scale.

References

- 1) M. Aono et al., *Oyoh Butsuri* **67**, 1361 (1998).
- 2) T. Nakayama et al., *SICE J. Control, Measurement, and System Integr.* **38**, 742 (1999).
- 3) S. Higuchi et al., *Rev. Sci. Instrum.* **81**, 073706 (2010).
- 4) O. Kubo et al., *Appl. Phys. Lett.* **88**, 254101 (2006).
- 5) S. Higuchi et al., *Nanotechn.* **22**, 285205 (2011).
- 6) S. Higuchi et al., *Rev. Sci. Instrum.* **82**, 043701 (2011).
- 7) M. Nakaya et al., *Adv. Mater.* **22**, 1622 (2010).
- 8) M. Nakaya et al., *Small* **4**, 538 (2008).
- 9) M. Nakaya et al., *ACS Nano* **5**, 7830 (2011).
- 10) J. Xu et al., *Small* **7**, 1169 (2011).
- 11) J. Xu et al., *Carbon* **49**, 2074 (2011).
- 12) T. Uchihashi et al., *Phys. Rev. Lett.* **107**, 207001 (2011).

Mesoscopic Superconductivity and Quantum Information Physics

MANA Principal Investigator
(Satellite at Tokyo Univ. Sci., Japan)
MANA Research Associate
Guest Researcher
Graduate Student

Hideaki TAKAYANAGI

S. Kim, K. Tsumura
R. Inoue, R. Ishiguro
M. Kamio, T. Hayashi, K. Muranaga, M. Yakabe,
K. Yokobatake



1. Outline of Research

Our research topic is so-called mesoscopic superconductivity which aims to explore new quantum phenomena in different kind of superconducting devices and to apply them to quantum information physics.

We are now developing an ultimate SQUID (Superconducting Quantum Interference Device), i.e., a nano-SQUID which can detect single or several spins. We will also clarify the quantum interaction between a nano-SQUID with embedded quantum dots and spins in dots. This leads to the implementation of an entangled state between a superconducting qubit and spin qubit. The combination of these qubits is a promising candidate for a quantum interface that will be indispensable in the future quantum information network.

We are also working on superconductor-based Light Emitting Diode. Superconductor-based LED is expected to be the key device in quantum information technology because of its promising giant oscillator strength due to the large coherence volume of the superconducting pairs together with the possibility of the *on-demand* generation of entangled photon pairs.

Our other research targets are (i) graphene SQUID and (ii) spin injection effect into superconductor.

2. Research Activities

(1) Spin Polarized Current Injection and Detection on p-InMnAs/n-InAs/Nb Junctions.

We study the transport properties of p-InMnAs/n-InAs/Nb junctions, where a p-InMnAs can be regarded as a spin injector (Fig. 1). We fabricate the junctions with different distance between InMnAs and Nb electrodes. These junctions

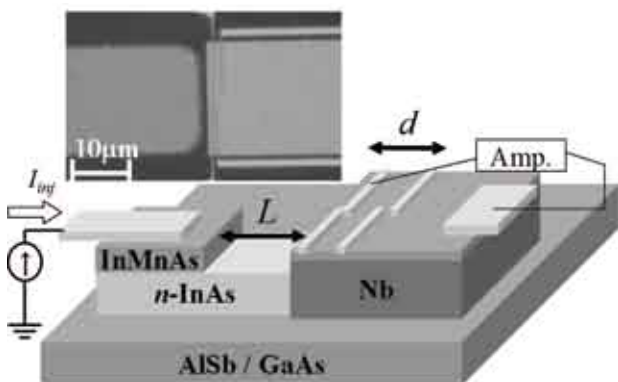


Fig. 1. Schematic diagrams of p-InMnAs/n-InAs/Nb junction. The distance (L) between InMnAs and Nb is designed to be 1.0, 5.0 and 10.0 μm and the probe electrodes is laid on Nb at the distance d between probe electrodes and InAs/Nb interface to be 0.1, 0.5, 1.0 and 2.0 μm . The inset shows a micrograph of the device around InAs channel.

have the probe electrodes on Nb at different position away from the InAs/Nb interface. We measure the differential conductance of the Nb with spin-polarized carrier injected from InMnAs in order to investigate the spin injection effect on the superconductivity of Nb. The conductance minima appear at zero-bias voltage. The suppression of conductance minima due to spin-polarized carrier injection can be explained by the inverse proximity effect that the exchange field is induced in superconductor. We successfully obtained the spin-decay length in InAs and the spin penetration length in Nb from the distance dependence from a spin injector of the conductance behaviors. The obtained length in InAs and Nb are $1.95 \pm 1.5 \mu\text{m}$ and $550 \pm 50 \text{ nm}$, respectively. These results indicate that a superconductor has the potentiality to apply to a novel spin detector.

(2) Graphene SQUID.

We develop a graphene-based superconducting quantum interference device (SQUID) which consists of two superconductor/single layer graphene/superconductor (SGS) junctions connected in parallel on a SQUID based superconducting loop made of aluminum (Fig. 2). Transport properties of the device are studied at $T=35 \text{ mK}$ using four-lead technique. Differential resistance-bias voltage characteristic shows subharmonic energy gap structure due to multiple Andreev reflection. We observe supercurrent flowing through the device and the mean switching current can be modulated periodically with the applied magnetic fields. The observed period coincides very well with the estimated one from the device geometry, which proves that our device works as a SQUID based on graphene.

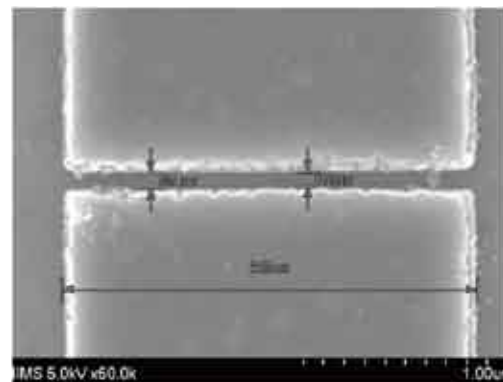


Fig. 2. A SEM photograph of the sample. The sizes of the junction is $W \sim 2.03 \mu\text{m}$ and $L \sim 70 \text{ nm}$.

Gate-Induced In-Plane p-i-n Tunnel Junction in Bilayer Graphene

MANA Principal Investigator
MANA Scientist
Post-doc

Kazuhito TSUKAGOSHI
Takeo Minari
Hisao Miyazaki, Songlin Li, Haisheng Song



1. Outline of Research

Control of the energy-band profile in semiconductors is one of the basic features of semiconductor electronics. When dopant atoms are introduced into the semiconductor bulk, conduction charge carriers are generated. Depending on the energy level of the dopant atoms in the host semiconductor, the carrier polarity can be tuned for either p-type or n-type conduction. When a p-type and an n-type semiconductor are coupled, a p-n junction is built in the host semiconductor. The energy-band profile varies at the junction such that the Fermi levels of the p-type and the n-type regions align. Unlike conventional p-n control in normal semiconductors, the ambipolar nature of graphene enables a control of the carrier polarity in an atomic film by modulation of the gate electric field without impurity doping. A p-n junction can be formed by spatially modulating the electric field. One of the important advantages of such a p-n junction is that both the carrier density in each homogeneous (p-type or n-type) region and the potential profile are gate-tunable. The physical mechanism determining the

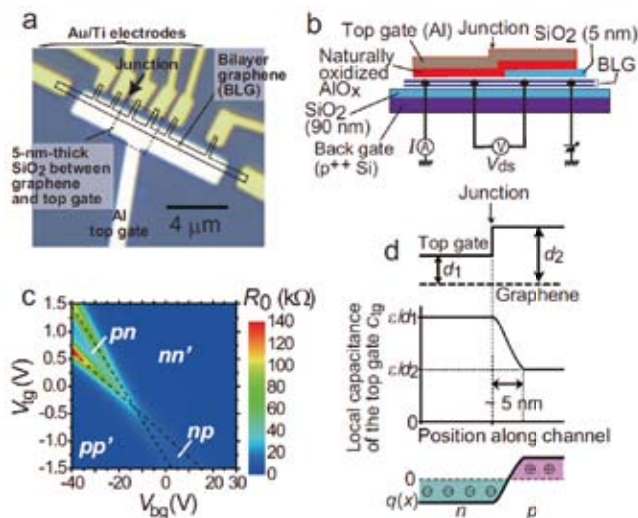


Fig. 1. (a) An optical micrograph of a bilayer graphene p-n junction with a stepwise top gate. The solid lines show the shape of the graphene channel made by oxygen plasma etching. The dashed lines show the area in which the graphene is covered by a 5-nm-thick SiO₂ layer. (b) A schematic illustration of the cross-sectional view of the p-n junction. The locally inserted SiO₂ layer creates the stepwise structure in the top gate. The instrumental configuration for a four terminal measurement is also shown. All transport properties shown in this paper were acquired in the configuration. (c) A color map of the linear resistance, R_0 , as a function of V_{bg} and V_{tg} at $T = 80$ K. The dashed lines show the ridges of the CNPs separating the p and n regions. (d) A schematic view of the geometrical structure of the stepwise top gate (top), the profile of the top gate capacitance (middle), and the charge distribution (bottom). A model for determining the top gate capacitance profile is illustrated in the supporting information.

potential profile differs from that of an ordinary p-n junction. In an ordinary p-n junction, the dopant ions determine the potential profile such that the Fermi energies in the p-type and n-type regions align. As a result, the two regions are connected through a depletion region. In contrast, the potential profile in a graphene p-n junction can be controlled by the external gate electric field. This feature allows for flexibility in designing the potential profile in the graphene pn junction because the profile can be designed in the geometry of the gate electrodes.^{1,2)}

2. Research Activities

In our experiment, we have developed the transport properties across a p-i-n junction in a semiconducting bilayer of graphene (Fig. 1). A spatial in-plane charge modulation using a top gate with a stepwise structure was fabricated, in which the thickness of the gate dielectric layer changes by a step at the middle of the channel. The nonlinear current observed with differential resistance indicates that the p region and the n region in the bilayer graphene can be connected through the tunneling barrier induced by the gate electric field (Fig. 2). Further analysis of the nonlinear current trends with temperature consistently suggests tunneling transport between the singularity peaks in a disordered density of states in the semiconductor graphene.

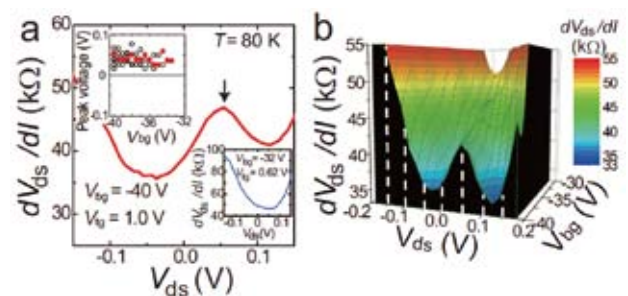


Fig. 2. (a) The differential resistance, dV_{ds}/dI , as a function of the source-drain voltage V_{ds} for bilayer graphene under a relatively large electric field ($V_{bg} = -40$ V). The arrow indicates the dV_{ds}/dI peak. The bottom-right inset shows the corresponding data for a relatively small electric field ($V_{bg} = -32$ V). The top-left inset shows a distribution of the V_{ds} values for the dV_{ds}/dI peaks as a function of V_{bg} with various values of V_{tg} . The red closed symbols correspond to the data shown in (b). (b) dV_{ds}/dI as a function of V_{ds} and V_{bg} . The V_{tg} value is selected along the middle point of two ridges of CNPs in Fig. 1c. All data were acquired at $T = 80$ K.

References

- 1) H. Miyazaki, S.L. Li, H. Hiura, K. Tsukagoshi, A. Kanda, *J. Phys. Soc. Jpn.*, in press.
- 2) S.L. Li, H. Miyazaki, M.V. Lee, C. Liu, A. Kanda, K. Tsukagoshi, *Small* **7**, 1552 (2011).

Bio-Inspired Materials for Sustainable Energy

MANA Principal Investigator
(Satellite at Univ. Cambridge, UK)

Research Co-Director
MANA Research Student

Mark WELLAND

David Bowler
Rami Louca, Conn O'Rourke, Umberto Terranova



1. Outline of Research

Our ultimate aim is to combine biological inspiration with electronics to give high efficiency materials and solar cells with applications to energy and sustainability. We will use a combination of self-assembly and directed assembly via lithography to create appropriate structures, taking our inspiration from biological systems. Our research combines experiment and theoretical modeling to give a detailed insight into the properties of the materials.

We have established a network of collaboration between three different institutions: MANA in NIMS, Nanoscience Centre in University of Cambridge and the London Centre for Nanotechnology in University College London. In this year, we have arranged collaborative research visits to MANA for the PI and the co-director, as well as visits to UCL from collaborators in NIMS (Y. Tateyama). We also hosted the MANA/UCLA/Cambridge Summer School with 11 MANA students presenting papers and three MANA PIs attending.

2. Research Activities

(1) Synthesis of metal oxide nanowires for DSSCs.

We are investigating unique low temperature methods to grow highly crystalline titanium dioxide nanowires directly on transparent conducting substrates. These structures are being incorporated into solid state excitonic solar cells, improving the electron transport properties compared to nanocrystalline electrodes. We are obtaining promising device performance and conversion efficiencies. We have developed the growth methods to achieve high uniformity of the nanowire films on a macro scale, as well as optimum nanowire morphology and dimensions.

Different nanowire morphologies have been obtained; we are continuing to optimise the morphology to give the best performance in a DSSC device. Using recently developed techniques to apply thin inorganic shell layers to cover the nanowires, we can investigate the effect these shells have on suppressing charge recombination and passivating surface traps. Fig. 1 shows an example of two DSSC fabricated with core-shell nanowires and the nanowires.

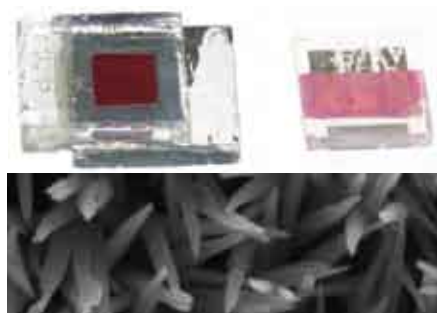


Fig. 1. Top: liquid and solid state DSSCs fabricated with core-shell nanowires. Bottom: SEM image of Al₂O₃ coated TiO₂ nanowires.

(2) Atomic and Electronic Structure of Dye Molecules on Substrates.

Using standard DFT, we are characterising the interaction of different dyes with TiO₂ surfaces found on nanoparticles.¹⁾ We have shown that both the bonding and the density of states of the dye depend strongly on its protonation state. We have also looked at the nucleation of Al₂O₃ on TiO₂,²⁾ as part of a study on the mechanisms underlying the change in electronic structure and dye efficiency following growth of thin oxide layers on TiO₂. We have extended this study to investigate the binding of dyes to amorphous Al₂O₃ layers, shown in Fig. 2, and the effect on dye properties.³⁾

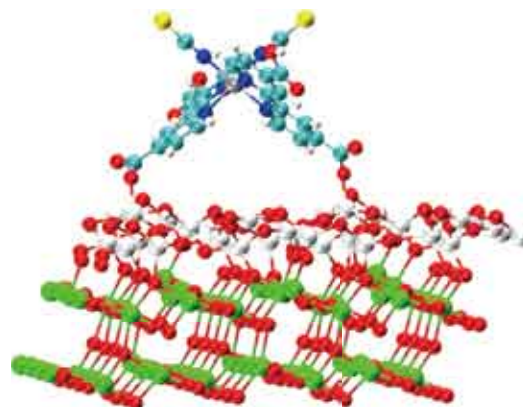


Fig. 2. Binding of N₃ dye to an amorphous Al₂O₃ layer on TiO₂.

(3) Development of novel methods.

Despite its success, DFT is not suitable for all applications, and we are continuing to develop novel approaches to extend the functionality of DFT for: large systems; energy levels; and charge transfer. It is hard to address large system sizes with standard implementations of DFT (which have a computer effort which increases with the cube of the number of atoms); we are using the CONQUEST linear scaling code⁴⁾ (which has linear scaling computer effort, and has been applied to systems containing millions of atoms) as a basis for this work. This code is the result of an on-going collaboration between NIMS and UCL. We have already implemented the constrained DFT technique for studying charge transfer excitations with the code,⁵⁾ and are testing a new implementation of time-dependent DFT within the code as a route to reliable energy level calculations for large systems.

References

- 1) K. Sodeyama, M. Sumita, C. O'Rourke, U. Terranova, A. Islam, L. Han, D. R. Bowler, Y. Tateyama, *J. Phys. Chem. Lett.*, in press.
- 2) U. Terranova, D.R. Bowler, *J. Mater. Chem.* **21**, 4197 (2011).
- 3) U. Terranova, D.R. Bowler, *J. Phys. Chem. C*, in press.
- 4) D. R. Bowler, T. Miyazaki, *Rep. Prog. Phys.*, in press.
- 5) A.M.P. Sena, T. Miyazaki, D.R. Bowler, *J. Chem. Theor. Comput.* **7** 884 (2011).

Construction of Interphases with Atomic/Molecular Order for Efficient Conversion of Energy/Materials

MANA Principal Investigator Kohei UOSAKI

(Field Coordinator)

MANA Scientist
MANA Research Associate
Graduate Student

Visiting Scientist

Hidenori Noguchi, Satoshi Tominaka
Qin Xu, Sedden Beyhan, Hicham Hamoudi
Yu Sun, Shongfu Tong, Yukihisa Okawa, Ya Zhang,
Ganesan Elumalai, Cepi Kurniawan
Aleksandra Pacula



1. Outline of Research

One of the most challenging problems for chemists/material scientists is construction of efficient energy/materials conversion systems. In this study, we would like to establish techniques to construct interfacial phases for highly efficient energy/materials conversion, mainly at solid/liquid interfaces, by arranging metal, semiconductor and organic molecules with atomic/molecular resolution. Furthermore, the detailed *in situ* analyses by STM, non-linear spectroscopy, and x-ray techniques of the structure and functions of the interfaces as well as theoretical study are carried out so that structure-function relations should be established and rational design and construction of the desired interfacial phases become possible. Specifically, we have carried out 1. construction of catalytic interfaces by arranging atoms on metal surfaces in ordered manner, 2. construction of photoenergy conversion interfaces by forming ordered molecular layers on metal and semiconductor surfaces, and 3. experimental and theoretical investigations of structure and electron transfer processes at solid/liquid interfaces.

2. Research Activities

(1) *Construction of catalytic interfaces by atomically ordered modification of metal surfaces and microfabrication techniques.*

Development of highly efficient multi-functional electro-catalysts attracted considerable attention because of their important applications for interfacial energy conversion. Catalytic activities depend on the composition and structure of the catalysts. For example, the atomic ratio giving maximum catalytic activity for electrochemical methanol oxidation reaction, which is one of the most important reactions in fuel cell, is suggested to be Pt₅₀Ru₅₀. It is, however, not easy to prepare the catalysts with precise atomic arrangement. Usually two metal complexes are mixed together and decomposed thermally to obtain alloy. In this case, bulk ratio can be controlled but not nano-scale arrangement at the surface where reactions take place. Here, we employed a new method, in which multi-nuclear metal complex is adsorbed on a substrate and then decomposed thermally so that atomically arranged nano-alloys can be formed. We have already demonstrated that Pt-Ru and Pt-Ni complexes are adsorbed on a gold (111) electrode surface in

ordered manner and subsequent decomposition of the adsorbed species by heating followed by electrochemical treatment resulted in highly dispersed PtRu¹⁾ and PtNi particles, respectively, on the surface with very high electrocatalytic activity for methanol oxidation. This year we have carried out XAFS measurements to examine the precise structures of PtNi catalysts prepared by the traditional

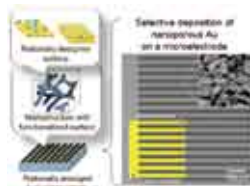


Fig. 1. Illustration for rational design of catalytic electrodes for advanced fuel cell (left) and SEM image of a rationally arranged nanoporous Au electrode (right).

method using Pt and Ru complexes and that prepared by the present method and it was proved that Pt and Ru are mixed much better in the latter.

Rational design of catalytic electrodes for advanced fuel cell systems is also investigated by arranging materials from atomic scale to macroscopic scale (Fig. 1, left). Electrochemical co-deposition of precious metals such as Au and Pd with Cu followed by selective dissolution of the latter enabled us to yield such rationally designed nanostructured electrodes. The SEM image (Fig. 1, right) shows a nanoporous Au electrode rationally arranged at micrometer scale.

(2) *Photoenergy Conversion at Metal and Semiconductor Surfaces Modified with Ordered Molecular Layer.*

It is very important to produce hydrogen from water and form useful compounds by reducing CO₂ using solar energy.

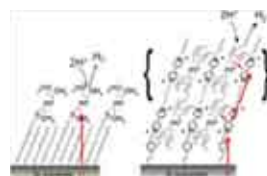


Fig. 2. Schematic model of confined molecular catalyst for HER on (left) and within molecular layer formed on Si(111) electrode surface.

Up-hill electron transfer is the basis of these processes. We have achieved enhancement of the visible light induced up-hill electron transfer at porphyrin-ferrocene thiol modified gold electrode by the addition of gold nanoparticles, which acted as plasmonic photon-antennas.²⁾ It was also demonstrated that Pt complexes

attached on and within molecular layers with viologen moiety, electron relay, formed on Si(111) electrode surface act as “confined molecular catalysts” for photoelectrochemical hydrogen evolution reaction (HER) (Fig. 2) as proved by *in situ* XAFS measurements.³⁾

(3) *Experimental and Theoretical Investigations of Structure and Electron Transfer Processes at Solid/liquid Interfaces.*

To construct interfacial phases for highly efficient energy/materials conversion, it is essential to have information on the structure and electron transfer dynamics at solid/liquid interfaces. This year we studied self-assembly process of polyproline, which is a very interesting peptide with solvent dependent structure, on a gold surface by using various techniques such as electrochemistry, IR, and ellipsometry⁴⁾ (Fig. 3).



Fig. 3. Schematic model of the formation process of polyproline SAM on a gold surface in aqueous solution.

References

- 1) H. Uehara, Y. Okawa, Y. Sasaki, K. Uosaki, *Chem. Lett.* **38**, 148 (2009).
- 2) K. Ikeda, K. Takahashi, T. Masuda, K. Uosaki, *Angew. Chem. Int. Ed.* **50**, 1280 (2011).
- 3) T. Masuda, H. Fukumitsu, S. Takakusagi, W.J. Chun, T. Kondo, K. Asakura, K. Uosaki, *Adv. Mater.* **24**, 268 (2012).
- 4) Y. Han, H. Noguchi, K. Sakaguchi, K. Uosaki, *Langmuir* **27**, 11951 (2011).

Solid State Batteries

MANA Principal Investigator

MANA Scientist
MANA Research Associate

Kazunori TAKADA

Tsuyoshi Ohnishi
Taeri Kwon



1. Outline of Research

Lithium batteries have been powering portable electronics including cellular phones and note PC's for 20 years. In addition, now they are expected to play new roles for realizing a low-carbon society as power sources in electric vehicles and energy storage device in smart grids. However, the safety issue arising from their combustible organic electrolytes remains unsolved.

Solid electrolytes will make a breakthrough due to their non-flammability. In addition, single-ion conduction in solid electrolytes will effectively suppress the side reaction deteriorating battery performance. These features will pave a way to next-generation batteries. Our goal is to realize all-solid-state lithium batteries through the researches on ionic conduction in solids.

2. Research Activities

(1) Self-organized core-shell structure for high-power solid-state lithium batteries.^{1,2)}

Solid-state lithium batteries had been suffering from the low power density. We found that the rate-determining step is in the lithium-depleted layer formed at the interface between $\text{Li}_{1-x}\text{CoO}_2$ cathode and the sulfide solid electrolyte and succeeded in improving it by surface coating on the LiCoO_2 particles with an oxide solid electrolyte as a buffer layer to suppress the lithium depletion. However, the coating technique does not fit to the mass production, because it is a batch process and needs expensive precursors and precise process control.

Recently, we have found a very simple alternative, where an Al compound was added among the starting materials for LiCoO_2 synthesis. Most of the Al occupies the Co sites to form a $\text{LiAl}_x\text{Co}_{1-x}\text{O}_2$ solid solution, whereas the rest is segregated on the surface of the particle to form an Al-enriched layer there. Because $\text{Li}_{1-x}\text{CoO}_2$ is originally an electron-ion mixed conductor, the enriched Al suppressing the electronic conduction makes the surface act as an oxide solid electrolyte layer, i.e. a self-formed buffer layer. Therefore, it reduces the interfacial resistance and increases the power density without any complicated process to almost the same extent as the coating layer of $\text{Li}_4\text{Ti}_5\text{O}_{12}$ (Fig. 1).

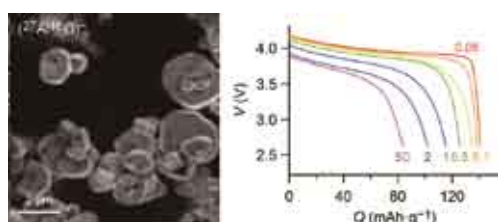


Fig. 1. Distribution of Al in $\text{LiAl}_{0.08}\text{Co}_{0.92}\text{O}_2$ particles observed by scanning secondary ion mass spectrometry (left) and the rate capability of the $\text{LiAl}_{0.08}\text{Co}_{0.92}\text{O}_2$ in a sulfide solid electrolyte (right).

(2) Nanosheet for ionic devices.³⁾

Because interfacial ionic conduction plays a critical role in ionic devices, two-dimensional nanomaterials will be effective in enhancing the performance by for controlling the interfacial phenomena. Although NIMS has developed many kinds of oxide nanosheets, which show outstanding functionalities including gigantic magneto-optical effects, and high dielectric constants, they have seldom been investigated as ionic materials.

A TaO_3 nanosheet has a mesh structure. Its openings are almost the same in size as lithium ion and thus are expected to allow lithium ions to penetrate the nanosheet. In addition, its wide band-gap with 5.3 eV guarantees the electronic insulation. Therefore, the TaO_3 nanosheet can be a self-standing solid electrolyte layer with an ultimate thinness of 1 nm. We have confirmed it by investigating the effects as a buffer layer at a $\text{Li}_{1-x}\text{CoO}_2$ /sulfide solid electrolyte interface.

The TaO_3 nanosheets interposed at the interface reduced the interfacial resistance by two orders of magnitude; that is, to the same degree as a typical oxide solid electrolyte of Li_3PO_4 . On the other hand, a nanosheet without openings, $\text{Ti}_{0.91}\text{O}_2$, did not decrease the interfacial resistance. These results strongly suggest that the TaO_3 nanosheet is a self-standing oxide electrolyte layer with an ultimate thinness of 1 nm, where the openings act as conduction channels for lithium ions (Fig. 2).

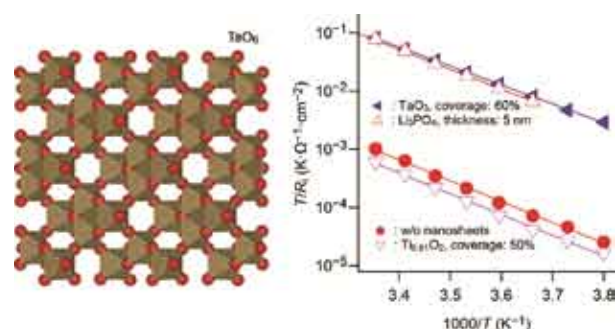


Fig. 2. Crystal structure of the TaO_3 nanosheet (left) and the effect of surface coating on the interfacial resistance (R_i) between $\text{Li}_{1-x}\text{CoO}_2$ and a sulfide solid electrolyte (right).

References

- 1) N. Ohta, K. Takada, L.Q. Zhang, R.Z. Ma, M. Osada, T. Sasaki, *Adv. Mater.* **18**, 2226 (2006).
- 2) X.X. Xu, K. Takada, K. Watanabe, I. Sakaguchi, K. Akatsuka, B.T. Hang, T. Ohnishi, T. Sasaki, *Chem. Mater.* **23**, 3798 (2011).
- 3) X.X. Xu, K. Takada, K. Fukuda, T. Ohnishi, K. Akatsuka, M. Osada, B.T. Hang, K. Kumagai, T. Sekiguchi, T. Sasaki, *Energy Environ. Sci.* **4**, 3509 (2011).

Reticular Materials

MANA Principal Investigator

MANA Researcher
MANA Research Associate

Omar M. YAGHI

Kentaro Tashiro
Alejandro M. Fracaroli, Piramuthu S. Lakshminarayanan



1. Outline of Research

The synthesis of mononuclear metal complexes by design is a well-established process. In sharp contrast, however, a protocol for the synthesis of complexes containing multiple homo- or hetero-metals, in a designed fashion, remains largely absent so far, where it is inevitable to get a mixture of products with respect to the number, nuclearity, or sequence of metal centers. In this project so far, we have developed a conceptually new synthetic methodology to create metal complex arrays with controlled number, nuclearity, or sequence of metal centers (Fig. 1).¹⁻³ This methodology is now opening a new era of metal complex-based materials science by producing multimetallic systems that are inaccessible via traditional synthetic methodologies. Especially, the controlled sequence of metal centers in the arrays, like those in proteins and nucleic acids, will be the most attractive characteristics of this type of materials. Moreover, since our methodology is potentially extendable to automated, parallel processes, high-throughput preparation of the libraries of metal complex arrays will be expected.

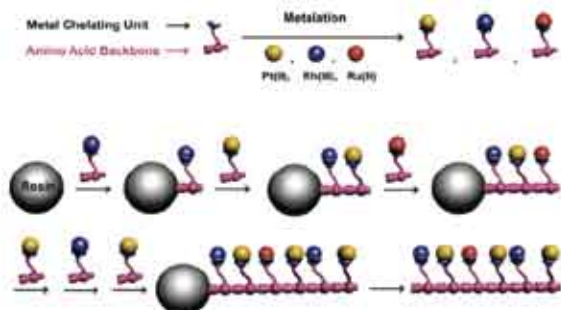


Fig. 1. Schematic representation of solid-phase synthesis of metal-organic complex arrays.

2. Research Activities

(1) Synthesis of a Series of MOCA Isomers.⁴⁾

Merrifield solid-phase peptide synthesis is a well-established synthetic technique for polypeptides, where the order in which the amino acids are added determines their sequence in the product. By taking advantage of the consecutive nature of this procedure, we have successfully constructed and isolated a series of sequential isomers of heterometallic triad complexes composed of Pt(II), Ru(II), and Re(I) metal centers with a hexapeptidic backbone (Fig. 2). These isomers are the first set of isolated heteronuclear trimetallic complex isomers so far. We also found that these isomers exhibit a sequence-dependent self-assembling property, where the Re–Ru–Pt sequence has a distinctively stronger gelation capability than the other sequences such as Ru–Pt–Re and Ru–Re–Pt (Fig. 3).

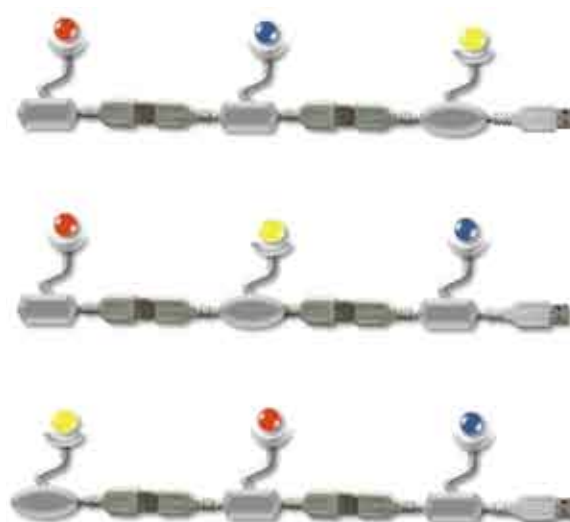


Fig. 2. Schematic representation of isomeric metal-organic complex array triads.



Fig. 3. Sequence-dependent gelation capability of isomeric metal-organic complex array triads.

(2) Catalytic Applications.

The synthetic intermediates of MOCAs on the resin could be nice candidates for metal complex-based immobilized catalyst with ultimately controlled orientations of metal centers. To investigate their potential, as the first survey, we have evaluated the catalytic activity of the metal complex monomers loaded on the resin, where Rh and Pt complexes actually can serve as catalysts for oxygenation and hydrogen production reactions.

References

- 1) P. Vairaprakash, H. Ueki, K. Tashiro, O.M. Yaghi, *J. Am. Chem. Soc.* **133**, 759 (2011).
- 2) M. Jacoby, *C&EN* **89**, 8 (2011).
- 3) K. Tashiro, *Gendaikagaku* **484**, 48 (2011).
- 4) A.M. Fracaroli, K. Tashiro, O.M. Yaghi, submitted.

Nanoarchitectonics of Hybrid Artificial Photosynthetic System

MANA Principal Investigator

MANA Research Associate
Graduate Student

Jinhua YE

Y. Bi, H. Tong,
X. Chen, J. Cao, B. Yue, N. Zhang, P. Li



1. Outline of Research

Fundamental research and development of artificial photosynthesis technology comprising of nano-structured metal/inorganic/organic semiconductor hybrid system will be conducted. Special attention will be paid to the design of new nano semiconductor materials harvesting major part of solar light, understanding of interactions between photon, carrier, molecules, and manipulation of these interactions for realization of higher photon efficiency by nanoarchitectonics. A breakthrough in the efficiency of solar-chemical energy conversion is expected.

In order to accomplish this purpose, we set following four sub-themes and are conducting the materials exploration research effectively by organically coordinating these sub-themes (Fig. 1):

- 1) Design and fabrication of new semiconductors which can utilize solar energy sufficiently by energy band structure engineering, with the help of theoretical calculation basing on the first principle theory. Engineering of band gap as well as CB, VB potentials will be carried out simultaneously to meet the potential requirement of photosynthetic reaction.
- 2) Nanoarchitectonics of the photosynthesis system will be conducted, by not only fabrication of nano particles using various soft chemical method, but also assembling of nano-metal/nano-oxide hybridized system to achieve efficient transportation and separation of electron-hole charge carriers.
- 3) Evaluation of photon efficiency in various reactions will be performed using a solar-simulator and various gas chromatography.
- 4) Photosynthetic mechanism will be investigated experimentally and theoretically, to establish guidelines for development of higher efficient system.

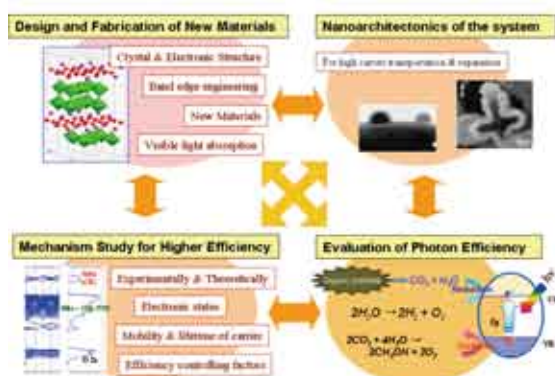


Fig. 1. Four sub-themes and their organic coordination for conducting effective materials exploration research.

2. Research Activities

(1) *Facet controlled growth of Ag_3PO_4 for higher photocatalytic activity.*¹⁾

We have developed a facile route for high-yield fabrication of single-crystalline Ag_3PO_4 rhombic dodecahedrons exposed totally with {110} facets and cubes bounded entirely by {100} facets (Fig. 2) without using any capping agent. The rhombic dodecahedrons were found to exhibit much higher photocatalytic activities than cubes and particles for the organic contaminants degradation, owing to it higher surface energy.

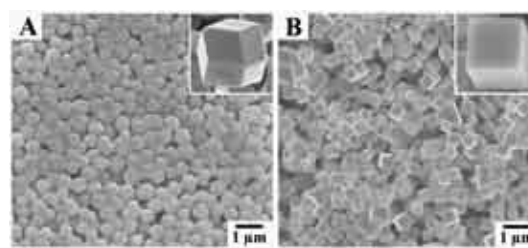


Fig. 2. SEM images of Ag_3PO_4 nano-crystals with different morphologies: (A) rhombic dodecahedrons; (B) cubes.

(2) *Discovery of a new doping-free strategy to the energy-band engineering of semiconductor materials.*^{2,3)}

We have discovered an innovative doping-free strategy to the energy-band engineering of semiconductor materials via proper assembly of semiconductor nanocrystals (Fig. 3). Both experimental investigations and theoretical calculations manifested that a much narrower band-gap than those of not only separate ones but also corresponding bulk materials can be achieved by energy-band reconstruction due to the formation of interface metal-metal bonds.

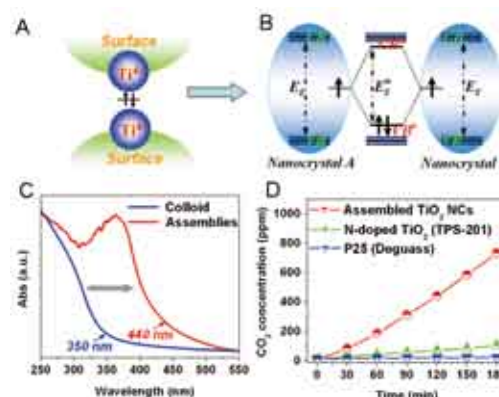


Fig. 3. A), B) Scheme of nano-assembly. C) Red shift of Uv-vis spectra. D) Photocatalytic activity of various TiO_2 .

References

- 1) Y. Bi, S. Ouyang, N. Umezawa, J. Cao, J. Ye, *J. Am. Chem. Soc.* **133**, 6490 (2011).
- 2) H. Tong, N. Umezawa, J. Ye, *Chem. Commun.* **47**, 4219 (2011).
- 3) H. Tong, N. Umezawa, J. Ye, T. Ohno, *Energy Environ. Sci.* **4**, 1684 (2011).

Smart Nano-Biomaterials

MANA Principal Investigator
(Field Coordinator)

MANA Scientist
NIMS Post-doc

Takao AOYAGI

Mitsuhiro Ebara
Koichiro Uto



1. Outline of Research

Shape-memory materials are a class of “smart” materials that have the capability to change from a temporary shape to a memorized permanent shape upon application of an external stimulus such as heating. By molecular designing and tailoring the nano-architectures of branched Poly(ϵ -caprolactone) (abbreviated as PCL) macromonomers, the switching temperatures for the shape-memory effect can be easily adjusted to near body temperature while keeping a sharp transition in a narrow temperature range. In this study, surface topography control using such unique materials was studied for cell biomedical application.¹⁾

2. Research Activities

To realize polymeric shape-memory materials, temperature-responsive materials were prepared by cross-linking of multi-branched PCL macromonomers. It is well-known that PCL is semi-crystalline polymer and its melting point is around 60°C. We carried out fundamental studies about PCL nano-architecture such as branch number, molecular weight and cross-linking on elasticity change in response to temperature alteration. By precise molecular design, we successfully prepared PCL membrane with around 20–40°C of softening points. That materials could be realized by combination of molecular-weight-controlled two branched (2b20) and four branched (4b10) macromonomers. The adjusting softening point near body temperature of these materials is surely critical to consider the biomedical application.

To prepare shape memory surfaces with permanent surface patterns, a PCL macromonomer solution was injected between a glass master and a flat slide glass with a 0.2 mm thick Teflon spacer and cured for 180 min at 80 °C. To program temporary surface patterns, the films were compressed in a thermo chamber. A compressive stress of 0.1 MPa was applied to the samples at 37 °C and held for 5 min. The embossing stress was then released at 4 °C after 10 min of cooling. When a flat PCL film was embossed with a grooved pattern by application of pressure at 37 °C and subsequent cooling, the film was deformed and fixed into the grooved topography of the master (grooves with width of 1 μ m and a height of 300 nm are spaced 2 μ m apart). The temporary surface pattern was quickly erased by heating and the permanent shape, a flat surface in this case, was completely recovered. When a PCL film with a grooved topography (grooves with width of 1 μ m and a height of 100 nm are spaced 2 μ m apart) was embossed with a flat master, the film was deformed and a flat surface was fixed. The permanent grooved topography quickly appeared after heating. It was also succeeded that shape-memory transition from a grooved topography (grooves with width of 5 μ m and a height of 300 nm are spaced 10 μ m apart) to another

grooved topography perpendicular to the original shape (grooves with width of 1 μ m and a height of 150 nm are spaced 2 μ m apart). Thus, temporary surface patterns can be easily programmed into the films and the transition to the permanent surface patterns is rapid and complete, regardless of the temporary or permanent topography.

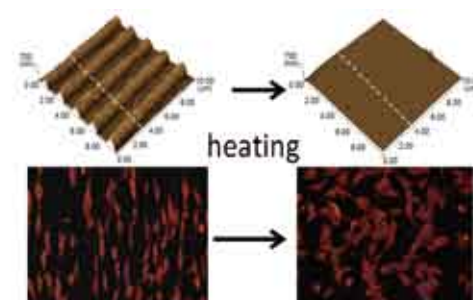


Fig. 1. Fluorescent microscope images of NIH3T3 fibroblasts seeded on the fibronectin-coated PCL films (4b10 / 2b10 = 50 / 50 wt%) with the temporal grooved surface.

To investigate the role of dynamic and reversible surface nanopatterns on cell proliferation, specifically cell alignment on the PCL films before and after a topographic transition, NIH3T3 fibroblasts were seeded on fibronectin-coated PCL films with a temporary grooved topography (grooves with width of 1 μ m and a height of 300 nm are spaced 2 μ m apart) and cultured at 32 °C for 6 h. Cells aligned parallel to the grooves as seen in Fig. 1. Cells migrated and grew horizontally to the surface grooves with cultivation time. Upon transition from the grooved topography to a flat surface, cell alignment was lost and random cell migration and growth ensued. The cell angle dispersion (defined as the angle between the pattern and cell orientation) increased with time even though the incubation temperature was returned to 32 °C after 2 h incubation at 37 °C. Cells seeded on flat films grew randomly regardless of incubation temperature. The distribution of cell-orientation angles correlated well with the topographic features of the underlying substrates before transition. On the other hand, angular histograms show clearly the time-dependent dispersion of cell angles after shape-memory transition to a flat shape. Thus, the shape memory surfaces demonstrated the important role of surface nanotopology in time-dependent cell migration and alignment. In the future, this approach will also enable unprecedented observations of time-dependent cell–substrate interactions without the need for invasive forces against intact adherent cells.

Reference

- 1) M. Ebara, K. Uto, N. Idota, J.M. Hoffman, T. Aoyagi, *Adv. Mater.* **24**, 273 (2012).

Nano- and Micro-Structured Porous Scaffolds for Tissue Engineering

MANA Principal Investigator

MANA Scientist
MANA Research Associate
JSPS Fellow

Guoping CHEN

Naoki Kawazoe
Hongxu Lu
Takashi Hoshiba



1. Outline of Research

By combining cells, biomaterial scaffolds, and biologically active molecules, tissue engineering has been proven to be a promising therapeutic approach in treating disease and injury in light of a variety of problems confronting currently available treatment methods. Nano- and micro-structured porous scaffolds play an important role in tissue engineering to control cell functions and to promote the formation of new tissues and organs. The scaffolds provide initial support to the seeded cells, localize the cells in the appropriate spaces, provide physical and biological cues for adhesion, migration, proliferation and differentiation, and assemble the propagated cells and secreted matrices into functional tissues and organs. Ideally, the scaffolds can provide the same nano- and micro-environments to the seeded cells as those of extracellular matrices (ECM) existing *in vivo*.

We developed a method of preparing ECM scaffolds by culture of cells in a selectively removable template. The intracellular components and the biodegradable polymer template are selectively removed after cell culture to obtain the ECM scaffolds. If autologous cells are used, the method can be used to prepare autologous ECM scaffolds. Stepwise tissue development-mimicking matrices can also be prepared to mimic the dynamically remolded *in vivo* native ECM by controlling the differentiation stage of stem cells.

2. Research Activities

ECM scaffolds derived from bone marrow-derived mesenchymal stem cells (MSCs), chondrocytes, and fibroblasts were prepared by culturing these cells in a selectively removable poly(lactic-co-glycolic acid) (PLGA) template. The ECM scaffolds exhibited a mesh-like appearance similar to that of the temporary skeletal PLGA knitted mesh. The porous 3D structure, microscale and nanoscale ECM fibers, was observed by a scanning electron microscope (Fig. 1). The geometrical properties, porosity, interconnectivity, and nanoscaled fibrous structure are meant to support cell proliferation and differentiation, and benefit tissue regeneration. The composition of the ECM scaffolds was dependent on the cell types used to prepare the scaffolds.¹⁾

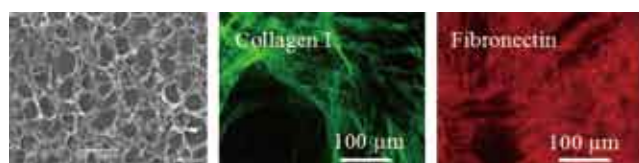


Fig. 1. SEM image of ECM scaffold and immunofluorescence images of collagen I and fibronectin composing the ECM scaffold.

The ECM scaffolds were used for *in vitro* cultures of MSCs and fibroblasts to examine their potential as scaffolds for cartilage and skin tissue engineering. The MSCs were cultured in MSC- and chondrocyte-derived ECM scaffolds. The ECM scaffolds supported cell adhesion, promoted both cell proliferation and the production of ECM and demonstrated a stronger stimulatory effect on the chondrogenesis of MSCs compared with a conventional pellet culture method. Histological and immunohistochemical staining indicated that cartilage-like tissues were regenerated after the MSCs were cultured in ECM scaffolds. Fibroblasts were cultured in the fibroblast-derived ECM scaffolds. Fibroblasts proliferated and produced ECM to fill the pores and spaces in the scaffold. After 2 weeks of culture, a uniform multilayered tissue was generated with homogeneously distributed fibroblasts. The cell-derived ECM scaffolds were demonstrated to facilitate tissue regeneration and will be a useful tool for tissue engineering.

This method can be used to prepare autologous scaffolds by culturing patient own cells. Biocompatibility of the autologous ECM scaffolds was demonstrated by implanting mouse fibroblast-derived autologous ECM scaffolds into the same mouse. The results from host tissue response analyses indicated excellent biocompatibility of the autologous ECM scaffolds, which is essential for ideal tissue engineering scaffolds. By using autologous ECM scaffolds for the culture of autologous cells, “full autologous tissue engineering” can be realized to make the tissue engineered construct more biocompatible with the host.²⁾

Furthermore, stepwise tissue development-mimicking matrices were prepared by controlling the stepwise osteogenic and adipogenic differentiation of MSCs.³⁾ The stepwise osteogenesis-mimicking matrices and adipogenesis-mimicking matrices showed different effects on osteogenesis and adipogenesis of MSCs. Osteogenic early stage matrices promoted osteogenesis of MSCs, while adipogenic early stage matrices facilitated adipogenesis of MSCs. The matrices showed tissue- and stage-specific effects on differentiation of MSCs. The ECM scaffolds and matrices will be useful for not only tissue engineering and biological therapy but also for basic biological research.

References

- 1) H. Lu, T. Hoshiba, N. Kawazoe, I. Koda, M. Song, G. Chen, *Biomater.* **32**, 9658 (2011).
- 2) H. Lu, T. Hoshiba, N. Kawazoe, T. Tateishi, G. Chen, *Biomater.* **32**, 2489 (2011).
- 3) T. Hoshiba, N. Kawazoe, G. Chen, *Biomater.* **33**, 2025 (2012).

Nanotherapy Based on Novel Materials Nanoarchitectonics

MANA Principal Investigator
(Satellite at Univ. Tsukuba, Japan)

Yukio NAGASAKI

Lecturer
Post-doc

Yutaka Ikeda
Yukichi Horiguchi, Toru Yoshitomi



1. Outline of Research

The objective of our research is to create new bioactive materials for high performance therapeutic system. In order to use materials *in vivo*, interactions between materials surface and bio-components such as blood and tissue must be controlled. Non-biofouling surface is one of the most important characters for high performance biomaterials design. Using our surface constructing technique thus developed, we have developed novel bionanoparticles. Highly dispersion stable and biocompatible nanoparticle is known to increase its blood circulation tendency. In order to control these nanoparticles *in vivo*, we have to install further specific functionality via new concept by novel materials nanoarchitectonics technique. Based on these concept, we have been designing novel unique nanoparticles such as near-infrared nanophosphor for bioimaging, photo-NO-releasing nanoparticle for cancer therapy, pH-triggered redox nanoparticles for cerebral ischemia- reperfusion injury, boron-containing nanoparticles for neutron-capture therapy.

2. Research Activities

(1) Biointerface.

Non-biofouling surface is one of the most important subjects to detect sensitive and selective recognitions of biomolecular events. Poly(ethylene glycol) (PEG) chains tethered on substrate surface are well known technique to reduce non-biofouling character. Protein adsorption on the PEG tethered-chain surface was strongly influenced by the density of the PEG chain, and was almost completely suppressed by successive treatment of longer PEG chain (5KDa) followed by treatment of PEG(2KDa) (mixed PEG-tethered chain surface) because of significant increase in PEG chain density. For a modification on versatile substrate surface, PEG possessing pentaethylenehexamine at one end (N6-PEG) was prepared via a reductive amination reaction of aldehyde ended PEG with pentaethylenehexamine. Using N6-PEG, antibody/ PEG co-immobilization was carried out on substrate possessing active ester groups. After antibody was immobilized on the surface, PEG tethered-chain was constructed surrounding the immobilized antibody (Fig. 1). It is interesting to note that the PEG tethered chain works not only as a non-fouling character but also as an improvement in immune-response. Hybrid surface was also applied to oligoDNA immobilization. The oligoDNA/ PEG hybrid surface improved hybrid hybrid-

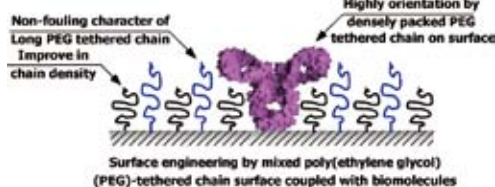


Fig. 1. Schematic illustration of PEG/antibody hybrid surface.

ization property, retaining non-fouling character. Densely packed PEG tethered-chains surrounding around antibody and/or oligoDNA improve their orientation on the surface. Thus, it is promising as a high performance biointerface for versatile applications.

(2) Bioimaging.

Using the surface modification technique, several types of nanoparticles were prepared. Er-doped yttrium oxide nanoparticle (Er:Y₂O₃) emits not only NIR light but visible light under the NIR excitation. The latter emission is called infrared-to-visible upconversion (UC) emission. PEG-b-poly(vinylbenzyl phosphoric acid) (PEG-b-PVBP) stabilized the UC-nanoparticle, which can be utilized as near-infrared bioimaging tools. PEG-b-PVBP also stabilized ion oxide and can be utilized *in vivo*. Ion oxide nanoparticles thus prepared can be utilized as MRI imaging probe as well as magnetite-assisted hyperthermia (Fig. 2).

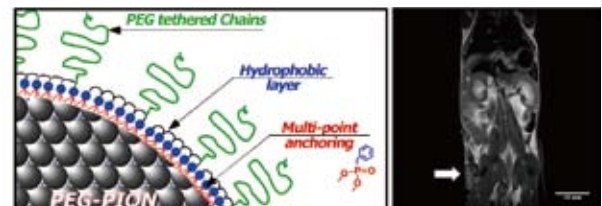


Fig. 2. Schematic illustration of ion oxide nanoparticle stabilized by PEG-b-poly(vinylbenzyl phosphoric acid) (PEG-b-PVBP) and MRI imaging assisted by ion oxide nanoparticle.

(3) Nanotherapy.

We have designed redox-nanoparticle (RNP), which reacts with reactive oxygen species (ROS). The RNP can be utilized for a scavenger of excessive generated ROS for several injuries such as cerebral and renal ischemia reperfusion injuries, Alzheimer's diseases and cancer. Recently, we have found that oral administration of RNP effectively accumulate in colon mucosa (Fig. 3) and almost cure ulcerative colitis by scavenging ROS. Our original redox nanoparticles are promising as novel nanotherapeutic system.

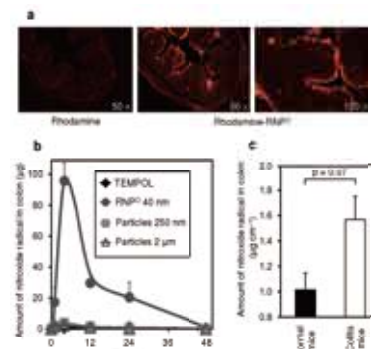


Fig. 3. Location of FL-labeled-RNP in colon mucosa and size dependent accumulation of nanoparticle in colon mucosa.

Nanoarchitectonics-Inspired Nanoparticles and Interfaces for Therapeutic Applications

MANA Principal Investigator **Françoise M. WINNIK**

(Satellite at Univ. Montreal, Canada)
Post-doc

Sayaka Toita, Fabien Perineau



1. Outline of Research

The ultimate aim of the project is to provide effective diagnostic and therapeutic modalities of minimal invasiveness for eventual clinical use. In one approach, we will exploit the ability of gold nano-objects to generate localized surface plasmons for which the resonance wavelength can be tuned by changes in the size, shape and geometry of the nanostructures. For *in-vivo* applications, the plasmon resonance peak should be within the near-infrared region (700 to 1000 nm), since this spectral domain of the electromagnetic field is safer and has much deeper tissue penetration, compared to visible or UV radiation. Nanoparticles endowed of this property can serve as NIR-responsive imaging agents or drug delivery systems when a dye or a drug is linked to their surface via a light-sensitive linker (Fig. 1A).

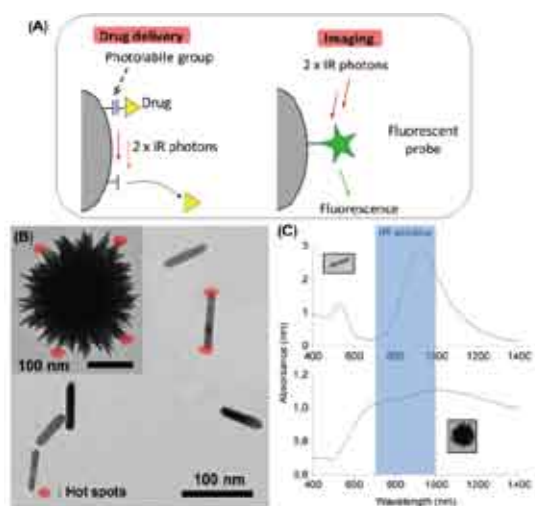


Fig. 1. (A) Plasmon-assisted drug delivery and imaging. (B) Transmission electron micrographs of gold nanourchins and nanorods. (C) Absorption spectra of the nanoparticles.

In a second approach, we will focus on the creation of chitosan-based photochemically tailored patterned interfaces for the recruitment of endothelial progenitor cells (EPC) for cardiovascular therapies. Chitosan is a cationic polysaccharide used extensively in the biomedical field in particular in gene therapy and tissue engineering. We discovered that phosphorylcholine-modified chitosan (CH-PC) (Fig. 2) constitutes an excellent supporting matrix for the survival and amplification of EPCs. This polymer will be used, upon further chemical modification, and photopatterning for controlled cell differentiation or light-triggered drug release.

2. Research Activities

(1) Nanoparticles for plasmon-assisted IR-induced imaging and drug delivery.

During the first months of this project, we concen-

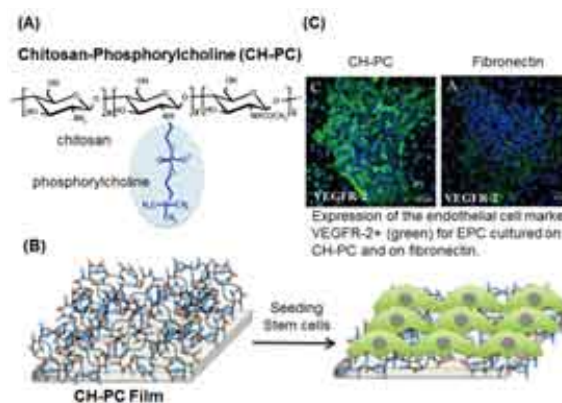


Fig. 2. (A) Chemical structure of CH-PC. (B) Schematic representation of CH-PC interfaces. (C) Images of EPC analyses (from Ref. 1).

trated our efforts on the elaboration of reproducible and scalable protocols for the synthesis of gold nanourchins, nanorods, and nanocages. Nanourchins were synthesized by reducing tetrachloroauric(III) acid grown on silver nanoseeds.³ Gold nanorods (60 nm in length, aspect ratio: 5.5) were prepared from gold nanoseeds by the reduction of tetrachloroauric(III) acid in a binary mixture of surfactants. The absorption spectrum of both gold nanourchins and nanorods extends to ~ 1000 nm (Fig. 1C), the desired spectral domain for the targeted applications. Current work focuses on the modification of the nanoparticles to render them compatible with the physiological environment and photoresponsive in the NIR spectral domain.

(2) Stem-cell based strategies for cardiovascular therapy.

In order to design matrices of optimal performance for EPC amplification, we assessed the physico-chemical properties of CH-PC matrices by tools such as quartz crystal microbalance, zeta potential and contact angle analysis. Samples of CH-PC with varying levels of PC incorporation were prepared and assessed. The CH-PC framework was used to prepare estradiol (E2) prodrugs in order to achieve controlled release of estradiol, a steroid known to inhibit neointima proliferation in coronary arteries following stent implantation. Initial studies of CH-PC-E2 films placed under simulated physiological conditions indicate that the release of estradiol occurs gradually over ~ 10 days. In-vitro studies of CH-PC-E2 films and nanoparticles will be carried out next on plain and patterned surfaces.

References

- 1) K. Tardif, I. Cloutier, Z. Miao, C. Lemieux, C. St-Denis, F.M. Winnik, J.F. Tanguay, *Biomater.* **32**, 5046 (2011).
- 2) E. Hutter, S. Boridy, S. Labrecque, M. Lalancette-Hébert, J. Kriz, F.M. Winnik, D. Maysinger, *ACS Nano* **4**, 2595 (2010).

Next-Generation Semiconductor Nanodevices

Group Leader
(Nano-Materials Field)

Naoki FUKATA



1. Outline of Research

Technical progress in silicon integrated circuits (Si VLSI) has, up to the present time, been driven by the miniaturization, or scaling, of gates, oxide layers, p-n junctions, substrates, and other elements in metal-oxide semiconductor field-effect transistors (MOSFETs), which are the building blocks of VLSI. Advances in performance and integration through conventional scaling of device geometries are, however, now reaching their practical limits in planar MOSFETs. To overcome the limiting factors in planar MOSFETs, vertical structural arrangements using semiconductor nanowires have been suggested as the basis for next-generation semiconductor devices.

Gaining an understanding the dynamic behaviors of dopant atoms in Si nanowires (SiNWs) is the key to achieving low-power and high-speed transistor devices using SiNWs. The behaviors of dopants atoms after doping are not yet fully understood. To be able to make MOSFETs based on SiNWs feasible, it is necessary to investigate the effects of the formation of gate oxides by thermal oxidation. Thermal oxidation thickens the surface oxide layer, resulting in a decrease in the diameter of the Si core of SiNWs. Our previous studies have shown that thermal oxidation exerts compressive stress toward the center of the SiNWs, due to expansion of the surrounding surface oxide layer.^{1,2)} The segregation of dopant atoms under stress should thus be taken into account during thermal oxidation.

2. Research Activities

(1) Oxidation effect of SiNWs.

A STEM image of typical P-doped n-type SiNWs is shown in Fig. 1a. A magnified image of a single SiNW is shown in Fig. 1b. It clearly shows a distinct contrast inside the SiNW. The darker region in the center of the SiNW is the crystalline Si region, while the surrounding layer is an amorphous SiO_x (x ≤ 2) layer. Thermal oxidation thickens the surface oxide layer, resulting in a decrease in the diameter of the Si core of SiNWs.

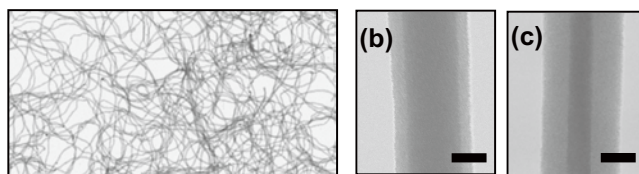


Fig. 1. Representative (a) STEM and (b) TEM images of the P-doped SiNWs synthesized using a Si₅₀(Ni₂P)₁₀ target. TEM images of P-doped SiNWs annealed at 900 °C in (c) O₂ and (d) Ar. Annealing time was 120 min. in each. The scale bars of (b)-(d) are 15 nm.

(2) Segregation of B and P atoms.

The segregation behavior of boron (B) and phosphorus (P) atoms in B- and P-doped SiNWs during thermal oxidation was closely observed using B local vibrational peaks and Fano broadening in optical phonon peaks of B-doped SiNWs by micro-Raman scattering. Electron spin resonance (ESR) signals from conduction electrons were used for P-doped SiNWs. The results showed that B atoms preferentially segregate in the surface oxide layer, whereas P atoms tend to accumulate in the Si region around the interface of SiNWs (Fig. 2). This is the first results about the behaviors of dopant atoms in SiNWs.³⁾

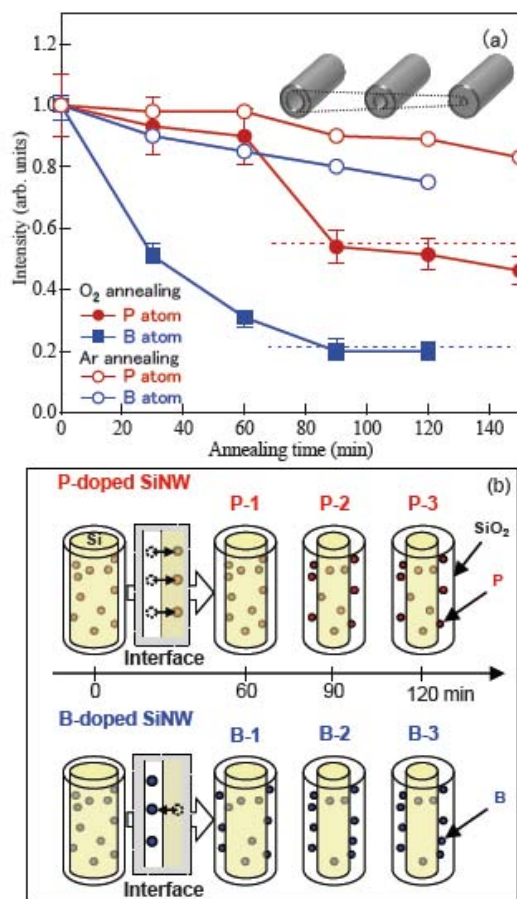


Fig. 2. (a) Dependence of the peak intensity of ¹¹B local vibrational peak and the ESR signal from conduction electrons on annealing time in O₂ and Ar. The Si₅₀Ni₂B₁₀ targets were used to synthesize the B-doped SiNWs and the Si₅₀(Ni₂P)₁₀ targets were used to synthesize the P-doped SiNWs. (b) Illustration of P and B segregation behaviors in SiNWs by thermal oxidation.

References

- 1) N. Fukata, *Adv. Mater.* **21**, 2829 (2009).
- 2) N. Fukata et al., *ACS Nano* **4**, 3807 (2010).
- 3) N. Fukata et al., *Nano Lett.* **11**, 651 (2011).

Development of Nano Biomedicines

Group Leader
(Nano-Bio Field)

Nobutaka HANAGATA



1. Outline of Research

My challenge is to apply beneficial technologies to society by integrating original biological discoveries with original materials technologies and nanotechnology. The integration of life sciences and nanotechnology/materials science has two approaches. The first approach is to link critical knowledge in the life sciences to technological innovations through the use of nanotechnology and materials science. The other approach is to use nanotechnology and materials science to lead to important discoveries in the life sciences. To accomplish research using these two approaches, I use the following foundational technologies; global gene expression analysis, protein interaction analysis and bioimaging as fundamental technologies in life science, and manufacturing of nanoparticles, nanotubes and nano-patterned surfaces as fundamental technologies in materials science and nanotechnology.

2. Research Activities

(1) *Development of natural CpG DNA drugs consisting entirely of phosphodiester backbone.¹⁾*

Unmethylated cytosine-guanine (CpG) motif-containing oligodeoxynucleotides (ODNs) have been well characterized as agonists of Toll-like receptor 9 (TLR9). In human, TLR9 is mainly expressed by B cells and plasmacytoid dendritic cells. ODNs with a phosphorothioate (PTO) backbone have been studied as TLR9 agonists since natural ODNs with a phosphodiester (PD) backbone are easily degraded by a serum nuclease, which makes them problematic for therapeutic applications. However, ODNs with a PTO backbone have been shown to have undesirable side effects. Thus, our goal was to develop nuclease-resistant, PD ODNs that are effective as human TLR9 (hTLR9) agonists. The sequence of ODN2006, a CpG ODN that acts as an hTLR9 agonist, was used as the basic CpG ODN material. The 3'-end modification of ODN2006 with a PD backbone (PD-ODN2006) improved its potential as an hTLR9 agonist because of increased resistance to nucleolytic degradation. Moreover, 3'-end modification with oligonucleotides showed higher induction than modification with biotin, FITC, and amino groups. Further, enhancement of hTLR9 activity was found to be dependent on the number of CpG core motifs (GTCGTT) in the PD ODN containing the 3'-end oligonucleotides. In particular, ODN sequences consisting of two to three linked ODN2006 sequences with a PD backbone (e. g., PD-ODN2006-2006

and PD-ODN2006-2006-2006) acted as effective agonists of hTLR9 even at lower concentrations. These CpG ODNs can be used as potentially safe agonists for hTLR9 activation instead of CpG ODNs with a PTO backbone.

(2) *Development of intracellular delivery system for CpG DNAs.^{2,5)}*

Delivery systems for CpG ODN using nanoparticles as carriers differ greatly from delivery systems of other nucleic acid drugs such as antisense DNA and small interfering RNA (siRNA) for cancer treatment. For delivery of antisense DNA and siRNA, after they have been taken up by cells as a result of endocytosis, their nucleic acids must move from the endosome to the nucleus. However, with the delivery of CpG ODN, because the TLR9 is localized in the endolysosome, CpG ODN must be retained in the endolysosome for a long period of time. Therefore, delivery systems using CpG ODN require a design strategy different from conventional drug delivery systems. We have developed mesoporous silica nanoparticles, boron nitride nanoparticles and silicon quantum dot nanoparticles for CpG DNA delivery. The advantages of using these nanoparticles as CpG ODN carriers include protection from DNase degradation, decrease in the amount administered because cellular uptake efficiency is improved, the ability to change the structure of CpG ODN, the ability to deliver to target tissues, and the ability to slow-release CpG ODN over a long period of time.

(3) *Safety and toxicity assessment on nanomaterials.⁶⁾*

In recent years, products that include nanoparticles have increased drastically in recent years. However, no standards have been established concerning the safety of nanoparticles. From global gene expression analysis of cells exposed to nanoparticles, we are elucidating molecular mechanisms involved in nanoparticles' cellular toxicity.

References

- 1) W. Meng, T. Yamazaki, Y. Nishida, N. Hanagata, *BMC Biotechnol.* **11**, 88 (2011).
- 2) Y. Zhu, W. Meng, X. Li, H. Gao, N. Hanagata, *J. Phys. Chem. C* **115**, 447 (2011).
- 3) Y. Zhu, W. Meng, H. Gao, N. Hanagata, *J. Phys. Chem. C* **115**, 13630 (2011).
- 4) C. Zhi, W. Meng, T. Yamazaki, Y. Bando, D. Golberg, C. Tang, N. Hanagata, *J. Mater. Chem.* **21**, 5219 (2011).
- 5) Y. Zhu, W. Meng, N. Hanagata, *Dalton Trans.* **40**, 10203 (2011).
- 6) N. Hanagata, F. Zhuang, S. Connolly, J. Li, N. Ogawa, M. Xu., *ACS Nano* **5**: 9326 (2011).

Bioactive Ceramics Materials

Group Leader
(Nano-Bio Field)

Masanori KIKUCHI



1. Outline of Research

Bioactive ceramics is divided into two types. One is conventional one that can directly bond with bone but not influences cell functions so much. Another type can activate target cell functions. We have been investigating both type of bioactive ceramics and ceramic/polymer composites for tissue regeneration. This year, we investigated hydroxyapatite/collagen bone-like nanocomposite (HAp/Col, Fig. 1) with properties that cell function activation and incorporating into bone remodeling process, after commercialization of unidirectional porous hydroxyapatite ceramics from Kuraray Co. of our collaborator. In addition, to support practical use (commercialization) of new biomaterials, studies on bioactive ceramics evaluation methods for establishment of new international standards.

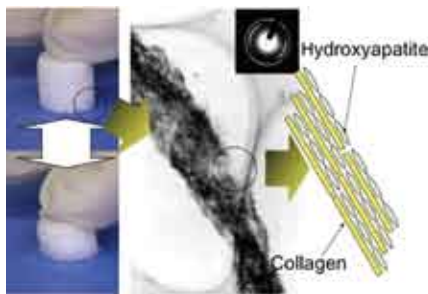


Fig. 1. Hydroxyapatite/collagen self-organized nanocomposite has nanostructure in which apatite and collagen are regularly aligned, and can be formed to sponge-like porous body.

2. Research Activities

(1) Injectable HAp/Col materials.¹⁾

Injectable artificial bone with bioresorbability is strongly desired in practical medicine to realize good minimum invasive surgery to reduce potential risk of bone fractures as well as inhibition of new bone formation due to remaining of cements in body. Injectable HAp/Col could be good candidate. We utilize sodium alginate (Na-Alg) for gelation and lubrication agent. Mass ratio of the HAp/Col powder with or without Ca adsorption treatment, and Na-Alg was fixed at 9/1. Injectable HAp/Col was prepared by mixing the HAp/Col powder with Na-Alg solution at several powder (HAp/Col)/liquid (Na-Alg solution) ratios (P/L ratio, g/cm³). According to the consistency measurement and practical feelings during mixing, P/L=1/1.67 (80-120 cP) and 1/1.89 (300-400, 500-600 cP) were the highest P/L ratio. At the P/L=1/2.33 (80-120 cP), the paste prepared with the non-treated HAp/Col powder, placed in an incubator (37 °C, relative humidity 100%) for 24h, demonstrated gel-like property, while the paste prepared with Ca-treated HAp/Col powder did putty-like property (Fig. 2). Their operability and coalescence/setting property could be used as the injectable bone filler.

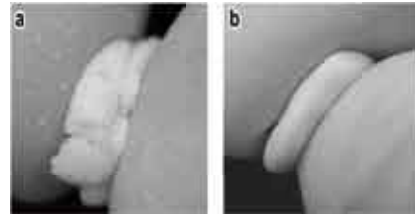


Fig. 2. Photo images of HAp/Col (a) and Ca-HAp/Col (b) coagulates placed in 100% humidified 37°C incubator for 24h.

(2) Influence of Ca²⁺ and Mg²⁺ Supplementation on In Vitro Biological Properties of HAp/Col Membrane.²⁾

We already reported that HAp/Col shows excellent bioactivity in vivo. However, they show quite high absorbability for cationic ions and lower culture medium ionic concentrations which adversely affects bone cell proliferation and osteogenic differentiation in *in vitro* cell culture condition. To address this limitation, in this study we have supplemented Ca²⁺ and Mg²⁺ ions to the HAp/Col nanocomposite membrane sample prior to cell culture to improve its *in vitro* biological properties. The HAp/Col nanocomposite membrane samples were fabricated by the simultaneous titration method using Ca(OH)₂, type-I atelocollagen and H₃PO₄ as starting precursor materials. Prior to *in vitro* cell culture experiments, the HAp/Col samples were pretreated with Ca²⁺ and/or Mg²⁺ ions by immersing in 10 ml of 20 mM CaCl₂ solution, 20 mM MgCl₂ solution, or a solution containing 20 mM CaCl₂ and 20 mM MgCl₂ for 7 days. *In vitro* bone cell-material interactions on the pretreated and untreated HAp/Col samples were studied by culturing MC3T3-E1 cells up to 7 days. Enhanced bone cell proliferation was found on all the pretreated HAp/col samples as confirmed by the CCK-8 assay (Fig. 3). Interestingly, the HAp/Col samples pretreated with both Ca²⁺ and Mg²⁺ ions showed the maximum viable bone cell density.

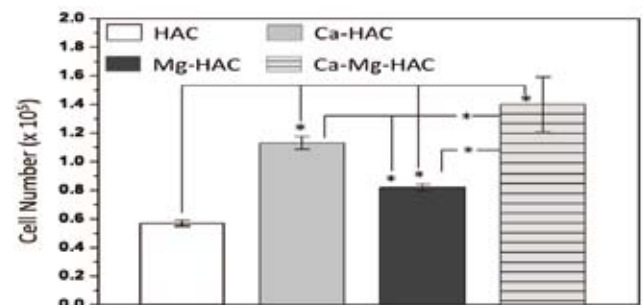


Fig. 3. Cell number on untreated and pretreated HAp/Col samples after 3 days culture. (* = P < 0.05).

References

- 1) A. Kochi, M. Kikuchi, Y. Shirosaki, S. Hayakawa, A. Osaka, *Key Eng. Mater.* **493-494**, 689 (2012).
- 2) S. Bodhak, M. Kikuchi, A. Oyane, Y. Sogo, H. Tsurushima, A. Ito, *Key Eng. Mater.* **493-494**, 126 (2012).

Materials for Functional Nanomedicine

Group Leader
(Nano-Bio Field)

Hisatoshi KOBAYASHI



1. Outline of Research

In general, organism selected quite limited molecules such as amino acids, lipids, sugar moieties, and limited metals and inorganics, and combined the limited molecules and finally constructed such highly functionalized complex systems. From the structure point of view, the organism is constructed by various nano-fibers and nano-particles under the highly dimensionally controlled condition.

We are challenging functionalization of a medical device using various nanomaterials and nanotechnologies till now. For example, in order to construct highly biofunctionalized cell-ECM composite, we are aiming to develop nano-micro-macro structure-regulated biofunctional materials (Fig. 1) which inspired natural ECM. Because it is the way in which organism selected under the evolution.

Towards the clinical use, we are carefully studying the cell-matrices interaction from the view point of material science under the world wide collaboration with various medical engineering, medical institutes etc.

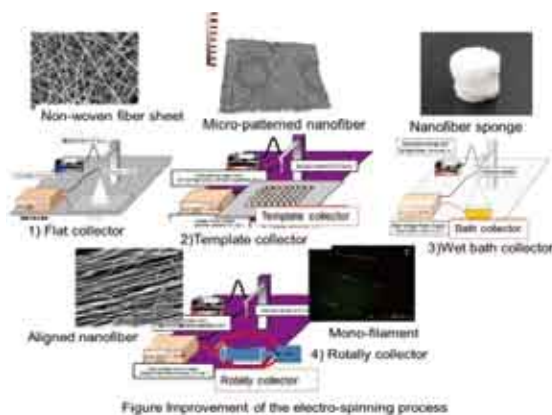


Fig. 1. Improvement of electrospinning process to produce controlled nano-micro-macro architecture.

2. Research Activities

(1) *Transient charge-masking effect of applied voltage on electrospinning of pure chitosan nanofibers from aqueous solutions.*¹⁾

The processing of a polyelectrolyte (whose functionality is derived from its ionized functional groups) into a nanofiber may improve its functionality and yield multiple functionalities. However, the electrospinning of nanofibers from polyelectrolytes is imperfect because polyelectrolytes differ considerably from neutral polymers in their rheological properties. In our study, we attempt to solve this problem by applying a voltage of opposite polarity to charges on a polyelectrolyte. The application of this “countervoltage” can temporarily mask or screen a specific rheological property of the polyelectrolyte (Fig. 2), making it behave as a neutral polymer. This approach can significantly contribute to the development of new functional nanofiber materials.

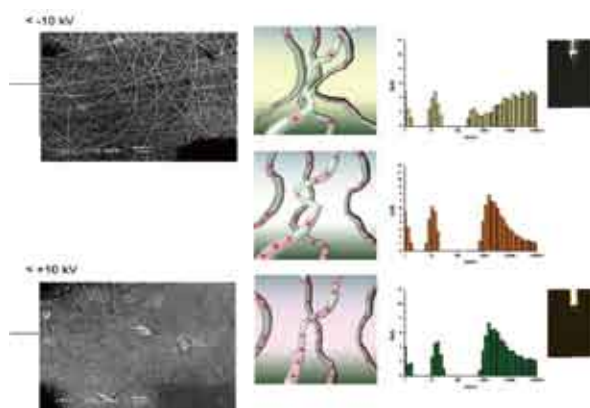


Fig. 2. Charge effects against polyelectrolyte: Expands difference of the Chitosan chain in aqueous solution between add +10kV and add -10kV.

(2) *An ultra sensitive saccharides detection assay using carboxyl functionalized chitosan containing $\text{Gd}_2\text{O}_3:\text{Eu}^{3+}$ nanoparticles probe.*²⁾

A novel saccharides detection assay based on covalent immobilization of amino phenyl boronic acid (APBA) in thin films of carboxyl functionalized chitosan (HOOC-chitosan) containing $< 5\text{ nm Gd}_2\text{O}_3:\text{Eu}^{3+}$ nanoparticles at a platinum disc electrode was developed (Fig. 3). The resulting HOOC-chitosan/ $\text{Gd}_2\text{O}_3:\text{Eu}^{3+}$ nanocomposite film exhibited excellent electrochemical response to changes in the pKa values of boronate esters yielded from different vicinal diols of sugars. The covalent interaction of APBA onto the HOOC-chitosan/ $\text{Gd}_2\text{O}_3:$ A wide linear response was measured to boronate esters ranging from 25 nM to 13.5 mM ($r^2 = 0.963$) with good reproducibility.

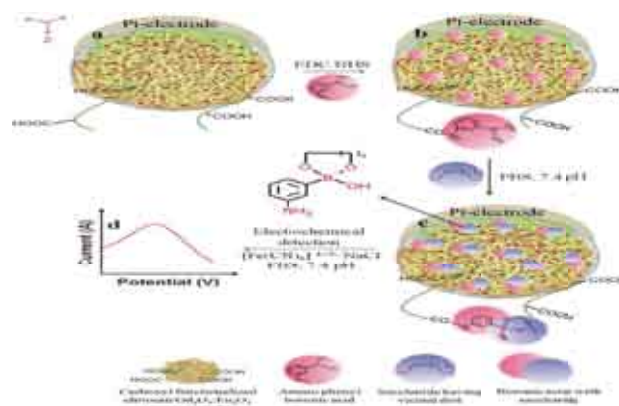


Fig. 3. Schematic illustration of electrodes fabrication and electrochemical saccharide detection process.

References

- 1) D. Terada, H. Kobayashi, K. Zhang, A. Tiwari, C. Yoshikawa, N. Hanagata, *Sci. Technol. Adv. Mater.*, in press.
- 2) A. Tiwari, D. Terada, P.K. Sharma, V. Paeashar, C. Yoshikawa, A.C. Pandey, H. Kobayashi, *Analyt. Meth.* **3**, 217 (2011).

Functionalization of Atomic Network Materials

Group Leader
(Nano-Materials Field)

Takao MORI



1. Outline of Research

Approximately two thirds of all primary energy (fossil fuels, etc) being consumed in the world, sadly turns out to be unutilized, with much of the waste being in the form of heat. The useful and direct energy conversion of waste heat to electricity is a large incentive to find viable thermoelectric materials. Traditionally, thermoelectric materials with attractive properties have tended to be mainly composed of elements which are not good from an element strategy viewpoint, namely, elements such as Bi, Te, Pb. One need exists to develop effective thermoelectric materials composed of abundant and safe elements. Another need exists for materials to have good thermal stability when considering mid to high temperature applications. To this end, we aim to functionalize covalent materials composed of elements like XIII~XV group elements (C, B, Si, Al, Sn, etc) by utilizing their atomic network structure, i.e. clusters, 2D atomic nets, cage-like structures in which the structural order plays a large role in the physical properties.¹⁻²⁾

2. Research Activities

(1) *Control of TE properties by microstructure control: Zinc doping effect.*

REB₄₄Si₂ exhibit Seebeck coefficients greater than 200 $\mu\text{V}/\text{K}$ at high temperatures and unlike most compounds, the figure of merit, ZT, shows a steep increase at $T > 1000$ K. We discovered a zinc doping method which was found to control the morphology (i.e. crystallinity) of the borosilicide compound and significantly improve the power factor by more than 30%.³⁾ Borosilicides and silicides tend to have a problem with Si aggregations (silicon “threads”) forming easily in the materials, and the zinc doping method was found to help remove them (Fig. 1). This method also has the potential to be an easy, inexpensive, and nonobtrusive method to apply to other high temperature materials.³⁾



Fig. 1. Zinc doping effect (SEM pictures).

(2) *Control of TE properties by microstructure control: Utilization of SPS.*

A series of homologous RE-B-C(N) compounds; RE-B₁₇CN, REB₂₂C₂N, and REB_{28.5}C₄, was recently discovered to be the long awaited n-type counterpart to boron carbide. Boron carbide is one of the few TE materials which have been commercialized, however, the lack of a compatible n-type counterpart has been a long standing obstacle, with great effort over 20 years being made to find one.

A challenge facing these materials for application is that densification processes have not been fully developed yet. Conventional hot press methods and cold pressing and annealing methods yield samples with densities of only around 50% the theoretical value. Straightforwardly applying spark plasma sintering (SPS) has been found to increase the density to ~70% which is still too low.

We utilized sintering additives and were able to control morphology and obtain a dramatic increase of the density to over 93%.⁴⁻⁵⁾ We are trying to develop a systematic strategy for additives selection, to find additives which are beneficial for densification and simultaneously beneficial as electronic dopants for thermoelectric properties.

(3) *Developing properties of 2D net layered compounds.*

We have taken a systematic approach to the AIB₂-type analogous “tiling” compounds, composed of 2D boron atomic sheets (based on hexagonal graphitic structure) sandwiching rare-earth and transition metal atoms. REAIB₄ in particular has attracted attention with recent discoveries, such as frustrated magnetism in α -HoAIB₄ and ErAIB₄, and multiple magnetic anomalies in α -TmAIB₄ below the Neel temperature indicated to be due to building defects.⁶⁾ With a counterintuitive approach to crystal growth, single crystals of α -TmAIB₄ were successfully grown, which were indicated from TEM and advanced XRD analysis to be virtually free from the ubiquitous building defects. The physical properties show a striking difference from those of conventional α -TmAIB₄ crystals (Fig. 2), and the large effect of the building defects on the physical properties could be directly confirmed, such as the origin of “missing entropy”. These building defects are quite subtle and may in some cases be unperceived, and might possibly be the origin of anomalous behavior in other layered systems also.⁷⁾

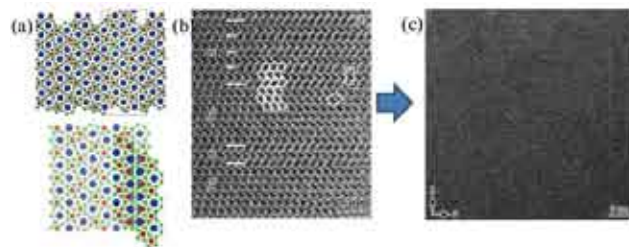


Fig. 2. (a) Schematic structure and (b) TEM pic of typical TmAIB₄ crystal. (c) TEM pic of crystal grown with new method.

References

- 1) T. Mori, in *Handbook on the Physics and Chemistry of Rare Earths*, Vol. 38, (North-Holland, Amsterdam, 2008) p. 105-173.
- 2) T. Mori, in *Modules, Systems and Applications*, (Taylor and Francis, London, 2012), in press.
- 3) T. Mori et al., *Dalton Trans.* **39**, 1027 (2010). Hot Article.
- 4) D. Berthebaud et al., *J. Electron. Mat.* **40**, 682 (2011).
- 5) D. Berthebaud et al., *J. Solid State Chem.* **184**, 1682 (2011).
- 6) T. Mori et al., *Phys. Rev. B* **76**, 064404 (2007), *J. Appl. Phys.* **105**, 07E124 (2009), *J. Appl. Phys.* **109**, 07E111 (2011).
- 7) T. Mori et al., *J. Appl. Phys.*, in press.

Controlling the Light in Nanospace

Group Leader
(Nano-System Field)

Tadaaki NAGAO



1. Outline of Research

The technology for amplifying, confining, and scattering the light in nanoscale is strongly desired as a key technology in communication, optical sensing, and energy harvesting. By hybridizing the plasma oscillation with the electromagnetic field near the metal surface we can manipulate the light at a much shorter wavelength than that in free space. Such hybridized waves with contracted wavelength are called plasmon polaritons.

When the size of the object shrinks beyond the micrometer scale and when it reaches down to the nanometer or sub-nanometer scale, novel effects that originate from its smallness and its shape come into play.^{1,2)} Atom-scale size effects become pronounced especially in metallic objects, since the Fermi wavelengths of metals are in the Ångström range.¹⁾ Plasmon polaritons in metal nanostructures show maximum tunability by changing the shape, the size, and thus the dimensionality of the objects. Such feature can be utilized for tailoring optical properties for future nano-photonics/optics devices for information technology as well as high-sensitivity sensors and efficient energy harvesting devices.²⁾

2. Research Activities

We focused ourselves to the fabrication of various nanoscale optical antennas in visible to infrared spectral region by using both lithographic and self assembly techniques.¹⁻⁴⁾ The electromagnetic waves in visible to mid-infrared region can be confined in nanometer-scale and even down to the subnanometer scale structures.

Fig. 1 shows an example of single-crystalline nano-hexagon with atomically smooth surface. The structure exhibited single-peaked antenna resonance and its resonance frequency was found to be fully tuneable in the entire infrared region by tuning its lateral size.

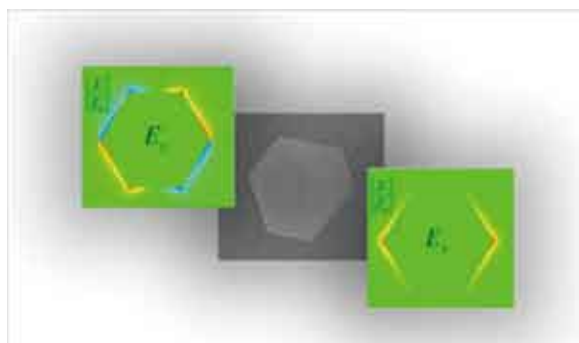


Fig. 1. An SEM image of the atomically flat Ag nano-hexagon fabricated by surfactant epitaxy (center). The structure acts as tunable infrared plasmonic antenna. Electrical field intensity for two orthogonal directions is shown for the incident beam polarization in the horizontal direction (left and right).

We also engineer the broadband plasmonic resonance by adopting an ensemble of gap-tuned random antennas with high filling factors (Fig. 2). As also evidenced by the electromagnetic simulations, the fabricated Au nanostructure showed enhanced vibrational signals for proteins and nucleic acids. Our plasmonic sensor shows an excellent detection limit in the zepto molar level and a multi-component detecting function. Although the current result is effectively applied to the infrared spectral region, we also expect that such broadband plasmonic absorber can be also applied for photovoltaic applications as well as photocatalysis.

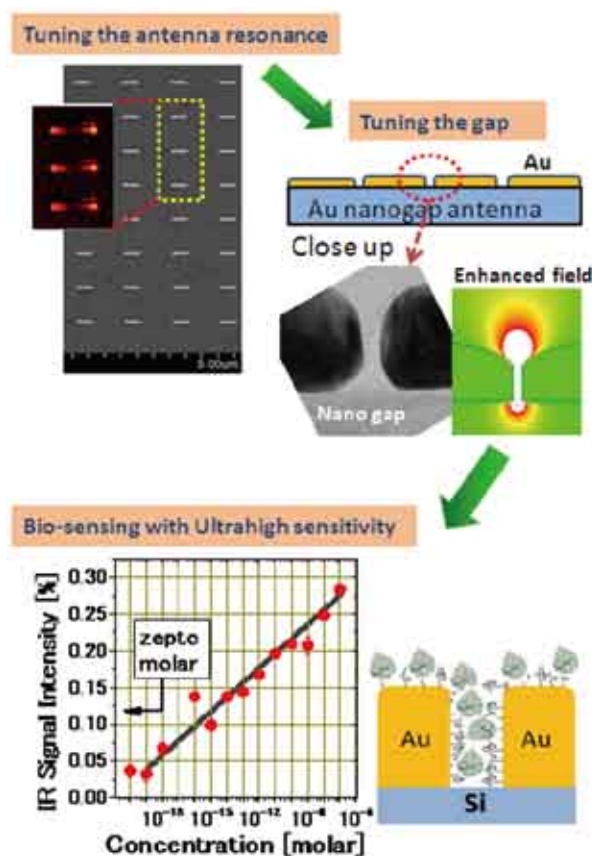


Fig. 2. A scheme for designing the optical nanoantennas. Typical nanoantenna fabricated in our group are also shown. One of the fabricated antennas has recorded extremely high sensitivity at concentration as low as zepto-molar level.

References

- 1) T. Nagao et al., *Phys. Rev. Lett.* **97**, 116802 (2006).
- 2) T. Nagao et al., *Sci. Technol. Adv. Mater.* **11**, 054506 (2011).
- 3) G. Han, D. Weber, F. Neubrech, I. Yamada, M. Mitome, Y. Bando, A. Pucci, T. Nagao, *Nanotechn.* **22**, 20572 (2011).
- 4) D. Enders et al., *Phys. Chem. Chem. Phys.* **13**, 4935 (2011).

Characterization of Semiconductor Nanostructures by Using EBIC and CL Techniques

Group Leader
(Nano-Materials Field)

Takashi SEKIGUCHI



1. Outline of Research

We are applying electron beam characterization techniques, such as electron-beam-induced current (EBIC) and cathodoluminescence (CL) for the study of semiconductor nanostructures and devices. First, we have improved the spatial resolution of EBIC/CL by introducing a better electro-optics and optimizing the light collection system. Second, the new specimen preparation techniques, such as cross sectional polisher (CP) and focus ion beam (FIB) have been introduced.

2. Research Activities

(1) EBIC study of III-V/Si interfaces.

III-V channel is a promising candidate for More Moore technology. However, the control of the heterointerface is extremely difficult because of the introduction of misfit dislocations. We have tried to observe the misfit dislocation arrays by using EBIC. The test structure is Ga_{0.30}In_{0.70}As(9nm) channel embedded in Al_{0.48}In_{0.52}As layer grown on GaAs substrate. (As for present stage, it is impossible to create high-quality III-V structure on Si). Fig. 1 shows the secondary electron (SE) and EBIC images taken at various electron beam energies.

These images indicates that the misfit dislocations along [1-10] lies deeper than those along [110]. Such preferential alignment indicates the nonuniformity of the defect generation, which suggests that the reduction of carrier recombination may be possible by aligning these dislocations parallel to the carrier motion.

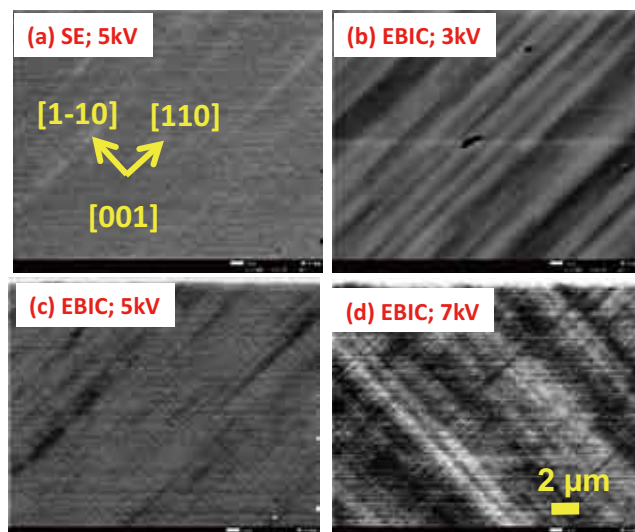


Fig. 1. (a) SE and (b,c,d) EBIC images of III-V heterointerface. The observation depths of EBIC are (b) 120 nm, (c) 270 nm, (d) 480 nm.

(2) CL study of Ga(O)N.

At the beginning, we have characterized the pit type defects in HVPE grown GaN thick films by using CL technique. During this study, we have found pit type defects are generated by the bundle of threading dislocations and are surrounded by the N facet. The slow growth rate of this N-facet is the cause of pit type defects and moreover, N-facet tends to incorporate oxygen impurities rather than Ga-facets.¹⁾

Then, we have characterized GaON nanowires grown by ammonolysis of Ga(NO₃)₃ with Ni as a catalysis. Fig. 2 shows the SE images of GaON nanowires grown at 800 °C and 1000 °C. Blue emission was dominant in the CL spectrum of nanowires grown at 800 °C, while band edge emission of GaN is dominant in that of 1000 °C. This suggests that oxygen concentration of GaON depends on the synthesis temperature. The electrical properties of these GaON nanowires were characterized by Dr. K. Kirihara (AIST) and correlated with the CL data.²⁾

The study of GaON nanostructures was done with the cooperation with Dr. Y. Masubuchi and Prof. S. Kikkawa in Hokkaido Univ.

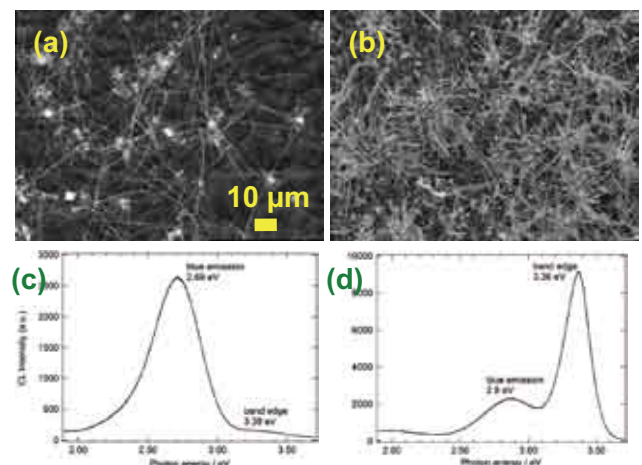


Fig. 2. (a,b) SE images and (c,d) CL spectra of GaON nanowires grown at (a,c) 800°C and (b,d) 1000°C.

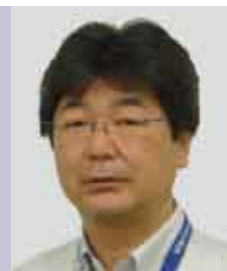
References

- 1) W. Lee et al., *J. Electron Microsc.*, in press.
- 2) Y. Masubuchi et al., *J. Crystal Growth* **337**, 87 (2011).

Development of Sensor Cells for Nanomaterials Safety Evaluation

Group Leader
(Nano-Bio Field)

Akiyoshi TANIGUCHI



1. Outline of Research

Live cell-based sensors are well accepted and used for investigating various signaling cascades caused by cytotoxic effects of reagents, because of their high specificity and sensitivity to their targets' specific gene expression.^{1,2)} In our laboratory, next-generation sensor cells are fabricated by molecular biology techniques that can detect changes in gene expression in response to toxic substances or other external stimuli (Figs. 1 and 2). We attempted to investigate the interaction between nanoparticles (NPs) and cells through our sensor cells, which can detect stimulation caused by TiO₂ NPs through monitoring the activation of the HSP70B' promoter.

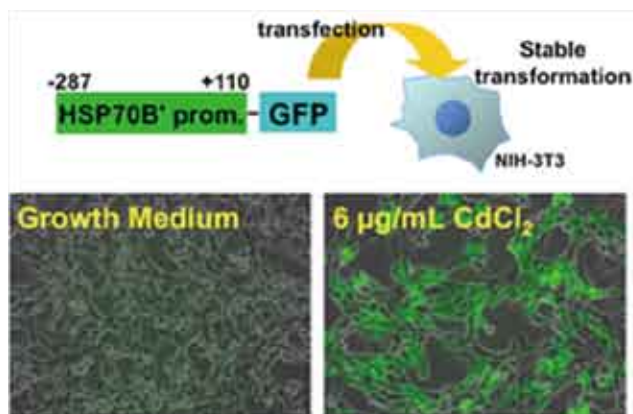


Fig. 1. Construction of sensor cells. Sensor cells were constructed by transfecting plasmids that contain promoter and reporter genes such as HSP70B' and GFP genes in to animal cells.

2. Research Activities

Nanomaterials, expressly nanoparticles, have been manufactured for varied applications. In particular, titanium dioxide nanoparticles (TiO₂ NPs) are an important both for lab research and industry products. Although they posed a safety risk to our health and environment, recent data have shown the worries concerning their potential toxicity. On the other hand, the development of various bio-

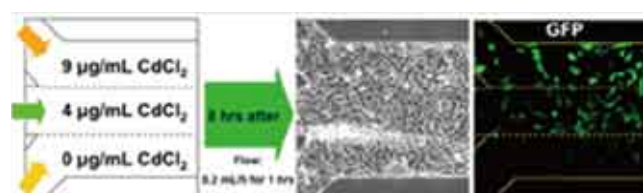


Fig. 2. Cytotoxic response of the sensor cell line in the 3-inlet microfluidic channels.

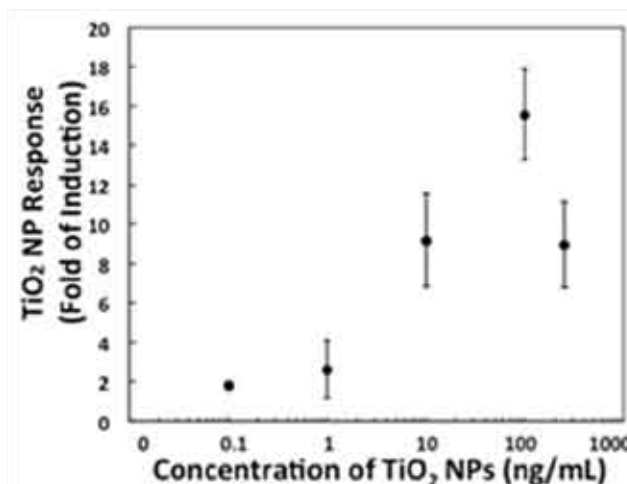


Fig. 3. TiO₂ NP dose response by HepG2 sensor cells. Scattergram of dose response plots of TiO₂ NP response (fold induction) by HepG2 sensor cells exposed to different concentrations (0.1, 1, 10, 100, and 250 ng/mL) of TiO₂ NPs for 48 h.

sensors, such as sensor cells, which monitoring expression levels of specific genes by receptor gene assays using functional promoters, has received a lot of attention because of their high specificity and sensitivity for their targets. The induction of heat shock protein (HSP) gene is a probable biomarker to investigate the potential mechanism of different stimuli. In this work, a HSP70B' promoter-reporter plasmid, which contains the HSP70B' promoter gene upstream of the luciferase gene, was transfected into different cell-lines to prepare live sensor cells for nanomaterials detection. Our data show the sensor cells we constructed have high response with the TiO₂ NPs exposure (Fig. 3) and our work could offer some useful information for the interaction investigation between the nanomaterials and cells.³⁻⁴⁾ Moreover, cooperated with different kinds of devices, our sensor cells would be hopeful to be applied for a bio-nanomaterials safety evaluation in the future.

References

- 1) A. Taniguchi, *Biomater.* **31**, 5911 (2010).
- 2) S. Migita, K.I. Wada, A. Taniguchi, *Biotechnol. Bioeng.* **107**, 561 (2010).
- 3) P. Chen, S. Migita, K. Kanehira, S. Sonezaki, A. Taniguchi, *Sensors* **11**, 7219 (2011).
- 4) J. Okuda-Shimazaki, S. Takaku, K. Kanehira, S. Sonezaki, A. Taniguchi, *Int. J. Mol. Sci.* **11**, 2383 (2010).

Nano-System Computational Science

Group Leader
(Nano-System Field)

Yoshitaka TATEYAMA



1. Outline of Research

We are challenging to make novel theoretical frameworks for physicochemical phenomena such as electron transfer, proton transfer & photoexcitation (Fig. 1), since their quantitative calculations are still less established than the conventional techniques for ground state properties.

Our main projects are as follows; (1) development and/or establishment of theories and computational methods for problems in physical chemistry based on the “density functional theory (DFT) and ab-initio calculation techniques”, and (2) understanding microscopic mechanisms of elementary reactions in physical chemistry problems by applying these computational techniques. Of particular interest are surface/interface chemistry, electrochemistry and photochemistry in these years.

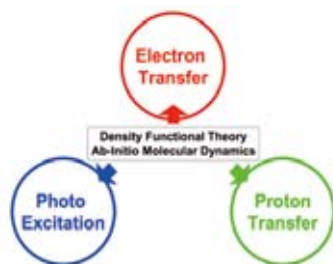


Fig. 1. Research targets in the computational physical chemistry (Tateyama independent scientist) group in MANA.

2. Research Activities

(1) *TiO₂ anatase (101)/liquid acetonitrile (MeCN) interface and its water contamination effect for durable dye-sensitized solar cell (DSC).*¹⁾

Water contamination in the fabrication processes of DSC is inevitable. Here, water contamination in the TiO₂ anatase (101)/liquid (MeCN) interface are investigated by using First-principles molecular dynamics (FPMD). Water molecule in the TiO₂/MeCN interfaces energetically favors structure II (Fig. 2), which has possibility to become cation radical by irradiation. Therefore, we recommend the fabrication process where H₂O should be eliminated from the TiO₂ surface before immersing MeCN solvent.



Fig. 2. Snapshot in the equilibrium trajectory of the TiO₂ anatase/acetonitrile interface with water molecule contamination. Characteristic hydrogen bond appears between the H₂O molecule and TiO₂ surface.

(2) *Protonated carboxyl anchor for stable adsorption of Ru N749 Dye (black dye) on TiO₂ anatase (101) surface.*²⁾

We have investigated the adsorption stability of Ru N749 dye (black dye) on the TiO₂ anatase (101) surface. Geometry optimization and UV spectrum calculation were carried out. Hydrogen bonding between the proton retained in black dye and the surface oxygen is responsible for the stability of the protonated anchor (Fig. 3). We confirmed that the calculated UV spectrum of the most stable dye structure shows the best consistency with the experimental data. This novel aspect of adsorption via protonated carboxyl anchor gives a new perspective for interfacial electronic processes of DSCs.

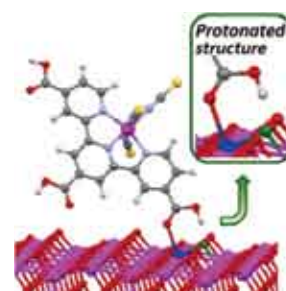


Fig. 3. Stable adsorption structure of black dye (Ru N749 dye) on TiO₂ anatase (101) surface.

(3) *First-principles large-scale calculation of polymerization of organic monomers for synthesis of nanowire.*³⁾

We have also examined the chain polymerisation of diacetylene compounds on a surface as well as the effect of phthalocyanine adsorption on the polymerisation, and given possible structure models, which are consistent with the STM observations in experiments (Fig. 4).

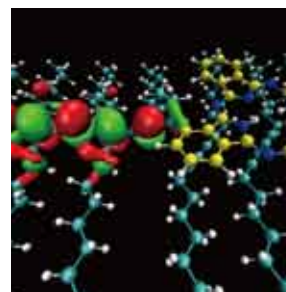


Fig. 4. HOMO distribution of polydiacetylene with adsorbed phthalocyanine on a surface, calculated by the first-principles wavelet-basis method.

References

- 1) M. Sumita, K. Sodeyama, L. Han, Y. Tateyama, *J. Phys. Chem. C* **115**, 19849 (2011).
- 2) K. Sodeyama, M. Sumita, C. O'Rourke, U. Terranova, A. Islam, L. Han, D. R. Bowler, Y. Tateyama, submitted.
- 3) Y. Okawa, S. K. Mandal, C. Hu, Y. Tateyama, S. Goedecker, S. Tsukamoto, T. Hasegawa, J. K. Gimzewski, M. Aono, *J. Am. Chem. Soc.* **133**, 8227 (2011).

Nano-Ionics Devices Based on Local Ion Transport

Group Leader

(Nano-System Field)
 MANA Research Associate
 NIMS Post-doc

Kazuya TERABE

Rui Yang
 Guangqiang Liu



1. Outline of Research

One possible way to extend Moore's law beyond the physical limits of the existing conventional semiconductor device is to achieve breakthroughs in nanotechnology materials and device architectures with increasingly capable. A promising type of nano-device is the nano-ionics device with multiple functions, which is operated by controlling local ion migration and electrochemical reaction phenomena. The ionics has been known to be a field in which the transport phenomenon of the ion in a solid is treated and, up to now, it has been different to electronics, which treats the transport phenomenon of the electron and the hole.

Unique properties and functions, such as analogue memory property, programming rectification, quantized conductance atomic switching, and nonvolatile resistance switching, have been founded in nano-ionics devices with simple layer structures (metal/electrolyte/metal).¹⁻³⁾ These properties and functions are realized by local ion migration in a nanoscale electrolyte layer of electronic-ionic mixed conductors or pure ionic conductors. Both cations and anions can be used as the migration ion. In a nano-ionics device functioning as an atomic switch, bipolar resistance switching (BRS), is achieved through the formation and annihilation of a metallic atom bridge by controlling the cation migration in the electrolyte or a nano-gap situated between two electrodes. The cations are usually supplied from chemically active electrodes. Meanwhile, in the transition-metal oxides based nano-ionics device with chemically non-active electrodes, the resistance switching is achieved by controlling the migration of anions, typically oxygen ions.

In this study, we examined the way to control the local migration of oxygen ion in the transition-metal oxide, and further explored the unique phenomena and function caused by the local ion transport in order to create unique nano-ionics devices.

2. Research Activities

Thin TiO_x and WO_x films with thickness of approximately 60 nm were fabricated by radio frequency sputtering on Pt bottom electrodes with quartz glass substrates at room temperature.⁴⁾ The depositions were performed with a WO_3 and TiO_2 targets in a gas mixture containing 80% Ar and 20% O_2 . The WO_x layer was then annealed in situ at 300 °C in an oxidizing atmosphere containing 50% Ar and 50% O_2 . Both top and bottom electrodes were approximately 100 nm thick. Each two-terminal device consisted of a cross-point structure with a junction area of $25 \times 25 \mu\text{m}$. The dc I - V curves were measured using a vacuum four-probe system equipped with a semiconductor characterization system. I - V measurements were performed at

room temperature.

The MO_x ($M=\text{Ti}$ and W) based nano-ionics devices with simple stacked structures show rectifying property as well as BRS by controlling the local migration of oxygen ions, as shown in Figs. 1a and 1b, respectively. The polarity dependence of the rectifying property in both devices can be changed by applying negative and positive bias voltages because the oxygen ion, namely oxygen vacancy ($V_{\text{O}}^{\cdot\cdot}$) could be migrated by the electric field as shown Fig. 1c. The interfaces of Pt/MO_x or Au/MO_x exhibit ohmic-like characteristics in the case of heavy $V_{\text{O}}^{\cdot\cdot}$ doping but exhibit rectification characteristics due to a Schottky-like barrier in the case of the light doping. It is found that the TiO_x based device shows the nonvolatile rectification but the WO_x based device shows the volatile rectification. We consider that the relaxation of $V_{\text{O}}^{\cdot\cdot}$ doping is easily occurred by relatively high oxygen mobility in the WO_x electrolyte. Moreover, both analogue memory property together with the rectification and BRS are achieved in the devices. These results demonstrate that the Pt/MO_x or Au/MO_x interface engineering realized by $V_{\text{O}}^{\cdot\cdot}$ local migration enables the creation of multi-functionality nanodevices. Such transition-metal oxide MO_x -based nano-ionic devices with simple stacked structure and multi-functionality are promising for practical application in programmable circuits, analog memory and artificial neural networks.

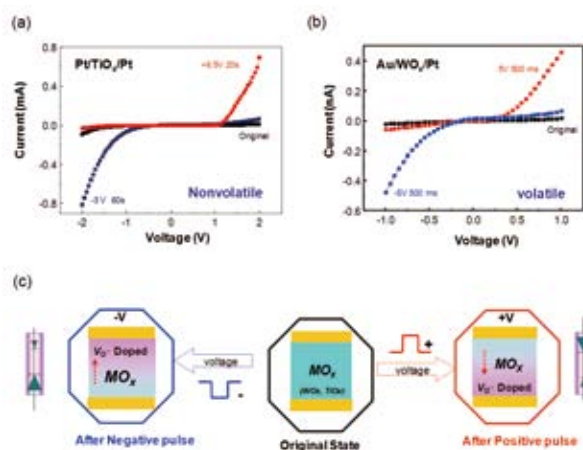


Fig. 1. (a): I - V curves of $\text{Pt}/\text{TiO}_x/\text{Pt}$ device after negative and positive pulse bias respectively without forming process. (b): I - V curves of $\text{Au}/\text{WO}_x/\text{Pt}$ device after negative and positive pulse bias respectively without forming process. (c): Schematic illustrations of oxygen vacancy profiles in MO_x ($M=\text{Ti}, \text{W}$) when positive and negative pulses voltage was applied, respectively.

References

- 1) K. Terabe et al., *Nature* **433**, 47 (2005).
- 2) T. Hasegawa et al., *Adv. Mater.* **24**, 252 (2012).
- 3) K. Terabe et al., *J. of IEICE*, in press.
- 4) R. Yang et al., submitted.

Controlling Initial Degradation of Bioabsorbable Mg Alloys to Improve Biocompatibility

Group Leader
(Nano-Bio Field)

Akiko YAMAMOTO



1. Outline of Research

Magnesium and its alloys are expected as bioabsorbable metals in the biomedical field because they are easily corroded inside the human body by reacting with water in the body fluid. Mg generates H₂ and OH⁻ along the progress of corrosion reaction with water, then, the pH of the fluid around Mg surface will increase, which makes it difficult for cells to grow on the Mg surface. Generation of H₂ and OH⁻ is unavoidable for Mg devices since they are required to be degraded. Therefore, not the permanent protection which is widely examined as the conventional approach in surface modification of Mg alloys, but retardation or control of the corrosion reaction of Mg devices is a key for their success.

Biodegradable polymers such as poly (L-lactic acid) (PLLA) and poly (ε-caprolactone) (PCL) generate H⁺ along their degradation by hydrolysis. This generated H⁺ could be effective to neutralize the generated OH⁻ by the degradation of Mg device and suppress the pH increase of surrounding fluid. In this study, application of biodegradable polymer coating to Mg surface is attempted to suppress the initial rapid degradation, pH increase, and to improve its cytocompatibility.¹⁾

2. Research Activities

Two kinds of biodegradable polymers, PLLA and PCL, with two different molecular weights (low molecular weight, LMW and high molecular weight, HMW) were employed for coating. Each polymer was spin-coated on to the pure Mg specimen separately at the same coating condition. The PCL coating was semi-crystalline and the PLLA coating is amorphous. The coating thicknesses of the LMW polymers are ca. 0.3 μm whereas those of HMW polymers are ca. 1.0 μm. Adhesive strengths of the four kinds of polymer coatings are 1.5-4.1 MPa.

Uncoated and polymer-coated Mg specimens were immersed into cell culture medium (D-MEM+10% FBS) in the CO₂ incubator for 24h to monitor the pH of the medium. The distance between the specimen surface and the

pH electrode was kept as 1 mm. As shown in Fig. 1, the pH decreases rapidly in the first 60 min due to the dissolution of CO₂ into D-MEM, and then, tends to be stable because of the buffering action of dissolved CO₂ as H₂CO₃. The pH of the medium with the uncoated Mg was is about 0.15-0.2 unit higher than that of the medium without a sample. Those of the medium with polymer-coated Mg were lower than that of uncoated one.

Human osteosarcoma, SaOS-2 was cultured on uncoated and polymer-coated Mg for 1, 4, and 7d. All polymer-coated samples promote significantly higher cell growth than uncoated Mg (Fig. 2a), suggesting the effective improvement in cytocompatibility by all polymer coatings. As shown in Fig. 2b, the Mg²⁺ ion release from the uncoated and polymer-coated Mg during the cell culture revealed that all polymer coatings effectively suppress the corrosion of Mg substrate. The HMW polymer coatings have lower pH, higher cell growth, and less Mg²⁺ release. This indicates that thicker polymer coating is more effective to retard the Mg substrate corrosion. It is also suggested that the lower pH of the medium with polymer-coated Mg that of uncoated Mg is mainly due to the less corrosion of the Mg substrate, but not to the H⁺ release by the degradation of polymer coatings. Even so, the suppression of the pH increase is effective to improve cell proliferation on the polymer-coated Mg.

The best suppression of Mg substrate corrosion was obtained with the PLLA-HMW coating, but Mg²⁺ release was confirmed after 1-d incubation. This indicates that the protective effect of the biodegradable polymer coating is not perfect but appropriate because the Mg substrate is required to be degraded in the biological environment. The effect of the degradation of polymer coating on Mg substrate degradation will be investigated by an immersion test in longer period of time in future.

Reference

1) L. Xu, A. Yamamoto, *Colloids Surf. B: Biointerfaces* (2012). doi: 10.1016/j.colsurfb.2011.12.009

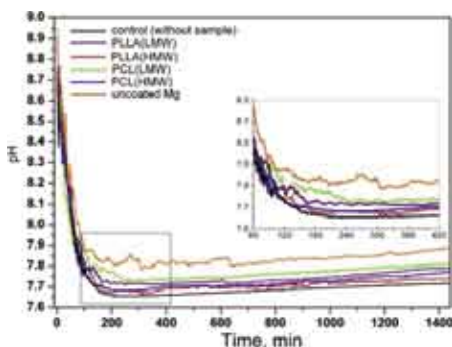


Fig. 1. The pH of the D-MEM+10%FBS with/without uncoated or polymer coated Mg samples.

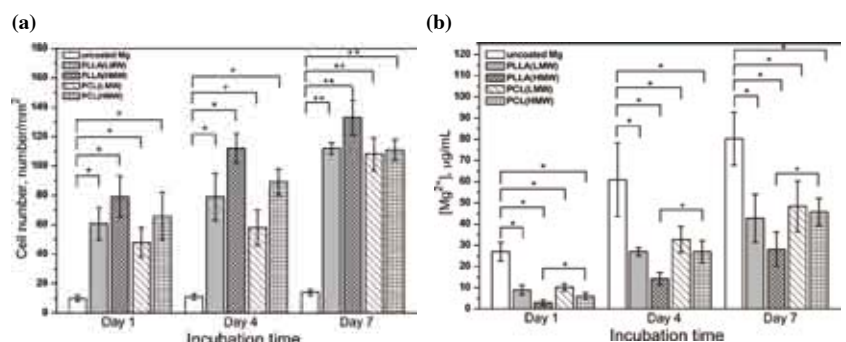


Fig. 2. (a) Proliferation of SaOS-2 on uncoated or polymer coated Mg samples during cell culture and (b) Mg²⁺ release during cell culture.

Laser-Based Inelastic Photoemission Spectroscopy

MANA Independent Scientist **Ryuichi ARAFUNE**



1. Outline of Research

My main objective is to explore and elucidate some aspects of the interaction between light and matter that take place uniquely at the solid surfaces. Currently, we concentrate on developing laser-photoemission spectroscopy (PES) into a novel technique to probe surface dynamics. Vibrational dynamics of adsorbate-substrate modes of adsorbed atoms and molecules can yield direct information on the nature of the bonding with the surface and on the energy exchange between the adsorbate and the substrate. Such modes appear at low-energy region (<100 meV). Unfortunately, no time-resolved surface vibrational technique that is applicable to low-energy vibrational modes has been developed thus far. Thus, a novel technique that can access such low energy vibrational modes is highly demanded.

Recently, we found that the photoemission spectra excited by the laser light contained the vibrationally induced inelastic components.¹⁾ This result indicates that the laser-excited and low-energy photoelectron strongly interacts with vibrational elementary excitations. We believe that this inelastic interaction has potentiality for measuring the dynamics of the electron-vibration interaction. The aim of this research project is the development of a novel PES and measurement of the vibrational dynamics (including the charge transport property) at solid surfaces. By measuring low energy photoelectron spectra of surfaces excited by the pulse laser light whose energy is tuned slightly higher than the work function of the solid surface, we will elucidate some aspects of the dynamic interactions between low-energy electrons and surface elementary excitations. This technique enables us to investigate vibrational and electronic dynamics of adsorbate on solid surfaces in the time range of picoseconds to femtoseconds.

2. Research Activities

(1) High energy-resolved two-photon photoemission.

Two-photon photoemission (2PPE) spectroscopy is a unique tool to probe surface electronic structures between the Fermi and vacuum level.²⁾ The fs-Ti:S based pulse lasers are generally used for the excitation light source. The measurement by the fs laser is powerful to investigate electron wavepacket dynamics near the surface in the real-time domain. However, from the spectroscopic point of view, such very short light pulses cause the spectral peak to broaden. Thus, it is difficult to discuss the unoccupied electronic structure in detail from the 2PPE spectra excited by the fs laser.

To reveal the unoccupied electronic structure with high energy-resolution, by careful experimental planning, we have succeeded in measuring the angle resolved 2PPE spectra with the enough S/N ratio. By using ps laser as

the excitation light source, we have succeeded in measuring the dispersion relation of the high order ($n=4$) image potential state of the Cu(001), which cannot be resolved in the spectra excited by the fs laser (Fig. 1). In addition, the dispersion curve of the image resonance of the Cu(110), which is essentially broad peak due to very short lifetime, has been obtained. We have found that these image-potential induced states are available above the vacuum level.

One of the next directions of inelastic photoemission spectroscopy is monitoring surface relaxation processes after photo excitation through the vibration states by means of the pump-probe method. In the pump-probe experiments, it is important to expose the sample to the pump and probe light pulses simultaneously. The precision of the overlapping two pulses determines the temporal resolution. Since 2PPE intensity is sensitive to temporal and spatial overlapping between two pulses, 2PPE technique is useful to examine simultaneity of two light pulses in the pump-probe method. Thus, we believe that this result is important from not only the viewpoint of determination of the surface band structure in the unoccupied region, but also next progress in inelastic photoemission spectroscopy.

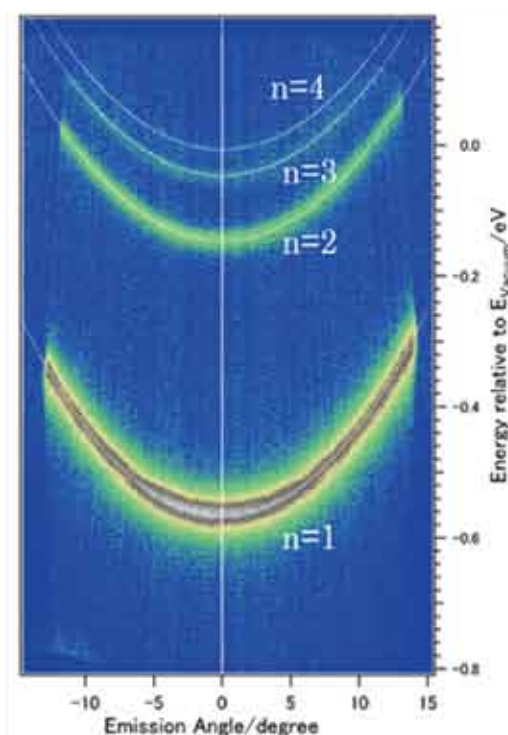


Fig. 1. Angle resolved 2PPE spectra of Cu(001).

References

- 1) R. Arafune et al., *Phys. Rev. Lett.* **95**, 207601 (2005).
- 2) U. Höfer et al., *Science* **277**, 1480 (1997).

Search for New Ferroelectric, Magnetic and Multiferroic Materials Using High-Pressure Technique

MANA Independent Scientist Alexei A. BELIK



1. Outline of Research

In multiferroic systems, two or all three of (anti)ferroelectricity, (anti)ferromagnetism, and ferroelasticity are observed in the same phase. These systems may have wide technological applications because they allow control of electric properties by magnetic field and control of magnetic properties by electric field (Fig. 1). The application would include, for example, multiple-state memory elements. Multiferroic materials have been studied in the past, but those studies did not attract wide attention most probably due to the lack of materials with strong magnetoelectric coupling and high ordering temperatures. Multiferroics have experienced revival interest and return to the forefront of condensed matter and materials research in the recent years because of the advanced preparation and characterization techniques. However in the field of multiferroic materials, two major problems still remain: (1) preparation of materials with multiferroic properties at and above room temperature (RT) and (2) preparation of materials with strong coupling between different order parameters.

Materials with a perovskite-type structure are of great interest in many fields of science and technology. Their applications range from the use as catalysts or sensors to superconductors, ferromagnetic, or ferroelectric materials. A new interest appeared recently for perovskite RCrO_3 and RMnO_3 as multiferroic materials.

We aim to develop new room-temperature multiferroic materials based on the perovskite-type structure using advanced high-pressure synthetic technique. We expect to find and develop new environmentally friendly lead-free materials with ferroelectric and multiferroic properties which will have superior properties compared with the known materials. The most attractive application of these materials is in non-volatile ferroelectric random access memory (FeRAM) elements.

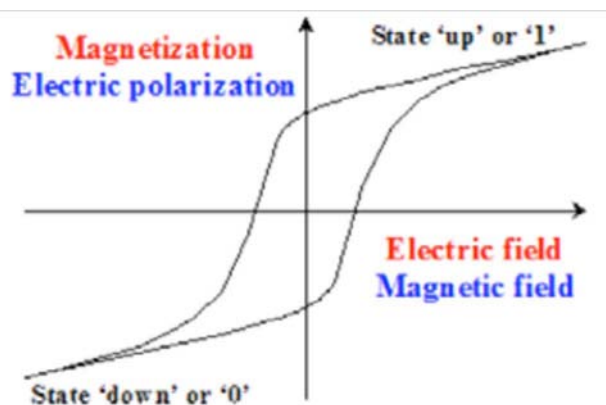


Fig. 1. Ferroelectric/ferromagnetic hysteresis loop: the basis of many memory elements.

2. Research Activities

(1) Structural Evolution of the BiFeO_3 - LaFeO_3 System.¹⁾

BiFeO_3 is the most studied multiferroic because the ferroelectric Curie temperature $T_E = 1100$ K and the antiferromagnetic Néel temperature $T_N = 640$ K are both well above RT; this compound continues to surprise by fascinating properties. However, “the exact nature and even the number of structural phase transitions as a function of La doping was still an open question.” We found four structural variations in the $(1-x)\text{BiFeO}_3$ - $x\text{LaFeO}_3$ system: $R3c$ for $0.0 \leq x \leq 0.10$, $Pnam$ (PbZrO_3 -related with $\sqrt{2}a_p \times 2\sqrt{2}a_p \times 4a_p$) for $\text{Bi}_{0.82}\text{La}_{0.18}\text{FeO}_3$, an incommensurately modulated phase with $\sqrt{2}a_p \times 2a_p \times \sqrt{2}a_p$ and the $Imma(00\gamma)s00$ superspace group for $0.19 \leq x \leq 0.3$, and $Pnma$ (GdFeO_3 -type with $\sqrt{2}a_p \times 2a_p \times \sqrt{2}a_p$) for $0.5 \leq x \leq 1$.

(2) Perovskite, LiNbO_3 , Corundum, and Hexagonal Polymorphs of $(\text{In}_{1-x}\text{M}_x)\text{MO}_3$.²⁾

ABO_3 compounds crystallize in a number of structure types, e.g., perovskite, LiNbO_3 , hexagonal LuMnO_3 -type, hexagonal BaMnO_3 -type, pyroxene, corundum, ilmenite (ordered corundum), rare earth sesquioxide structures (A, B, and C (bixbyite)), PbReO_3 , KSbO_3 , AlFeO_3 , CaIrO_3 , and others. Only limited number of ABO_3 compounds have more than two principally different modifications stable at or quenchable to ambient conditions. We prepared three modifications of $(\text{In}_{1-x}\text{M}_x)\text{MO}_3$ ($x = 0.143$; $M = \text{Fe}_{0.5}\text{Mn}_{0.5}$), which are stable at ambient pressure, and observed one unquenchable modification at high pressure. The irreversible transformation sequence of $\text{LiNbO}_3 > \text{corundum} > \text{hexagonal}$ on heating at ambient pressure is a new one and of interest because it has the order-disorder-order character.

(3) Low-temperature vacuum reduction of BiMnO_3 .³⁾

Transition metal oxides are very important for both fundamental and applied sciences. Their structural and physical properties are usually modified/improved by cation and anion doping. The oxygen content is known to have crucial and dramatic roles on properties of materials. In the case of oxygen deficient $\text{BiMnO}_{3-\delta}$, direct synthesis methods were unsuccessful. We found a method that gives an oxygen-deficient sample with the composition of $\text{BiMnO}_{2.81}$. The preparation method may be promising for the reduction of the oxygen content in other Bi- and Pb-based oxides.

References

- 1) D.A. Rusakov, A.M. Abakumov, K. Yamaura, A.A. Belik, G. Van Tendeloo, E. Takayama-Muromachi, *Chem. Mater.* **23**, 285 (2011).
- 2) A.A. Belik, T. Furubayashi, H. Yusa, E. Takayama-Muromachi, *J. Am. Chem. Soc.* **133**, 9405 (2011).
- 3) A.A. Belik, Y. Matsushita, M. Tanaka, E. Takayama-Muromachi, *Inorg. Chem.* **50**, 7685 (2011).

Graphene-Based Quantum-Dot Devices

MANA Independent Scientist Satoshi MORIYAMA



1. Outline of Research

Since the successful exfoliation of single-layer graphene sheets in 2004, the relationship between the structure and physical properties of π -conjugated graphene has attracted enormous interest. Furthermore, functionalization, which is routinely used to modify the properties of materials, has been extensively researched in graphene. The low-energy physics of graphene is described theoretically by (2+1)-dimensional Dirac fermions, where '2-dimensions' corresponds to a graphite sheet and '1-dimension' denotes time. The corresponding energy dispersion becomes the so-called Dirac cone, which leads to rich physics inherited from quantum electrodynamics.

Our research objective is the realization of quantum wires and quantum dots in graphene-based materials by using the nano-fabrication process, toward the novel graphene-based quantum devices. It will be expected that the fabricated quantum wires or quantum dots become integrated quantum circuits because of its 2-dimensional sheet structure. Furthermore, their low atomic weight and the low nuclear spin concentration, arising from the only 1.1% natural abundance of ^{13}C are expected for having weak spin-orbit interactions and hyperfine interactions. Therefore, graphene-based quantum devices are promising candidates for spin-based quantum information processing and spintronic devices.

2. Research Activities

(1) Selective edge modification in grapheme.¹⁾

The effect of edge structures in graphene sheets has been well investigated theoretically but most experimentally demonstrated functionalization schemes have been for bulk structures because not too many reported chemical methods selectively modify only the edges. We investigated a chemical method using the Lemieux-von Rudloff reagent that selectively oxidizes the edges of graphene sheets. Various functionalizations of the edge structure by conventional synthetic methods will be possible using the obtained edge-oxidized graphene as a starting material.

Raman line-mapping analysis of a graphene sheet before and after the weak oxidation provided clear evidence of selective modification of the edges of the graphene sheet. After the weak oxidation, the D-band ($\sim 1350\text{ cm}^{-1}$) intensity at the edges increased by a factor of about 10. In contrast, the D-band intensity remained nearly constant in the inner parts of the sheet and it was too weak to identify suggesting that the structure in the inner parts of graphene

remained largely unchanged after weak oxidation. Our experimental results indicate that selective oxidation occurred only at the edges of the graphene sheet and $-\text{COOH}$, $-\text{C}=\text{O}$, and other functional groups were introduced to edge structures. It is well-known that the edge structure of a graphene sheet strongly affects its electronic properties. Our findings regarding the edge modification will be useful for developing graphene chemistry in terms of both theoretical studies and applications because the oxidized edges of graphene can be further functionalized by various organic synthesis techniques.

(2) Field-induced quantum dots in grapheme.²⁾

In most cases, the formation of graphene quantum-dot devices relies on the removal of unwanted areas of graphene by etching.^{3,4)} The performance of such quantum dots is limited due to the detail of nano-constriction structures. Therefore, it is crucially important to develop other methods of creating graphene nanostructures and control the constriction. Here, I proposed novel quantum-dot device structures. We fabricated the perfectly isolated graphene islands, and contacted the electrodes directly to the graphene islands with no constrictions. As discussed above, it is free from the disturbance due to the detail of constrictions. We discovered the evolution of the Coulomb oscillations under a magnetic field i.e. 'magnetic-field-induced confinement', which leads to the transport spectroscopy (Fig. 1).

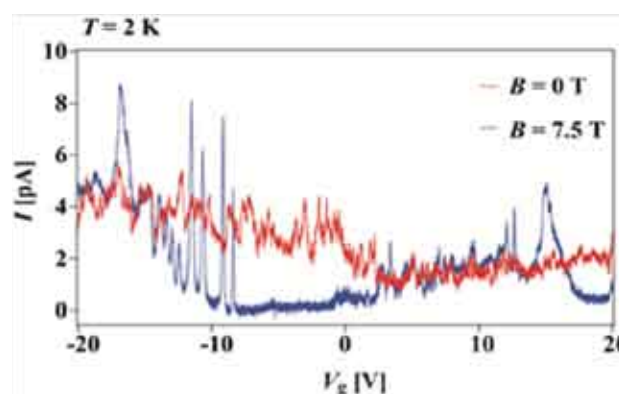


Fig. 1. Current as a function of back gate voltage at low bias ($V_{sd} = 0.1\text{ mV}$), measured at 2 K, $B = 0\text{ T}$ (red) and 7.5 T (blue). Magnetic fields were applied perpendicular to the graphene

References

- 1) M. Yang, S. Moriyama, M. Higuchi, submitted.
- 2) S. Moriyama, Y. Morita, E. Watanabe, D. Tsuya, in preparation.
- 3) S. Moriyama *et al.*, *Nano Lett.* **9**, 2891 (2009).
- 4) S. Moriyama *et al.*, *Sci. Technol. Adv. Mater.* **11**, 054601 (2010).

Development of Photoresponsive Biointerfaces

MANA Independent Scientist Jun NAKANISHI



1. Outline of Research

Biointerface is an interface between biomolecules and materials. It plays a pivotal role in biomedical devices such as materials for drug delivery, tissue engineering, and bioanalysis. The major purpose of the present study is to develop chemically functionalized biointerfaces with photochemically active compounds and apply them for analyzing and engineering cellular functions (Fig. 1).

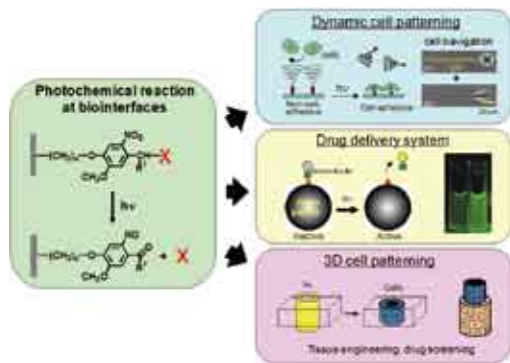


Fig. 1. Photoresponsive biointerfaces developing in this study.

2. Research Activities

(1) *Dynamic culture substrate that captures a specific extracellular matrix protein in response to light.*¹⁾

A chemically functionalized gold substrate that captures a genetically tagged extracellular matrix protein in response to light was developed (Fig. 2). The substrate was composed of mixed self-assembled monolayers of three disulfide compounds containing (i) a photocleavable poly(ethylene glycol) (PEG), (ii) nitrilotriacetic acid (NTA), and (iii) hepta(ethylene glycol) (EG7). Although the NTA group has an intrinsic high affinity for oligohistidine tag (His-tag) sequences in its Ni²⁺-ion complex, the interaction was suppressed by the steric hindrance of coexisting PEG on the substrate surface. Upon photoirradiation of the substrate to release the PEG chain from the surface, this interaction became possible and hence the protein was captured at the irradiated regions, while keeping the nonspecific adsorption of non-His-tagged proteins blocked by the EG₇ underbrush. In this way, we selectively immobilized a His-tagged fibronectin fragment (FNIII₇₋₁₀) to the irradiated regions. In contrast, when bovine serum albumin - a major

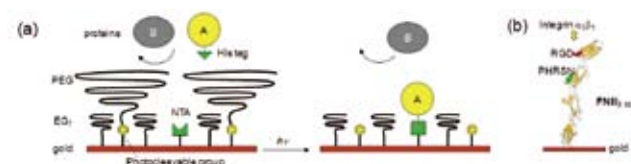


Fig. 2. Schematic of a dynamic substrate that captures His-tagged proteins in response to light.

serum protein - was added as a non-His-tagged protein, the surface did not permit its capture, with or without irradiation. In agreement with these results, cells were selectively attached to the irradiated patterns only when a His-tagged FNIII₇₋₁₀ was added to the medium. These results indicate that the present method is useful for studying the cellular behavior on the specific extracellular matrix protein in cell-culturing environments.

(2) *Photoactivatable Culture Substrate for the Assay of Collective Cell Migration.*²⁾

Collective cell migration plays a major role in cancer metastasis and wound healing, therefore, several in vitro assays for studying such behavior have been developed. Using photoactivatable culture substrates we studied collective sheet-like cell migration behavior of epithelial Madin-Darby canine kidney (MDCK) cells from initially precisely controlled adhesive patterns (Fig. 3). Poly(ethylene glycol) (PEG) was conjugated to a glass coverslip via a 2-nitrobenzyl group, which cleaves upon exposure to near-UV light, changing the surface from non-cell-adhesive to cell-adhesive. Initial cell attaching areas were generated in arbitrary geometries via projection exposure through a photomask placed at the field diaphragm of a fluorescence microscope. The cells were released from the initial geometrical confinement by a second flood exposure of the surface inducing cell migration. Our experiments showed that cluster size and boundary curvature affected the expansion of the cell sheet and the formation of leader cells. At a certain cluster size, characteristics of the expansion behavior changed. With donut-like ring structures, we demonstrated a break in symmetry between the behavior of cells along the outer convex boundary and along the inner concave boundary. Additionally, we observed that collective migration characteristics are modulated by the initial culture time of the cell sheet.

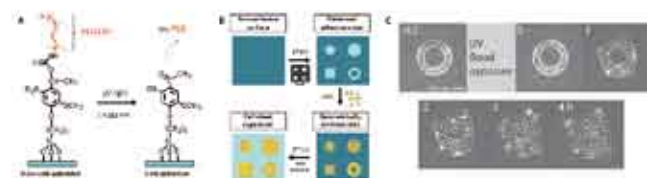


Fig. 3. (A) Photoactivatable substrate. (B) Procedure for cell patterning and cell migration induction. (C) Expansion of MDCK cells from a donut shape pattern.

References

- 1) J. Nakanishi, H. Nakayama, K. Yamaguchi, A.J. Garcia, Y. Horiike, *Sci. Technol. Adv. Mater.* **12**, 044608 (2011).
- 2) C.G. Rolli, H. Nakayama, K. Yamaguchi, J.P. Spatz, R. Kemkemer, J. Nakanishi, *Biomater.*, in press. doi: 10.1016/j.biomaterials.2011.12.012

Green Nanochemistry: Bandgap Engineering for Group IV Nanostructures

MANA Independent Scientist Naoto SHIRAHATA



1. Outline of Research

Findings of strong luminescence from nanostructures of group IV semiconductors and their compounds, i.e., Si, Ge, $\text{Si}_x\text{Ge}_{1-x}$, and silicide, have generated a great deal of excitement because their light emitters have a potential to open a new door to silicon photonics. Furthermore, the industrial use of efficiently luminescent group IV nanostructures possibly overcomes the unstable supply issue of rare-earth elements which raises a threat to the present industry of light emitters including LED and laser devices, and would give the significant contribution to realize a lighting industry for sustainable future.

2. Research Activities

(1) *A wide range of Multicolor Fine-Tuning: UV through visible to near-IR emission from Si nanostructures.*^{1,2)}

One of the impacts in the use of Si light emitters is definitely a wide continuous spectral tunability as shown in Fig. 1. Interestingly, Si is a solid element to allow the widening of color tunability ranging from UV through visible to near-IR wavelengths. Additionally, some of these emission colors are known to show highly luminescence features (PL QYs > 20%) which are comparable to the values of compound semiconductor QDs. The device application of Si simplifies the interior constitution of the device systems, leading to the good cost performance and the space-saving (being smaller, thinner, and lighter) of light-emitting devices.



Fig. 1. Color-tunable light emission from Si nanocrystals with controlled.

(2) *Minimum Size to Form a Diamond Cubic lattice.*²⁾

A wide variety of nanostructures can be theoretically and experimentally reported such as diamond cubic lattice as well as bulk Si, clusters, polysilanes including silanes, and amorphous structures unlike most of metal nanostructures, e.g., Au and Pt. The difference in structural phase of Si nanoparticles would influence significantly on the optical absorption and emission structures, making it more difficult to control precisely light emission properties. HR-TEM is one of the powerful tools to reveal the real atomic arrangement (Fig. 2). Si NCs were prepared by sodium biphenylide reduction of SiCl_4 in the presence of surfactant. In every high-resolution image, periodic arrangements of channel structures surrounded by Si tetrahedrons are clearly visible. NCs having diameter $d > 1.5$ nm have diamond cubic lattice structures. The same is true for 1.5-nm NCs; thus, a 1.5-nm NC is large enough to form a diamond cubic lattice. Surprisingly, a 1.1-nm NC, unlike other NCs,

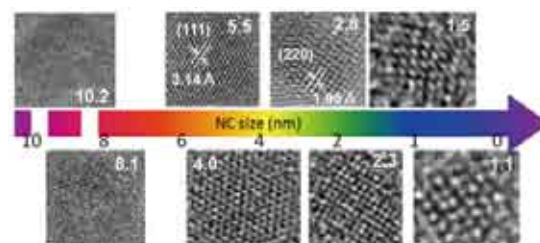


Fig. 2. HR-TEM images showing lattice fringes of the different size of Si NCs synthesized by inverse micelle method.

cannot have a diamond cubic lattice. At 1.1 nm, about 30 atoms are required to produce a diamond cubic lattice. Although a complementary simulation study is needed to determine the real atomic geometry, the minimum size that allows the formation of a diamond cubic lattice may be found to lie in the 1.2–1.5-nm size regime.

(3) *Laser Chemical Synthesis of Ge Nanoparticles.*³⁾

Color-tuned PL properties in a wide wavelength of UV-visible are observed from Ge NPs. The appearance of such unique light emission features required the careful control of their nanostructures including crystalline phase and surface chemistry. In the present study, a laser chemical method was used to produce Ge NPs capped monolayers. A molecular density of the surface monolayer was a key to control the PL features. In fact, we developed a color separation method to prepare NPs which efficiently emit the lights at UV, violet, blue, light-blue and green wavelength regions, respectively (Fig. 3).

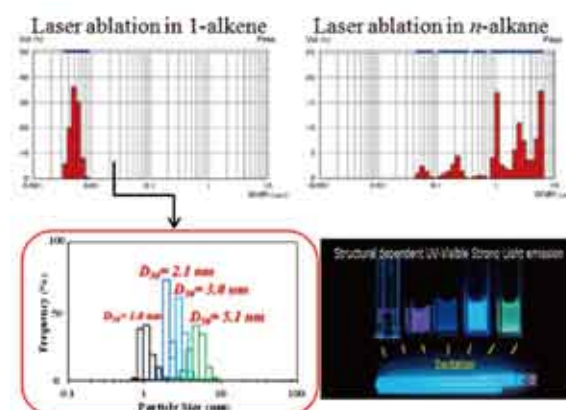


Fig. 3. Important role of 1-alkene as a solvent for liquid laser ablation, efficiently producing nanoparticles with size ranging from 1 to 10 nm. The well-controlled organic modification allows the emission color separation, and the structural-dependent light emissions at single excitation.

References

- 1) N. Shirahata, T. Tsuruoka, T. Hasegawa, Y. Sakka, *Small* **6**, 915 (2010).
- 2) N. Shirahata, *Phys. Chem. Chem. Phys.* **13**, 7284 (2011). Perspective Article.
- 3) N. Shirahata, D. Hirakawa, Y. Sakka, *Jpn. Patent Appl.* 2011-239933.

Metal Oxide Quantum-Confined Structures: Aqueous Design, Electronic Structure & Size Dependence on Chemical & Physical Properties

MANA Independent Scientist **Lionel VAYSSIERES**



1. Outline of Research

We aim to contribute to the development of a new generation of clean metal oxide materials using nanoscale and quantum confinement phenomena to create multifunctional structures and devices for renewable energy, environment, and health by cost-effective large scale fabrication techniques. We are developing series of novel materials for solar hydrogen generation, photovoltaics, sensors, and surface controlled nanoparticles and quantum dots for nanotoxicology studies utilizing low-cost and large scale materials chemistry such as aqueous chemical growth to fabricate structures and devices (Fig. 1) based on quantum-confined metal oxide (hetero)-nanostructures.¹⁻³⁾

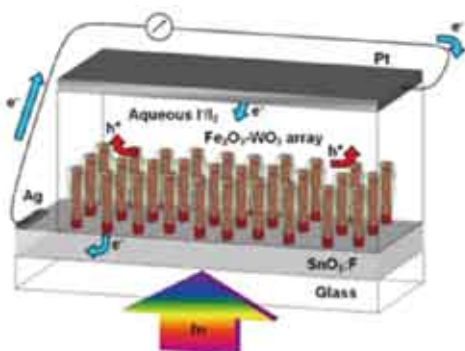


Fig. 1. Scheme of a hetero-nanostructured visible light active photoelectrochemical systems for water splitting applications. The anode consists of a quantum-rod based large bandgap semiconductor (e.g. iron oxide) coated with another photoactive semiconductor (e.g. tungsten oxide).

2. Research Activities

We have synthesized and characterized the electronic structure and basic structural, optical, and photoelectrochemical properties of novel visible light active iron oxide-based semiconductors consisting of vertically oriented quantum rod arrays. Doped and/or quantum dot sensitized bundle of iron oxide quantum rods which by intermediate band effects enable a full visible absorption profile while still being stable against photo-corrosion for efficient and low cost solar hydrogen generation by direct water splitting at neutral pH allowing therefore the use of the largest free natural resource on Earth, that is seawater, as unique electrolyte.⁴⁾

Another aspect of our research activities involved the controlled fabrication of quantum dots of tailored sizes in aqueous solutions without surfactant and thus the ability to control their surface acidity and properties. Size effect in general on the physical properties and electronic structure of metals and semiconductors are well established in the literature. However, the effect of quantum dot size on the chemical properties of materials and, in particular, on the surface chemistry of hydrated metal oxides has scarcely been reported. We have investigated the effect of the size of quantum dots of γ -Fe₂O₃ on their aqueous surface chem-

istry. Indeed, the effect of size on the surface chemistry of metal oxides was demonstrated by the reversal of the surface acidity from acidic to neutral to basic by changing the size from 12 to 7.5 to 3.5 nm, respectively.⁵⁾ Recent developments include the synthesis of large quantities of pure TiO₂ anatase quantum dots without the use of surfactant. Thermodynamically and kinetically stable aqueous suspensions have been obtained at various concentration of Ti from which powders have been extracted by ultracentrifugation. In depth analysis of the size dependence over two orders of magnitude (i.e. from 2-200 nm in diameter) electronic structure performed at synchrotron radiation reveals a direct effect of the nanoparticle size on the orbital character of TiO₂ anatase quantum dots⁶⁾ with important repercussion for enhanced electrical properties of large bandgap semiconductors.

Finally, a direct experimental observation of spontaneous electron enrichment of metal d orbitals in a new transition metal oxide heterostructure (Fig. 2) with nanoscale dimensionality has been recorded. Such a study has direct implications for the understanding of electron gradient formation at the interface of heteronanostructures.⁷⁾

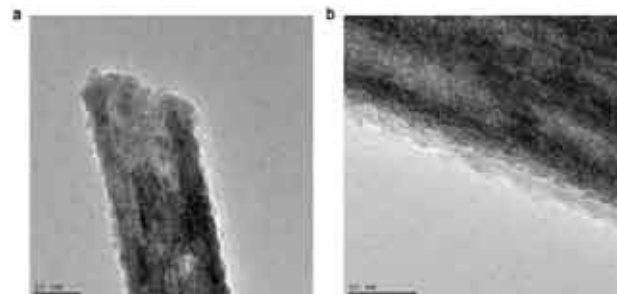


Fig. 2. Transmission electron microscopy of a representative Ti-O-Fe₂O₃ hetero-nanostructure: (a) tip of a complete structure and (b) magnified view of the core-shell interface highlighting the faceted structure of the Ti-O nanocrystalline layer, with lattice fringes in alpha-Fe₂O₃ single crystals evident.

References

- 1) C.X. Kronawitter, L.Vayssieres, S. Shen, L. Guo, D. Wheeler, J.Z. Zhang, B.R. Antoun, S.S. Mao, *Energy Environ. Sci.* **4**, 3889 (2011).
- 2) L.Vayssieres, *Proc. Am. Chem. Soc., Div. Fuel Chem.* **56**, 135 (2011).
- 3) L.Vayssieres, in *Advances in Spectroscopy and Imaging of Surfaces and Nanostructures*, edited by J. Cumings, D. Fong, J. Huang, S. Lindsay, G. Zhou, J. Guo, H. Bluhm, M. Havecker, S.Yamaguchi, F.M. Granozio, G. Koster, G. Eres, C-B. Eom, N. Ingle, O.V. Kolosov, B.D. Huey, S. Hong and H. Shin (*Mater. Res. Soc. Symp. Proc.* **1318**, Warrendale, PA, 2011), pp. 1-12.
- 4) L.Vayssieres, "Quantum confined visible-light active metal oxide nanostructures for direct solar-to-hydrogen generation" in *On Solar Hydrogen & Nanotechnology*, L.Vayssieres editor (John Wiley & Sons, 2009), Chapter 17, pp. 523-558.
- 5) L.Vayssieres, *J. Phys. Chem. C* **113**, 4733 (2009).
- 6) L.Vayssieres, C. Persson, J. Guo, *Appl. Phys. Lett.* **99**, 183101 (2011).
- 7) C.X. Kronawitter, J.R. Bakke, D. Wheeler, W.C. Wang, C. L. Chang, B.R. Antoun, J.Z. Zhang, J.H. Guo, S. F. Bent, S.S. Mao, L.Vayssieres, *Nano Lett.* **11**, 3855 (2011).

Theoretical Research on Electronic Properties of Nano-Carbon Systems

MANA Independent Scientist Katsunori WAKABAYASHI



1. Outline of Research

Our research target is to theoretically reveal the peculiar electronic, magnetic, transport and optical properties in nano-carbon materials such as graphene, nano-graphene, graphene nanoribbons, nanotubes using theoretical and/or computation method. Recently graphene, one-atomic thickness carbon sheet, has attracted much attention both from the fundamental and applied sciences, since the electronic states are described by the massless Dirac Fermion in sharp contrast with the conventional two-dimensional electron gas on the semiconductor devices.

The successive miniaturization of the graphene electronic devices inevitably demands the clarification of edge effects on the electronic structures, electronic transport and magnetic properties of nanometer-sized graphene. The presence of edges in graphene has strong implications for the low-energy spectrum of the π -electrons. There are two basic shapes of edges, armchair and zigzag, which determine the properties of graphene ribbons. It was shown that ribbons with zigzag edges (zigzag ribbon) possess localized edge states with energies close to the Fermi level.

On the background mentioned above, the main purpose of our research is to clarify the peculiar features in electronic, magnetic and transport properties of nano- and meso-scopic systems based on carbon materials. Also, we aim to design and explore theoretically the new functionalities as the next-generation devices based on the peculiar electronic properties.

2. Research Activities

(1) Perfect Conducting Channel.^{1,3)}

Numerical calculations have been performed to elucidate unconventional electronic transport properties in disordered zigzag nanoribbons. The energy band structure of zigzag nanoribbons has two valleys that are well separated in momentum space, related to the two Dirac points of the graphene spectrum. The partial flat bands due to edge states make the imbalance between left- and right-going modes in each valley, i.e. appearance of a single chiral mode. This feature gives rise to a perfectly conducting channel in the disordered system, i.e. the average of conductance $\langle g \rangle$ converges exponentially to 1 conductance quantum per spin with increasing system length, provided impurity scattering does not connect the two valleys, as is the case for long-range impurity potentials. We have also identified that these peculiar transport properties are related to the time-reversal symmetry breaking for pseudospin in graphene due to the presence of zigzag edge boundary.

(2) Development of Analytic Method.^{4,7)}

The development of analytic method for massless Dirac Fermion systems is necessary not only for improvement of computational code but also for the intuitive understanding of quantum phenomena in the system. Recently we have succeeded to derive the full spectrum and corresponding wave function of graphene nanoribbons within the tight-binding model using wave-mechanics approach and transfer matrix approach. These analytical approaches revealed the scattering mechanism of pseudospins near the graphene edges. The states of pseudospins are conserved in the scattering process at the armchair edge, however the states of pseudospins are flipped in the scattering process at the zigzag edge. This striking difference in the scattering process of pseudospins at the graphene edges are decisive in the response of Raman spectroscopy and Berry's phase structures at the low-energy electronic properties of graphene near the edges.

(3) Electronic states of graphene corner edge and magic corner angle.⁸⁾

The electronic states of graphene corner edge are of crucial issues from the experimental point of view, because the edge structures are relevant with the structural stability of the system. Recently we have studied the electronic states of semi-infinite graphene with a corner edge. The 60, 90, 120, and 150° corner edges are examined. We have numerically studied the local density of states (LDOS) on the basis of a nearest-neighbor tight-binding model using Haydock's recursion method. It was found that edge localized states appear along a zigzag edge of each corner edge structure except for the 120° case. This magic angle was analyzed within the framework of an effective mass equation.

References

- 1) K. Wakabayashi, Y. Takane, M. Yamamoto, M. Sigrist, *New J. Phys.* **11**, 095016 (2009).
- 2) K. Wakabayashi, Y. Takane, M. Yamamoto, M. Sigrist, *Carbon (Elsevier)* **47**, 124 (2009).
- 3) M. Yamamoto, Y. Takane, K. Wakabayashi, *Phys. Rev. B* **79**, 125421 (2009).
- 4) K. Sasaki, K. Wakabayashi, T. Enoki, *New J. Phys.* **12**, 083023 (2010).
- 5) K. Wakabayashi, K. Sasaki, T. Nakanishi, T. Enoki, *Sci. Technol. Adv. Mater.* **11**, 054504 (2010).
- 6) K. Wakabayashi, "Electronic Properties of Nanographene", published as the Chapter 4 of "Physics and Chemistry of Graphene: Graphene to Nanographene", Pan Stanford Publisher (2012). (in press)
- 7) K. Sasaki, K. Wakabayashi, T. Enoki, *J. Phys. Soc. Jpn.* **80**, 044710 (2011).
- 8) Y. Shimomura, Y. Takane, K. Wakabayashi, *J. Phys. Soc. Jpn.* **80**, 054710 (2011).

Synthesis and Application of Mesoporous Pt

MANA Independent Scientist Yusuke YAMAUCHI



1. Outline of Research

Because of their scientific and practical significance, research on mesoporous materials, conducted mainly by using surfactant assemblies as templates, has been increasing rapidly. The specific features of regular pore arrangement, uniform mesopore size, and high surface area make these materials very promising for various applications. Especially, mesoporous metals with high electroconductivity have attracted particular interest for their very wide range of applications in such items as batteries, fuel cells, solar cells, chemical sensors, field emitters, and photonic devices. Although several mesoporous metals have been prepared in the past, the mesostructures of these metals are less ordered than those reported for inorganic oxides such as silica. Therefore, the rational design of highly ordered mesoporous metals with controlled compositions and morphologies for practical applications is a most attractive and challenging objective.¹⁻¹³⁾

2. Research Activities

Compared to silica and carbon, mesoporous metals have fascinating properties inherent to metal frameworks (e.g., high electroconductivity, catalytic activities, etc.) along with the general characteristics of mesoporous materials. Therefore, we can anticipate various electrochemical applications which cannot be realized by traditional mesoporous silica. Several approaches have been reported for the preparation of mesoporous/mesostructured metals. The lyotropic liquid crystals made of highly concentrated surfactants or block copolymers have been utilized as soft-template. By using chemical or electrochemical reduction, ordered mesoporous metal powders or films can be synthesized, respectively. However, the ordered arrangement of the rod-self assemblies in the liquid crystals is often distorted during metal deposition process, thereby lacking a long range order of mesoporous structures in the final product. Comparing to the soft-templating method, hard-templating method is a very attractive pathway which is widely applicable to various compositions. Mesoporous silica with a robust framework and high thermal stability is used as a hard template to synthesize a metal replica. So far, various Pt nanostructures such as 1D nanowires and 3D nanowire networks were prepared by using MCM-41 (p6mm), SBA-15 (p6mm), KIT-6 (Ia-3d), and MCM-48 (Ia-3d) as hard-templates.

Despite those recent advances in the soft- and hard-templates, the obtained morphologies of mesoporous metals have been very limited to only powders with irregular morphology or films on conductive substrates. The lack of

the controllability in the particle sizes and morphologies is serious problem for further development of mesoporous metals. The shape and size distribution of the nanoparticles are critical parameters of the function and utility for applications. To bring out shape- and size-dependent physicochemical properties, it is extremely important to prepare uniform-sized particles with the same shapes in high yield.

Very recently, we proposed new concept on shape- and size-controlled synthesis of mesoporous metals in hard-templates. We demonstrated a facile synthesis of uniformly-sized mesoporous Pt nanoparticles by using mesoporous silica KIT-6 (Ia-3d) or SBA-15 (p6mm) as hard-templates and ascorbic acid as reducing agent (Fig. 1).¹⁾

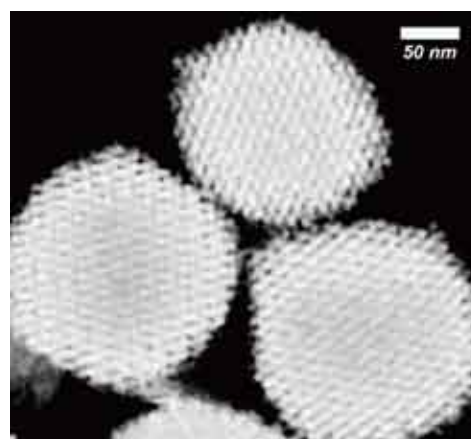


Fig. 1. TEM image of Mesoporous Pt particles.

References

- 1) H. Wang, H.Y. Jeong, M. Imura, L. Wang, L. Radhakrishnan, N. Fujita, C. Toen, O. Terasaki, Y. Yamauchi, *J. Am. Chem. Soc.* **133**, 14526 (2011).
- 2) M. Hu, J. Reboul, S. Furukawa, L. Radhakrishnan, Y. Zhang, P. Srinivasu, H. Iwai, H. Wang, Y. Nemoto, N. Suzuki, S. Kitagawa, Y. Yamauchi, *Chem. Commun.* **47**, 8124 (2011).
- 3) L. Wang, Y. Nemoto, Y. Yamauchi, *J. Am. Chem. Soc.* **133**, 9674 (2011).
- 4) A. Takai, H. Atae-Esfahani, Y. Doi, M. Fuziwara, Y. Yamauchi, K. Kuroda, *Chem. Commun.* **47**, 7701 (2011).
- 5) C. Urata, H. Yamada, R. Wakabayashi, Y. Aoyama, S. Hirose, S. Arai, S. Takeoka, Y. Yamauchi, K. Kuroda, *J. Am. Chem. Soc.* **133**, 8102 (2011).
- 6) H. Oveisi, X. Jiang, M. Imura, Y. Nemoto, Y. Sakamoto, Y. Yamauchi, *Angew. Chem. Int. Ed.* **50**, 7410 (2011).
- 7) L. Wang, Y. Yamauchi, *Chem. Eur. J.* **17**, 8810 (2011).
- 8) X. Jiang, H. Oveisi, Y. Nemoto, N. Suzuki, K.C.W. Wu, Y. Yamauchi, *Dalton Trans.* **40**, 10851 (2011).
- 9) M. Hu, Y. Yamauchi, *Chem. Asian J.* **6**, 2282 (2011).
- 10) L. Wang, Y. Yamauchi, *Chem. Mater.* **23**, 2457 (2011).
- 11) K.C. W. Wu, X. Jiang, Y. Yamauchi, *J. Mater. Chem.* **21**, 8934 (2011).
- 12) H. Atae-Esfahani, Y. Nemoto, L. Wang, Y. Yamauchi, *Chem. Commun.* **47**, 3885 (2011).
- 13) N. Suzuki, S. Kiba, Y. Yamauchi, *Phys. Chem. Chem. Phys.* **13**, 4957 (2011).

Nanomechanical Sensors for Medical, Security and Environmental Applications

MANA Independent Scientist Genki YOSHIKAWA



1. Outline of Research

The demands for new sensors are rapidly growing in various fields; for medical, security and environmental applications.

In a conventional blood test, for example, at least several days are required to identify the infectious bacteria. Accordingly, medical doctors prescribe an antibiotic based on their experiences (empiric therapy) as the first choice, thereby running the risk of fostering antibiotic-resistant bacteria everyday all over the world. Moreover, recent studies indicate that such overuse of antibiotics could be fuelling the dramatic increase in conditions such as obesity, type 1 diabetes, inflammatory bowel disease, allergies and asthma, because antibiotics kill the beneficial bacteria that we do want, as well as we do not, and our friendly flora has been found to be never fully recovered once the natural balance is upset.¹⁾

In the environmental field, the pollutions of air, water, and soil have been the long-standing issues. We have to keep monitoring any tiny indications to prevent new pollution from being widely spread. The sick house syndrome or various allergies could be also attributed to the pollution of our surrounding environment.

As for the security issues, many countries are still suffering from the tremendous numbers of land mines (the total number is estimated at more than 70 million). Detection of drugs and explosives is one of the critical requirements to oppose terrorism and antisocial forces.

Nanomechanical sensors have potential to contribute to these global grand challenges owing to their intrinsic versatility. Nanomechanical sensors detect volume and/or mass of target molecules, while there are no substances which do not have volume and mass. Therefore, nanomechanical sensors can be used for detecting virtually any kinds of substances. We are now trying to realize practically useful nanomechanical sensors which must fulfill the practical requirements, such as small, low-cost, easy to use anywhere in the world, in addition to the basic specifications, such as high sensitivity.

2. Research Activities

(1) Membrane-type Surface stress Sensors (MSS).

Recently, we made comprehensive optimization of a piezoresistive nanomechanical cantilever sensor and developed a membrane-type surface stress sensor (MSS; Fig. 1).²⁻³⁾ Experimental evaluation of a prototype MSS demonstrates a high sensitivity which is comparable with that of optical methods. Given the various conveniences and advantages of the integrated piezoresistive read-out, this platform is expected to open a new era of sensors, contributing to the above mentioned global grand challenges.

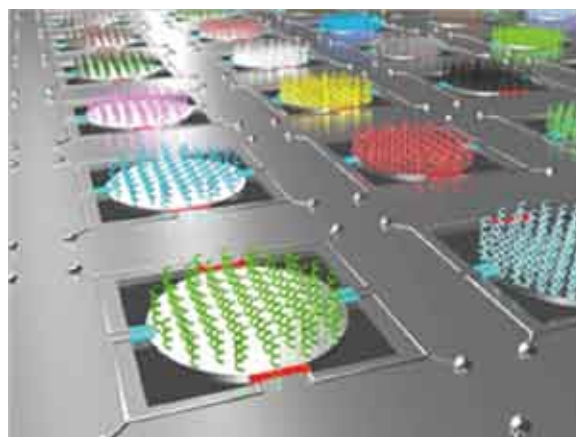


Fig. 1. Membrane-type Surface stress Sensor (MSS) and its arrayed structure.

(2) 2D array of MSS and visualization of smells.

To demonstrate the capability of MSS for the multi-dimensional array, we fabricated the two dimensionally arrayed MSS chip and succeeded in operating all channels simultaneously. In addition, the technological improvements in the micro-fabrication process led to much better sensitivity than that of the first prototype. Using this 2D MSS chip as a gas sensor, we succeeded in “visualizing smells” in real-time by converting signals from each channel in the 2D array into colored-pixels of the “picture.” We developed a mobile all-in-one device, which contains all required components for the gas measurements, including sensor chip, read-out electronics, pumps, etc., and successfully demonstrated the smell-visualization under ambient conditions.⁴⁾

(3) Optimization model for a receptor layer on nanomechanical sensors.

The functionalization and optimization of coating films on the sensor surfaces are the critically important challenges for actual applications. To provide a guideline for this issue, an analytical model for nanomechanical cantilever sensors coated with a solid receptor film is formulated, taking account of all relevant physical parameters of both cantilever and coating film.⁵⁾ This model provides accurate values verified by an excellent agreement with those simulated by finite element analyses. It will help toward analyzing the static behavior of nanomechanical sensors in conjunction with physical properties of coating films as well as optimizing the films for higher sensitivity.

References

- 1) M. Blaser, *Nature* **476**, 393 (2011).
- 2) G. Yoshikawa, H. Rohrer, *International Workshop on Nanomechanical Cantilever sensor*, Banff (2010).
- 3) G. Yoshikawa, T. Akiyama, S. Gautsch, P. Vettiger, H. Rohrer, *Nano Lett.* **11**, 1044 (2011).
- 4) G. Yoshikawa, A. M. Palumbo, *Patent pending*.
- 5) G. Yoshikawa, *Appl. Phys. Lett.* **98**, 173502 (2011).

Magneto-Responsive Soft Materials: Magnetically Reconfigurable in a Nonvolatile Fashion

ICYS-MANA Researcher

Fatin HAJJAJ



1. Outline of Research

The semiconductor industry has long sought a high-density, high-speed, low-power memory device that retains its data even when the power is interrupted. Nonvolatile memory concepts aimed at the horizon beyond 2013 are based on phase-change rather than charge storage where the transition between two different states represents the 1s and 0s of stored digital data. Responsive soft materials with phase-change capabilities under external stimuli, such as liquid crystals (LCs), are considered the most mature candidates for future nonvolatile data storage and reconfigurable electronics. The growing interest in integration of adaptive LC materials in devices brings about the need to utilize non-invasive stimuli to remotely trigger changes in the materials without induced degradation of the device performance. Among all potential external stimuli, a magnetic field has the benefits of contactless control, instant-nonharmful action, and easy integration into electronic devices, though it has only been used limitedly in manipulating supramolecular LC assemblies due to the complication of the forces that are involved. Magnetic-field-induced molecular switching is most suitable for ionic soft materials that are inconsistent with the application of electric fields. Despite these attractive features of the magnetic stimulus, up to date, there is no experimental evidence for a magnetically induced irreversible massive lattice distortion in LCs.

In this study, we demonstrated that the application of an external magnetic field can induce a massive structural transformation in ionic liquid crystalline material with orthorhombic phase structure.¹⁻²⁾

Due to structural features, this orthorhombic phase

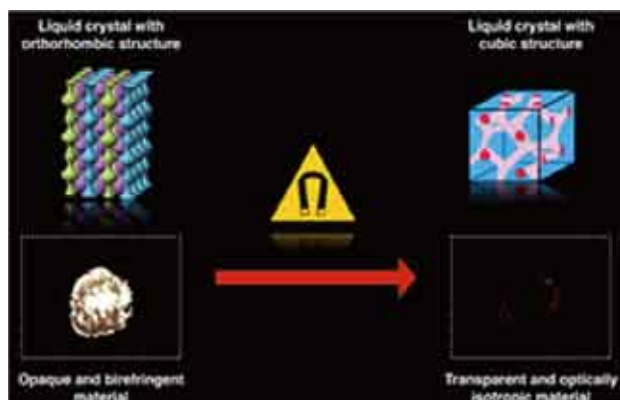


Fig. 1. Schematic representation and polarizing optical microscopic images of a magneto-responsive liquid crystalline material at 300 K before (orthorhombic phase) and after (cubic phase) exposure to a magnetic field.

structure (bright phase in Fig. 1) transfers preferentially into a more thermodynamically stable cubic phase structure (dark phase in Fig. 1) upon cooling its isotropic melt in the presence of magnetic fields. The transition is irreversible and accompanied by a spectacular change in the material property that confers a memory effect to the system. Our observations suggest that this new concept of magnetic-field-driven irreversible switching, based on magneto-responsive soft materials, may open up the doors for novel magneto-optical devices.

2. Research Activities

The synthesis of stable lanthanide-containing discotic liquid crystals (LCs) had been established. Depending on the ratio of added Ln^{3+} it is possible to engineer molecular assemblies with cubic, columnar orthorhombic, and columnar hexagonal structures at room temperature. The thermal stability and mesophase behavior were confirmed by X-ray diffraction (SPRING-8), polarized light optical microscopy (POM), and differential scanning calorimetry (DSC). Based on SQUID results, the samples show paramagnetic response from Ln^{3+} over a broad temperature range. *In situ* POM observations of the LCs phase growth on thin films indicate that the magnetic response of Ln^{3+} can make the material to undergo homeotropic alignment under a 5T magnetic field (Fig. 2). Permanent structural changes in the materials can be induced by cooling their isotropic melts $\sim 450\text{K}$ in the presence of a 5T magnetic field (Fig. 1). Such irreversible magnetic-field-induced phase transition is very promising for nonvolatile memory applications.



Fig. 2. Time-dependent magneto-optical response of orthorhombic liquid crystalline material at 420K under a 5T field. The optical images were taken with crossed-polarizers condition of the magneto-optical microscope.

References

- 1) F. Hajjaj, T. Kajitani, A. Yamaguchi, Y. Yamamoto, K. Kato, T. Fukushima, T. Aida, The 10th International Conference on Materials Chemistry, Manchester, UK (2011).
- 2) F. Hajjaj, T. Kajitani, K. Kato, H. Kitazawa, A. Yamaguchi, Y. Yamamoto, T. Fukushima, T. Aida, in preparation.

Optical Manipulation of Single-Electron Tunneling Through Photochromic Molecular Dots

ICYS-MANA Researcher

Ryoma HAYAKAWA



1. Outline of Research

A single-electron memory that adopt Si and Ge nano-dots as floating gates hold promise for future Si-based memory devices.^{1,2)} The reason is that the operating principle is based on the Coulomb blockade effect, which makes it possible to inject the carriers into the dots on the “single electron level”. Moreover, the device allows the multi-level operation and ultra-low power consumption, which are key challenges in future nano-electronics. In this study, we have proposed to use organic molecules as the floating gates.³⁾ Organic molecules are excellent quantum dots over inorganic counterparts. 1) Molecules have a uniform size in nanometer scale to achieve large number density of the quantum dot (10^{13} cm^{-2}). 2) Energy-levels of molecules are tunable by light irradiation, as represented by photochromic molecules. That is, the carrier injection for the memory can be manipulated by alternative external triggers those are light irradiation and gate voltage (Fig. 1). From these points of view, integration of unique molecular functions into single-electron memory is a prospective approach for achieving novel and practical molecular devices. We believe that the success of this study can provide a prototype device for “More than Moore”.

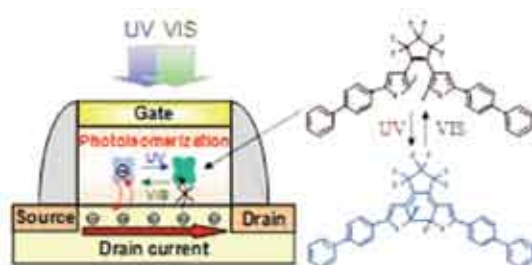


Fig. 1. Schematic illustration of optical single-electron memory devices with photochromic molecules as quantum dots.

2. Research Activities

(1) Photoisomerization of diarylethene thin films.

A derivative of diarylethene molecules was used to manipulate a single-electron tunneling by light irradiations. First of all, to clarify whether photoisomerization of the molecules takes place in a solid state, the 30 nm-thick films were formed on quartz substrates.

Fig. 2 shows optical images and UV-Vis spectra of the thin films after UV and VIS light irradiations. UV light irradiation induced the change in the color from transparent to blue. Meanwhile, the color was returned to original one by VIS light irradiation (Fig. 2a). Moreover, characteristic absorption peaks were observed at the wavelength of 320 nm for open-ring isomer and 610 nm for closed-ring one in UV-Vis spectra (Fig. 2b). These results clearly reveal that the solid-state diarylethene molecules are underwent photoisomerization due to the minimal change of molecular geometrical structure.

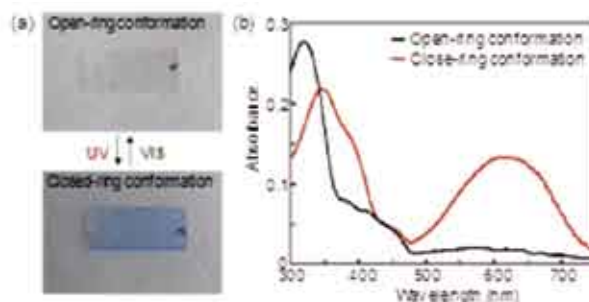


Fig. 2. Optical images (a) and UV-Vis spectra (b) of diarylethene thin films on quartz substrates.

(2) Optical control of single-electron tunneling via photochromic molecules in MIS structures.

A multilayer structure consisting of ITO/ Al_2O_3 /diarylethene molecule/ SiO_2 /Si was formed to manipulate single-electron tunneling (SET) by light irradiation. Multiple Coulomb staircases were seen in the I - V curve (Fig. 3). Meanwhile, no staircases were visible in the samples without molecules. These results clearly indicate that each diarylethene molecule works as a quantum dot for the SET in the double-tunnel-junction.

Subsequently, we successfully controlled the SET by light irradiations. Firstly, the threshold voltage of SET was shifted to lower voltage after UV light irradiation. After that, VIS light irradiation induced reversible change to higher voltage. In this manner, the reversible variation in the threshold voltage was repeatedly observed by alternate the UV and VIS light irradiations. These results demonstrate that the diarylethene molecules can work as optically-controllable quantum dots in the practical device configuration.

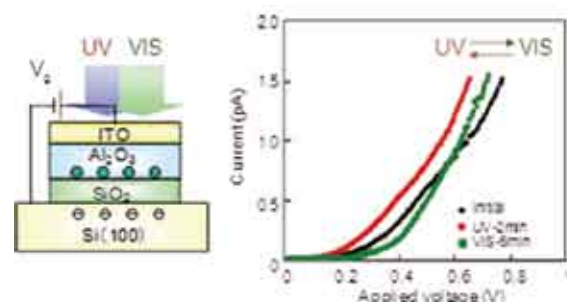


Fig. 3. Optical manipulation of single-electron tunneling in the samples with diarylethene molecules as quantum dots.

References

- 1) S. Tiwari, F. Rana, H. Hanafi, H. Haratstein, E.F. Crabbe, K. Chan, *Appl. Phys. Lett.* **68**, 1377 (1996).
- 2) C. Pace, F. Crupi, S. Lombardo, C. Gerardi, G. Cocorullo, *Appl. Phys. Lett.* **87**, 182106 (2005).
- 3) R. Hayakawa, N. Hiroshiba, T. Chikyow, Y. Wakayama, *Adv. Funct. Mater.* **21**, 2933 (2011).

Complementary-Like Graphene Logic Gates

ICYS-MANA Researcher

Song-Lin LI



1. Outline of Research

With the bulk silicon microelectronics approaching its physical limit, graphene (Fig. 1a), a two-dimensional material, is very attractive for next-generation nanoelectronics due to its atomic thickness, ultrahigh carrier mobility, and compatibility with planar semiconductor process. However, the ambipolar conduction behavior intrinsic to graphene hinders the fabrication of logic devices directly in a conventional complementary architecture. We showed the possibility of fabricating high-performance elementary graphene logic gates and demonstrated basic logic operations with a self-adaptive complementary-like architecture, in which the ambipolar nature is used as a benefit rather than a drawback to form logic devices. The results represent an important step toward graphene nanoelectronics.

2. Research Activities

(1) Graphene voltage inverter.¹⁾

As an ambipolar material, graphene exhibits both p - and n -type conduction branches which are separated by a charge neutrality point (CNP). We found that a voltage inverter (NOT gate) could be easily formed in a complementary-like geometry by directly connecting two ambipolar transistors. The otherwise overlapped CNPs of the two transistors naturally split by the potential superposition effect from supply bias (V_{DD}) applied. Between the two CNPs, complementary geometry forms with each transistor contributing either a p or n conduction branch. In addition, a facile but high capacitive efficiency ($\sim 1.2 \mu\text{F}/\text{cm}^2$) top gate technique was introduced to increase the coupling capacitance and lower the operating bias. For the first time, voltage gain up to 6 was achieved in gapless monolayer graphene inverters at cryogenic temperature of 77 K, despite the extremely low switching ratio ~ 5 of monolayer graphene. A match between input and output voltage levels was realized, indicating the potential for direct cascading between multiple devices for large-scale integration.

(2) Band gap opening in bilayer grapheme.²⁾

In order to further improve the switching ratio of graphene and device performance, band gap engineering was also employed. Band structure calculation shows that a band gap can be introduced in bilayer graphene with breaking the symmetry between top and bottom layers. By applying perpendicular electric fields on bilayer graphene through top and bottom gates, large transport band gap of ~ 100 meV and high switching ratio of ~ 200 was observed. Corresponding inverters were also fabricated based on the semiconducting bilayer graphene, with voltage gain up to 8 and output voltage swing up to 80% V_{DD} . The transfer characteristics were considerably improved in low V_{DD} region

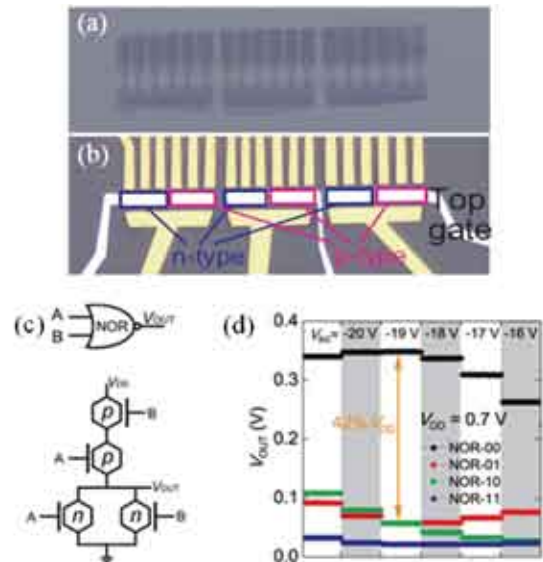


Fig. 1. (a) and (b) Optical images for a patterned bilayer graphene flake and corresponding logic devices. In (b) three voltage inverters are defined with three pairs of effective p - and n -type graphene transistors in each device. (c) Schematic diagram for a dual-input NOR gate, in which four transistors including two p -type and two n -type transistors are employed. (d) Logic operation for a NOR gate at $V_{DD} = 0.7$ V. The numbers XX (X = “0” or “1”) in NOR-XX denote the corresponding logic states of the two inputs.

due to the presence of band gap in the channels, indicating the potential for future low-bias logic circuits.

(3) Dual-input elementary logic gates.³⁾

Dual-input NAND and NOR gates are building pillars for various logic functions and devices in microelectronics. To extend the possible logic applications of graphene, these elementary logic gates were also fabricated by extending the complementary range using an asymmetric gating technique (Fig. 1c). We also developed a method to electrostatically control the relative positions of CNPs by gate coupling capacitances and to form equivalent p - and n -type transistors (Fig. 1b). This led to larger CNP splitting and makes the equivalent p - and n -type transistors more distinguishable on polarities and more effective to mimic the complementary function required by logic devices. The swing of output voltage reached about 40% for the formed NAND and NOR gates (Fig. 1d).

References

- 1) S.L. Li, H. Miyazaki, A. Kumatani, A. Kanda, K. Tsukagoshi, *Nano Lett.* **10**, 2357 (2010).
- 2) S.L. Li, H. Miyazaki, H. Hiura, C. Liu, K. Tsukagoshi, *ACS Nano* **5**, 500 (2011).
- 3) S.L. Li, H. Miyazaki, M.V. Lee, C. Liu, A. Kanda, K. Tsukagoshi, *Small* **7**, 1552 (2011).

C₆₀ Microcrystals with Diverse Morphologies

ICYS-MANA Researcher

Lok Kumar SHRESTHA



1. Outline of Research

Preparation of morphology-controlled nano-sized materials through self-assembly of functional units is a key issue in bottom up nanotechnology. In particular, functional molecules such as fullerenes require assembly into well defined forms in order to construct advanced electronic, photonic, or bionic devices. Such applications utilize the C₆₀ in a self-assembled one-dimensional (1-D) or two-dimensional (2-D) structure that promotes its electronic and optical properties. Therefore studies on morphology-controlled nanostructures of C₆₀ continue to grow.

To improve the utility of C₆₀, a various synthetic approaches have recently been explored to develop 1-D or 2-D C₆₀ structures. A slow evaporation method has been explored for producing C₆₀ nanorods. Similarly, a vapor-solid process has been used to produce disk-type C₆₀ structure. We followed a simple liquid-liquid interfacial precipitation (LLIP) method¹⁻² for the production of C₆₀ microcrystals with diverse morphologies; 1-D nanorods, nanotubes, 2-D nanosheets, and even a novel complex 3-D network structures. We adopted a concept of mixing solvents and/or antisolvents for the production of such morphologies. Regardless of the progress in controlling the size and morphology of C₆₀ nano/microstructures, a systematic approach is still needed to facilitate the morphologically controlled synthesis of C₆₀ crystals. Generally LLIP method utilizes pure liquids (solvents and anti-solvents) for the synthesis of C₆₀ microcrystals. We believe that systematic studies of the effects of mixing solvents and/or anti-solvents on the structure and properties of C₆₀ crystals may lead to a new direction for the free morphology control of C₆₀ crystals.

2. Research Activities

(1) Synthesis and characterization of C₆₀ microcrystal.

Interfaces containing saturated solution of C₆₀ in organic solvents [benzene and carbon tetrachloride (CCl₄) or their mixtures] and alcohols [isopropyl alcohol (IPA) and tertiary butyl alcohol (TBA) or their mixtures] were formed. First of all, C₆₀ crystals were synthesized at liquid-liquid interfaces of benzene and mixed anti-solvents (IPA and TBA were mixed at different mixing ratios; 1:9 to 1:0.11). Next, anti-solvent was fixed and mixing ratios of solvents (CCl₄ and benzene) were varied. In a typical crystallization, 1 mL of saturated C₆₀ solution was placed in a thoroughly cleaned 10 mL glass bottle then 5 mL of antisolvent was added slowly while the temperature was maintained at 15 °C using a water bath. The above mixture was kept for 15 min without disturbance and then sonicated gently for a min for homogeneous crystal growth. The resulting mixture was stored in an incubator to grow crystals of C₆₀. The thus obtained C₆₀ microcrystals were characterized by using

electron microscopy (SEM and TEM), X-ray diffraction (XRD), and Raman spectrometry. Note that morphology of C₆₀ crystals obtained from mixed anti-solvents and solvents are very much different from those obtained from individual solvent/antisolvents systems. Fig. 1 shows SEM images of C₆₀ microcrystal prepared in mixed IPA-TBA/benzene systems. As is seen in SEM images, giant microcrystals consisting of well defined nanocrystals are formed in the mixed IPA-TBA system.

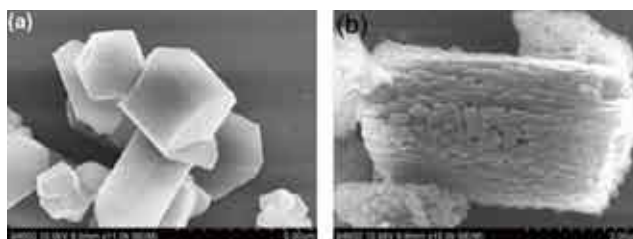


Fig. 1. SEM images of C₆₀ microcrystal prepared in mixed IPA-TBA/benzene systems via LLIP method for different mixing ratios IPA:TBA of 1:9 (a) and 2.3:1 (b).

Mesoporous crystalline C₆₀ could successfully be synthesized upon mixing benzene and CCl₄. When mixture of these solvents is interfaced with IPA, well-defined hexagonal-shaped crystals with macropores (conical shape) on the surface and mesopores in the bulk have been observed (see Fig. 2). The pore size could also flexibly be controlled by mixing fraction of the solvents.

Although the mechanism of crystal growth is yet to know, mixing solvents concept seems to be a novel route to the morphology control of fullerene crystals and also for the production of pore size controlled mesoporous crystalline fullerene. A detail investigation will be carried out to optimize the system and a particular attention will be paid to study of the application size of these self-assembled C₆₀ microcrystals.

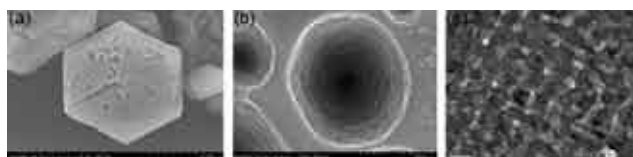


Fig. 2. Macro- and mesoporous crystalline fullerene from mixed solvent system: (a) SEM image, (b) HR-SEM image, and (c) cross-sectional HR-TEM image. The average pore size in panel (c) is ~ 25 nm.

References

- 1) K. Miyazawa, Y. Kuwasaki, A. Obayashi, M. Kuwabara, *J. Mater. Res.* **17**, 83 (2002).
- 2) M. Sathish, K. Miyazawa, J.P. Hill, K. Ariga, *J. Am. Chem. Soc.* **131**, 6372 (2009).

Low-Temperature Fluorination of Layered Iron Oxide

ICYS-MANA Researcher

Yoshihiro TSUJIMOTO



1. Outline of Research

The development of transition metal oxides with perovskite-based structure has stimulated the search for mixed-anion systems, because the incorporation of the two different anions in one structure provides further opportunities to effectively control and enhance the chemical and physical properties in the pure oxides. For example, the fluorine anion has almost the same ionic radius as the oxygen anion but different charge and electronegativity; this allows us to modify the electronic configuration of the transition-metal cation and the superexchange interactions mediated by the anion through substitution of F for O. However, the oxyfluoride phase is basically difficult to synthesize by a simple high-temperature reaction, because of the high chemical stability of the simple fluoride starting materials. This problem can be overcome using the following two techniques. One is a high-pressure synthesis,¹⁾ which allowed for access to the first example of layered cobalt oxyfluoride $\text{Sr}_2\text{CoO}_3\text{F}$. However, the number of materials that may be prepared via such a method is also quite limited, because the reaction technique requires specialized equipment. The other synthetic method is a low-temperature reaction. This is what I will report here.

2. Research Activities

Low-temperature reaction method is straightforward and contributes greatly to the development of oxyfluoride chemistry. To date, various fluorinating agents such as fluorine gas and NH_4F are known. For example, the reaction between fluorine gas and a layered iron oxide $\text{Sr}_3\text{Fe}_2\text{O}_6$ yields $\text{Sr}_3\text{Fe}_2\text{O}_6\text{F}_{0.87}$.²⁾ In this study, the synthesis of more highly fluorinated phase, namely $\text{Sr}_3\text{Fe}_2\text{O}_{5.44}\text{F}_{1.56}$, was successfully obtained using polytetrafluoroethylene (PTFE) or Teflon

powder, which possesses stronger reductive fluorinating power. $\text{Sr}_3\text{Fe}_2\text{O}_7$ and PTFE were thoroughly mixed, pelletized and heated in N_2 gas atmosphere at 275°C for 2d.

$\text{Sr}_3\text{Fe}_2\text{O}_{5.44}\text{F}_{1.56}$ powder was measured by neutron diffraction on HRPD at JRR-3 in JAEA with $\lambda = 1.5148 \text{ \AA}$. On the basis of Rietveld structure analysis (Fig. 1), the crystal structure was determined to be the tetragonal structure with the space group $I4/mmm$ ($a = 3.87264(6) \text{ \AA}$, $c = 21.3465(5) \text{ \AA}$). Close inspection of the NPD data revealed some additional peaks coming from magnetic reflection. The most reasonably refined magnetic structure is the model where each nearest neighbor iron moment in a double-layered block is aligned antiparallel and confined in the xy plane at a cant angle of $\theta \sim 45^\circ$ with the a -axis. Here, the magnetic cell (Fig. 2) is given as $a_m = b_m = \sqrt{2}a$, and $c_m = c$.

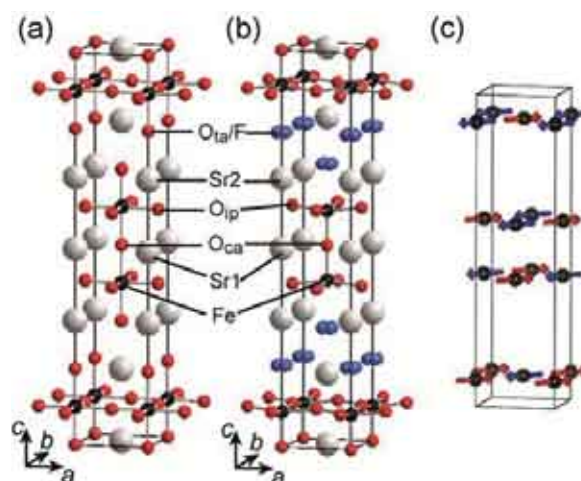


Fig. 2. Crystal structures of (a) $\text{Sr}_3\text{Fe}_2\text{O}_7$ and (b) $\text{Sr}_3\text{Fe}_2\text{O}_{5.44}\text{F}_{1.56}$, and (c) magnetic structure of the latter determined by the neutron experiments.

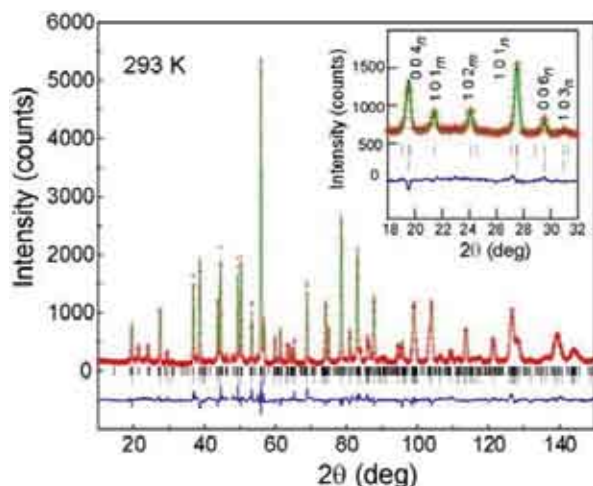


Fig.1. Neutron powder diffraction data collected at 293 K from $\text{Sr}_3\text{Fe}_2\text{O}_{5.44}\text{F}_{1.56}$.

In order to determine the valence state of Fe and anion composition, Mössbauer spectroscopy measurements were carried out in the temperature range from 4 to 410 K. Surprisingly, it was found that the iron charge was disproportionated into Fe(III) and Fe(V) with a ratio of 0.89 : 0.11 at 4 K. By taking into consideration the results of Mössbauer spectroscopy and NPD experiments, the composition of the iron oxyfluoride could be determined as $\text{Sr}_3\text{Fe}_2\text{O}_{5.44}\text{F}_{1.56}$.

References

- 1) Y. Tsujimoto, J.J. Li, K. Yamaura, Y. Matsushita, Y. Katsuya, M. Tanaka, Y. Shirako, M. Akaogi, E. Takayama-Muromachi, *Chem. Commun.* **47**, 3263 (2011).
- 2) Y. Tsujimoto, K. Yamaura, N. Hayashi, K. Kodama, N. Igawa, Y. Matsushita, Y. Katsuya, Y. Shirako, M. Akaogi, E. Takayama-Muromachi, *Chem. Mater.* **23**, 3652 (2011).

Visualization of the Grain Boundary as the Blocking Layer for Oxygen Tracer Diffusion

ICYS-MANA Researcher Ken WATANABE



1. Outline of Research

Metal oxides are important in many modern technological processes and one of the most important compounds is barium titanate (BaTiO_3) due to its applications in devices such as multilayer ceramics capacitors (MLCCs) and positive temperature coefficient resistors (PTCRs). The BaTiO_3 materials for both MLCCs and PTCRs are often formulated by incorporating them with rare-earth cations to control the microstructure of individual grains, conductivity, and electrical degradation.

Studies on oxygen diffusion bring direct information on oxygen defects (oxygen vacancies) in oxide materials. Itoh et al. reported a study on oxygen self-diffusion in non- and La-doped BaTiO_3 ceramics. They found that non-doped BaTiO_3 contained large numbers of oxygen vacancies.

Here, we focus on the diffusion path of oxygen in non-doped BaTiO_3 ceramics by means of secondary ion mass spectrometry (SIMS) and reveal our findings that the grain boundary acts as a blocking layer against oxygen self-diffusion in oxidized and reduced BaTiO_3 ceramics.¹⁾

2. Research Activities

Fig. 1 show the results obtained in BaTiO_3 ceramics that were pre-annealed in air. Fig. 1a is a concentration map of ^{18}O . This clearly reveals the ^{18}O diffusion feature in BaTiO_3 ceramics. The ^{18}O incorporates at the surface, and quickly diffuses into the grains. The BaTiO_3 grains can be found by observing the contrast in ^{18}O concentration due to discontinuous change when ^{18}O goes through the grain boundary. The decrease in ^{18}O concentration at the grain boundary is slight.

Fig. 1b shows the diffusion profile calculated along A-B in Fig. 1a. The $C[^{18}\text{O}]$ profile gradually decreases up to natural abundance, and then weak concentration steps can be found at the grain boundaries. The ^{18}O diffuses through the grains by a mechanism of bulk diffusion. The fitted curve is also in the same figure. To evaluate diffusion coefficient (D_b), the line profile calculated from the concentration map was fitted to the following equation

$$\left(\frac{C_{(x,t)} - C_o}{C_s - C_o} \right) = \text{erfc} \left(\frac{x}{2\sqrt{D_b \cdot t}} \right).$$

Here, C_s is the surface concentration, C_o is the background concentration, and x is the penetration depth. t is the duration of the diffusion treatment and $\text{erfc} = 1 - \text{erf}$ (erf is the Gaussian error function). The evaluated oxygen bulk diffusion coefficient (D_b) is $2 \times 10^{-11} \text{ cm}^2/\text{s}$. This value is in excellent agreement with the value of $2 \times 10^{-11} \text{ cm}^2/\text{s}$ at 850°C determined by the method of depth-profiling with SIMS.

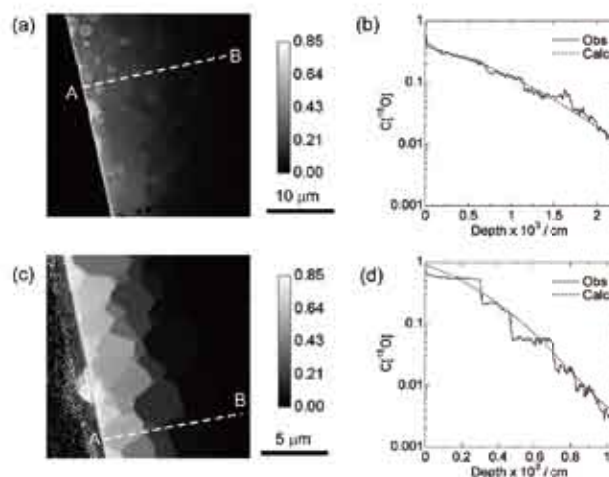


Fig. 1. High-resolution concentration maps of ^{18}O and $C_s[^{18}\text{O}]$ profiles obtained in (a and b) oxidized and (c and d) reduced BaTiO_3 ceramics. $C[^{18}\text{O}]$ profiles were obtained from lines (A-B) in each map.

Fig. 1c and d show the results obtained for the reduced BaTiO_3 ceramics. Fig. 1c is a concentration map of ^{18}O , which reveals the feature of ^{18}O diffusion, the concentration inside the samples, and the morphology. The ^{18}O in this map enters the sample surface and quickly diffuses up to the grain boundaries. Then, ^{18}O is prevented from diffusing at the grain boundaries, indicating steps in the ^{18}O concentration. Fig. 1d clearly shows the feature of oxygen diffusion in the ^{18}O concentration profile. The concentration profile indicates a uniform concentration in the grains and the concentration steps at the grain boundaries. The profile of $C[^{18}\text{O}]$ decreases up to natural abundance. Because the oxygen diffusion in the grains was too fast, it was not evaluated. Moreover, the concentration steps at the grain boundaries are larger than those in Fig. 1b. These results suggest that the reduced process acts to increase oxygen diffusivity in the grains and enhances the blocking effect at the grain boundary. The fitted curve is also plotted as the dashed line in Fig. 1b. The oxygen diffusion coefficient that was obtained as the apparent value is $3 \times 10^{-12} \text{ cm}^2/\text{s}$. This value is one order of magnitude smaller than that in Fig. 1b. These results indicate that the thermal history of samples plays an important role in controlling the structure of oxygen defects that are responsible for oxygen diffusion.

Reference

- 1) K. Watanabe, I. Sakaguchi, S. Hishita, N. Ohashi, H. Haneda, *Appl. Phys. Exp.* **4**, 055801 (2011).

Electron Emission from One-Atom-Thick Solids

ICYS-MANA Researcher

Xianlong WEI



1. Outline of Research

How electrons are emitted from a solid surface is an important problem from both fundamental and technological view points. In the past two decades, many kinds of solids with only one atom thickness (e.g. graphenes, carbon nanotubes (CNTs) et al.) became available for human beings. As compared to those in a three-dimensional (3D) bulk solid, electrons in a monatomic solid have two features: (i) they are confined in a quantum well along the direction normal to the surface; (ii) all electrons are always at a boundary with vacuum. Since those two features are closely related to electron emission processes, electron emission from a monatomic solid (Fig. 1) may be quite different from that from a 3D bulk one.

In this research, we are devoting to understanding how electrons are emitted from a monatomic solid, including possible new emission characteristics and mechanisms associated with its low dimensionality and monatomic thickness, and exploring possible applications based on the electron emission from it.

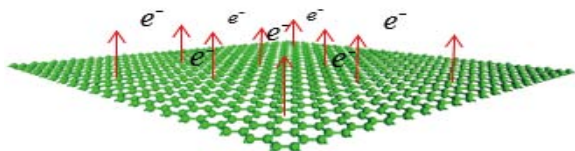


Fig. 1. A schematic drawing of electron emission from a one-atom-thick solid surface.

2. Research Activities

(1) Phonon-Assisted Electron Emission from Monatomic CNT Shells.

Electron emission from monatomic shells of individual electrically biased CNTs was studied both experimentally and theoretically.¹⁾ It was observed that electrons were emitted laterally from a CNT shell when a driving voltage higher than a threshold value of ~2-3 V was applied, and that emission current increased exponentially with the driving voltage (Fig. 2). More interestingly, the spatial distribution of the electron emission was asymmetric along tube axis and depended on the direction of electric field in CNT.²⁾ The average emission density of a half tube was found to increase along the direction of electric force. The phenomenon is absent in all pre-existing well-established emission mechanisms. In order to describe the regarded electron emission, a new kinetic model was proposed and well described all the experimental phenomena.¹⁻²⁾ It was shown that the electrons moving along a CNT under the drive of electric force can overflow from a monatomic CNT shell due to the absorption of hot forward-scattering optical phonons, and that the electron emission could be attributed to a new mechanism which was named by us as phonon-assisted electron emission (PAEE).

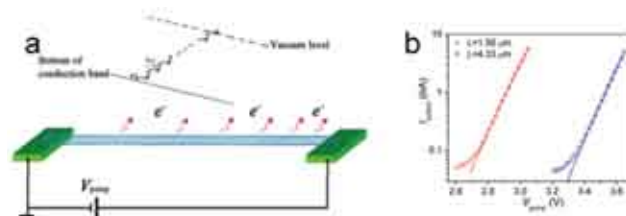


Fig. 2. (a) Electron emission from the shell of an electrically biased CNT and the energy diagram of PAEE. (b) Theoretical (lines) and experimental (symbols) emission curves.

(2) Electron Emission from Graphene Nanoribbons.

As compared to a CNT with seamless surface along its circumference, a graphene nanoribbon (GNR) has two open 1D edges. One atom thick character enables two different ways of electron emission from a GNR: (i) perpendicular emission from the monatomic surface and (ii) parallel emission from the 1D edges (Fig. 3).

We studied electron emission from individual GNRs driven by an internal electric field with a driving voltage of <3 V and analyzed the measured emission characteristics by taking into account monatomic thickness.³⁾ While deviating from the 2D Richardson equation for thermionic emission, they were well described by PAEE mechanism. Different from widely studied field emission from graphene edges, electrons were found to be emitted perpendicularly to the atomic graphene surfaces with an emission density as high as 12.7 A/cm² (Fig. 3). The internally driven electron emission is expected to be less sensitive to the microstructures of an emitter as compared to field emission. The low driving voltage, high emission density, and internal driving character make the regarded electron emission highly promising for electron source applications.

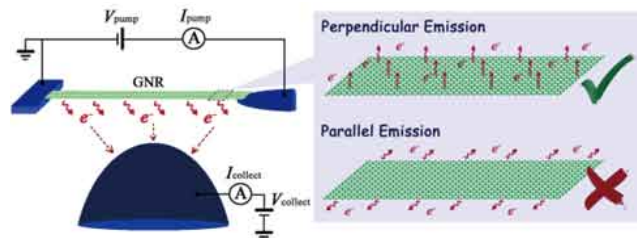


Fig. 3. The two different ways of electron emission from a GNR under internal drive with a preferable emission way marked.

References

- 1) X.L. Wei, D. Golberg, Q. Chen, Y. Bando, L.M. Peng, *Nano Lett.* **11**, 734 (2011).
- 2) X.L. Wei, D. Golberg, Q. Chen, Y. Bando, L.M. Peng, *Phys. Rev. B* **84**, 195462 (2011).
- 3) X.L. Wei, Y. Bando, D. Golberg *ACS Nano*, in press. doi: 10.1021/nm204172w

Direct Fabrication of Plasmonic Nanoparticles

ICYS-MANA Researcher

Jung-Sub WI



1. Outline of Research

Direct-fabrication of synthetic nanoparticles by top-down physical routes, in which materials are vacuum deposited in a nano-patterned polymer template, allows massive synthesis by a low-cost batch-type process and exquisite control over material composition, multilayer structure, particle size, and shape which are not achievable with chemical nanoparticle synthesis. The wide freedom of nanostructure design from various lithographic and deposition techniques allows us to engineer unique physical properties of custom designed nanoparticles, such as sub-lithographic-feature enhanced plasmonic nanoparticles. These plasmonic nanoparticles are designed to contain internal Raman hot spots,^{1,2} where a local electromagnetic field concentrated by surface plasmon resonance, or designed to interact with a broadband light.³

2. Research Activities

(1) Sombrero-shaped Raman-active Ag nanoparticles

Raman-active nanoparticles are fabricated using nano-imprint lithography and thin-film deposition as shown in Fig. 1, and are comprised of novel internal structures with sub-lithographic dimensions: a disk-shaped Ag core, a Petri dish-shaped SiO₂ base whose inner surface is coated with Ag film, and a sub-10 nm scale circular gap between the core and the base.¹

Confocal Raman measurements and electromagnetic simulations (Fig. 2) show that Raman hot spots appear at the inside perimeter of individual nanoparticles and serve as the source of a 1000 fold improvement of minimum molecular detection level that enables detection of signals from a few molecules near hot spots. Precisely controlled dimensions and unique internal structure of these sombrero-shaped nanoparticles enable detection of a few molecules.

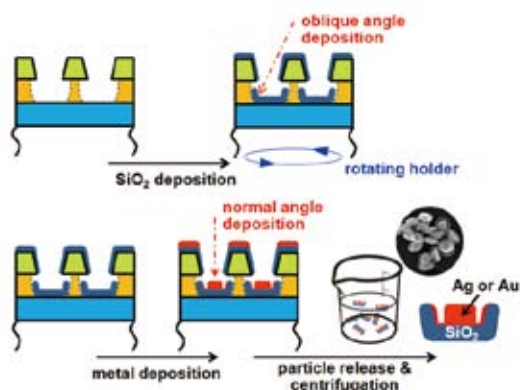


Fig. 1. Schematic illustration of the overall process: generation of polymer pocket array (details are described in Ref. 1), oblique angle deposition of SiO₂, metal deposition, nanoparticle release, and centrifugation. Inset SEM image shows the fabricated nanoparticles after centrifugation.

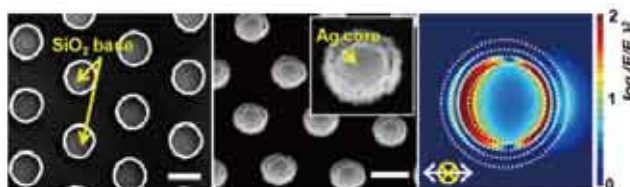


Fig. 2. SEM images of (left) SiO₂ bases and (middle) sombrero-shaped plasmonic nanoparticle arrays. The scale bars are 200 nm (right). The squared magnitude of the local electrical field amplitude of Ag Raman sombrero nanoparticle. The direction of incident light and its polarization are indicated in the inset as yellow and white colored arrows, respectively.

A multi-modality version of these nanoparticles, which includes the functionality offered by magnetic elements, is also simply available by successive deposition of plasmonic and magnetic films. These results illustrate the potential of direct fabrication for creating exotic monodisperse nanoparticles, which combine engineered internal nanostructures and multi-layer composite materials. Considering the present results, we expect that Raman sombrero nanoparticles can be used as an ultrasensitive molecular detection platform and that released nanoparticles that contain magnetic elements, distinguishable through the use of different Raman dyes, can be useful as multifunctional *in-vitro* or *in-vivo* imaging reagents.

(2) Three-tiered Au disks for trapping broadband light.

We have developed a straightforward method to enlarge the spectral window for light harvesting by creating a plasmonic nanostructure composed of closely spaced multiple Au nano-disks.³ The vertically stacked, three different-sized Au nano-disks make possible to merge the individual spectral windows of the internal nano-disks into one broadband window, as verified by numerical electromagnetic simulations and by direct observation of the relative scattering properties, and these nanostructures can be simply generated by a single e-beam lithography step with subsequent sputter deposition. The overhang structure from the sputtering process allows the self-adjustment of the diameters of the Au disks and enables the self-alignment of their central axes. We expect the proposed Au nanostructures to be useful for efficient Si PV cells through broadband light harvesting.

References

- 1) J.S. Wi, E.S. Barnard, R.J. Wilson, M. Zhang, M. Tang, M.L. Brongersma, S.X. Wang, *ACS Nano* **5**, 6449 (2011).
- 2) J.S. Wi, S. Sengupta, R.J. Wilson, Z. Zhang, M. Tang, S.X. Wang, *Small* **7**, 3276 (2011).
- 3) J.S. Wi, M. Rana, T. Nagao, *Jpn. Patent Appl.* 2011-279027.

High-Performance Solar-Blind Photodetectors

ICYS-MANA Researcher

Tianyou ZHAI



1. Outline of Research

One-dimensional (1D) inorganic nanostructures such as nanowires (NWs), nanobelts (NBs), and nanotubes (NTs) have stimulated numerous studies due to their importance in basic scientific research and potential technological applications. It is generally accepted that 1D inorganic nanostructures are ideal systems for exploring a large number of novel phenomena at the nanoscale and investigating the size and dimensionality dependence of functional properties. They are also expected to play important roles as both interconnects and key units in nanoscale electronic, optoelectronic, electrochemical, and electromechanical devices. Among many available nanoscale devices, the photodetectors are critical for applications as binary switches in imaging techniques and light-wave communications, as well as in future memory storage and optoelectronic circuits. In view of their high surface-to-volume ratios and Debye length comparable to their small size, 1D inorganic nanostructures have already displayed superior sensitivity to light in diverse experiments. We aim to develop an effective approach to construct high-performance solar-blind photodetectors based on 1D ZnS, $\text{In}_2\text{Ge}_2\text{O}_7$, and Ga_2O_3 nanostructures.¹⁻⁵⁾

2. Research Activities

(1) $\text{In}_2\text{Ge}_2\text{O}_7$ nanobelt-based photodetector.

High-quality single crystalline $\text{In}_2\text{Ge}_2\text{O}_7$ nanobelts were synthesized by vapor transport process. Individual $\text{In}_2\text{Ge}_2\text{O}_7$ nanobelts were designed for solar-blind DUV photodetectors. The detectors showed the ultrahigh photoconductive performance (Fig. 1): 1) High sensitivity and selectivity towards the solar-blind spectrum. 2) Excellent stability and reproducibility. 3) Fast response and decay time (~ 2 ms). 4) Ultrahigh responsivity ($3.9 \times 10^5 \text{ A W}^{-1}$) and quantum efficiency ($2.0 \times 10^8 \%$). Up to now, these values are the best working parameters of solar-blind photodetectors. A power-law dependence of the photocurrent of $\text{In}_2\text{Ge}_2\text{O}_7$

nanobelts on light intensity was determined. Based on the dependence of photocurrent on environment and quantum efficiency on light intensity, ultrahigh performance of $\text{In}_2\text{Ge}_2\text{O}_7$ nanobelts was ascribed mainly to surface traps, 1D dimensionality, and high-quality single crystals. Present $\text{In}_2\text{Ge}_2\text{O}_7$ nanobelt photodetectors may find wide optoelectronic applications in optical sensing, switches, and communications.

(2) Individual Ga_2O_3 nanobelt-based photodetector.

We designed solar-blind deep-ultraviolet range semiconductor photodetectors using individual Ga_2O_3 nanobelts and systematically studied their photoconductive behavior (Fig. 2). The photodetectors demonstrate high selectivity towards 250 nm light, fast response time of less than 0.3 s, and a large ratio of photocurrent to dark current, up to 4 orders of magnitude. The photoresponse parameters such as photocurrent, response time, and quantum efficiency depend strongly on the intensity of light, the detector environment, and the nanobelt size. The photoresponse mechanism was proposed, which was mainly attributed to the band bending, surface traps, and distribution of traps in the belts. Present Ga_2O_3 nanobelts can be exploited for future applications in photo sensing, light-emitting diodes, and optical switches.

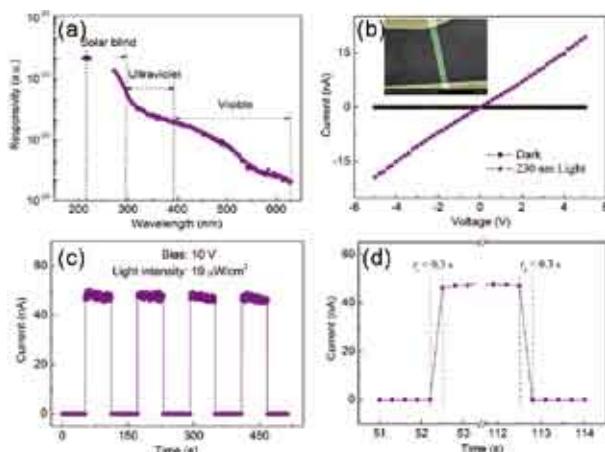


Fig. 1. Photoconductivity of $\text{In}_2\text{Ge}_2\text{O}_7$ -nanobelt-device.

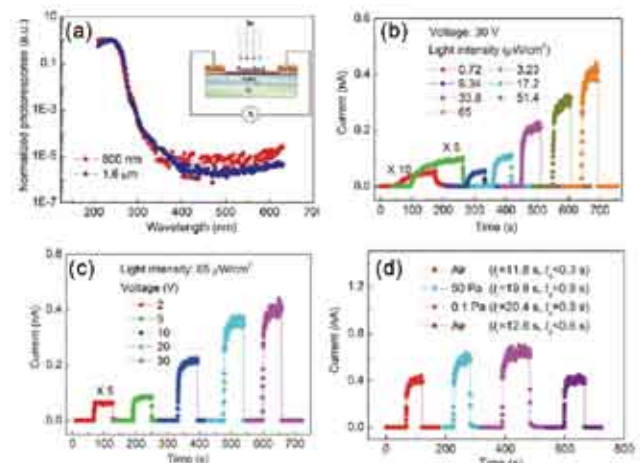


Fig. 2. Photoconductivity of Ga_2O_3 -nanobelt-device: (a) Spectral response; (b) under various light intensities; (c) under different applied voltage; (d) under air and different vacuum environments.

References

- 1) T. Zhai, L. Li, Y. Ma, M. Liao, X. Wang, X. Fang, J. Yao, Y. Bando, D. Golberg, *Chem. Soc. Rev.* **40**, 2986 (2011).
- 2) T. Zhai, L. Li, X.S. Fang, Y. Bando, D. Golberg, *Adv. Funct. Mater.* **20**, 4233 (2010).
- 3) L. Li, E. Auer, M. Liao, X. Fang, T. Zhai, U.K. Gautam, A. Lugstein, Y. Koide, Y. Bando, D. Golberg, *Nanoscale* **3**, 1120 (2011).
- 4) L. Li, P.S. Lee, C. Yan, T. Zhai, X. Fang, M. Liao, Y. Koide, Y. Bando, D. Golberg, *Adv. Mater.* **22**, 5145 (2010).
- 5) G. Li, T.Y. Zhai, Y. Jiang, Y. Bando, D. Golberg, *J. Phys. Chem. C* **115**, 9740 (2011).

Nano-Carbon Materials for Green Energy: Ambipolar Engineering of Graphitic Carbon Nitride via Graphene

ICYS-MANA Researcher Yuanjian ZHANG



1. Outline of Research

As one of the natural elements, carbon has already created a disproportionate amount of curiosities in science. Among various carbon allotropes, graphene, has attracted much attention and revealed interesting applications since 2004.¹⁾ Especially, the unique electric, optical and mechanical properties are of great interest, because of its one-atom thick, two-dimensional layer of sp^2 -bonded carbon structure (Fig. 1a). Among the most spectacular physical and chemical properties, graphene was found to be an electron collector and transporter, which may be used to boost performances of various energy conversion and storage devices or to be dispersible carrier for catalysts and templates for chemical reactions. Additionally, many efforts have also been devoted to modifying the electronic structure of graphene by physical cutting or chemical doping. However, graphene has seldom been used as a dopant with the purpose of manipulating the electronic structure of other semiconductors.

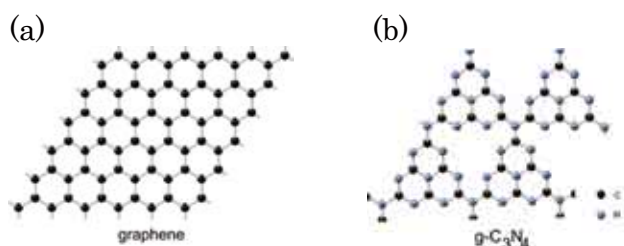


Fig. 1. Idealized motif of graphene (a) and graphitic C₃N₄ sheet (b).

As an analogue of graphite, graphitic carbon nitride also possesses a stacked two-dimensional structure (Fig. 1b shows one idealized structure of graphitic C₃N₄, g-C₃N₄).²⁾ Very recently, proof-of-concept studies by us and other groups showed organic semiconductors based on g-C₃N₄ are promising candidates for applications in optoelectronic conversion, and as photocatalysts in water splitting and degradation of organic pollutions. However, the efficiency of bulk g-C₃N₄ in visible light is rather low because it is hindered by the marginal absorption of visible light and grain boundary effects. In this regards, chemical doping such as ionic and covalent functionalization has been exemplified to be an effective strategy to modify the electronic structures of g-C₃N₄, and improve its performances.

Here we show that graphene was used as a dopant for semiconductors in band-structure engineering.³⁾ Like the union of tetrathiafulvalene (TTF) with tetracyanoquinodimethane (TCNQ) through π - π stacking forming a new molecule, we stacked graphene with its analogue, g-C₃N₄ sheet (Fig. 2). Our results showed that by doping with graphene (≤ 1 wt %) the band structure of g-C₃N₄ was modulated between more “n-type” and more “p-type”.



Fig. 2. Fused hybrid: graphene was used as a “dopant” for semiconducting graphitic carbon nitride in band-structure engineering via π - π stacking interaction.

Consequently, a significant increase of either anodic or cathodic photocurrent from g-C₃N₄ was obtained (e.g., when biased at 0.4 V vs. Ag/AgCl, the anodic photocurrent was 300% higher after doping). Complementary to previous ionic and covalent doping, the third strategy reported here, i.e., non-covalent doping would establish a more comprehensive understanding of the correlations between the chemical doping of g-C₃N₄ and enhanced performances.

Moreover, the host semiconductors are feasibly extended to other layered semiconductors; therefore, graphene would be promising as a general intercalating dopant. Meanwhile, it also implicated the rational combination of any other two-dimensional materials towards new properties.

2. Research Activities

(1) Preparation of graphene-doped carbon nitride.

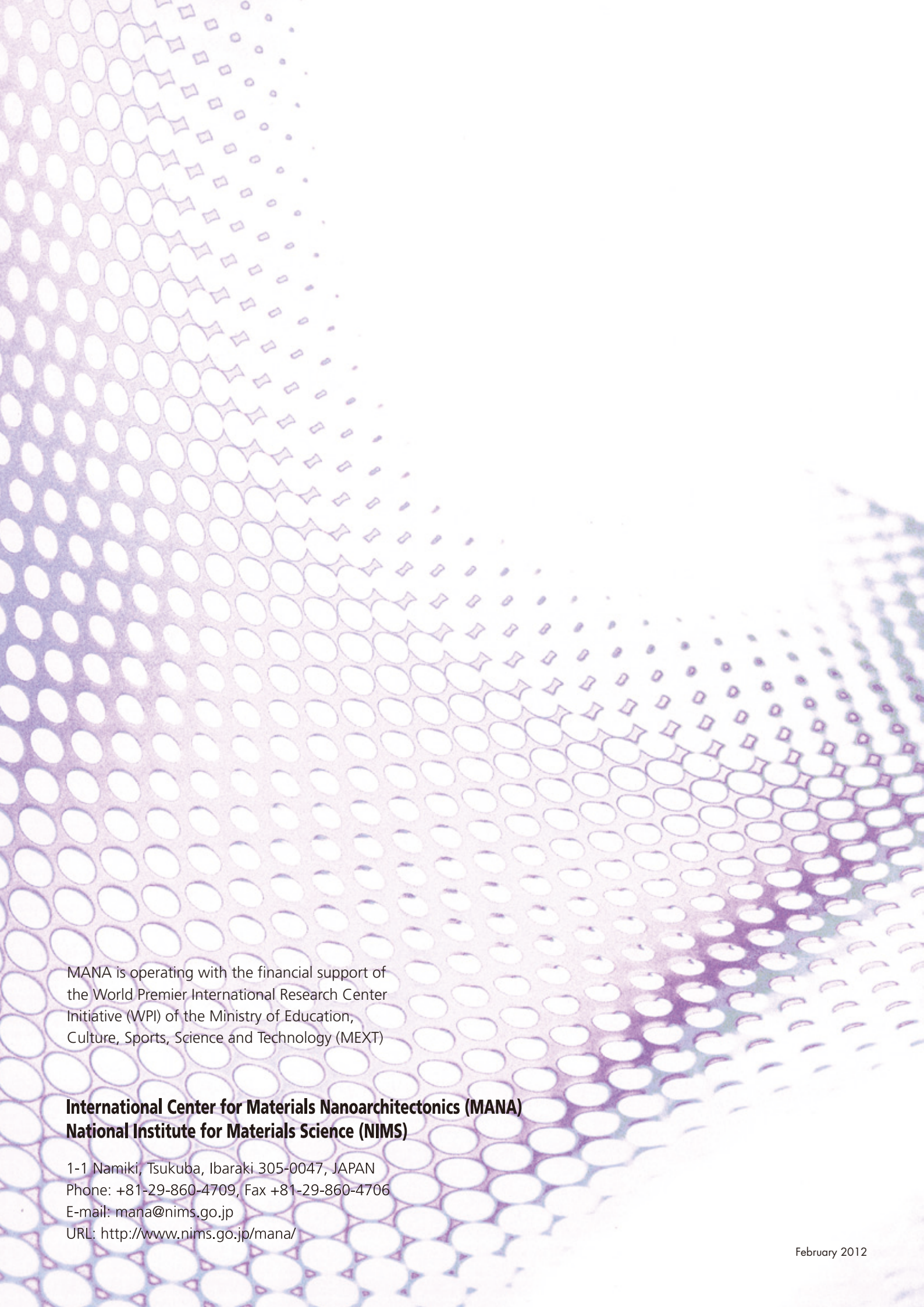
Graphene oxide (GO) was selected as the precursor for graphene. It was because GO could be exfoliated into single sheets, uniformly mixed with the monomer of g-C₃N₄ (dicyandiamide, DCDA) in water *via* electrostatic interaction, and converted back to graphene by the reduction. The graphene-doped g-C₃N₄ was prepared by heating the composite of GO and DCDA at 550 °C in air or in Ar for 4 hrs, during which, the polycondensation of DCDA was accompanied by the reduction of GO.

(2) Physicochemical properties.

Most of the molecular structure features of g-C₃N₄ were well retained after the intercalation of the graphene dopant. But depending on the concentration and the defects (oxygen-groups) of the graphene dopant, the electronic features had been seriously altered via photo electrochemical investigations.

References

- 1) K. Geim, K.S. Novoselov, *Nature Mater.* **6**, 183 (2007).
- 2) A. Thomas, A. Fischer, F. Goettmann, M. Antonietti, J.O. Müller, R. Schlögl, J.M. Carlsson, *J. Mater. Chem.* **18**, 4893 (2008).
- 3) Y. Zhang, T. Mori, L. Niu, J. Ye, *Energy Environ. Sci.* **4**, 157 (2011), and references therein.



MANA is operating with the financial support of the World Premier International Research Center Initiative (WPI) of the Ministry of Education, Culture, Sports, Science and Technology (MEXT)

**International Center for Materials Nanoarchitectonics (MANA)
National Institute for Materials Science (NIMS)**

1-1 Namiki, Tsukuba, Ibaraki 305-0047, JAPAN
Phone: +81-29-860-4709, Fax +81-29-860-4706
E-mail: mana@nims.go.jp
URL: <http://www.nims.go.jp/mana/>